

**Republic of Iraq
Ministry of Higher Education
& Scientific Research
University of Babylon
Faculty of Materials Engineering
Department of polymers and petrochemical industries**



Preparation of Super Hydrophobic Composite Nano Fibers by AC,DC- HV Electro spinning Technique

A Thesis

**Submitted to the Department of Polymers and
Petrochemical Industries at College of Materials
Engineering / University of Babylon in Partial
Fulfillment of the Requirements for the Master Degree
in Materials Engineering / Polymer**

By

Ammar Karim Kazem

Supervised by

Prof. Dr. Hanaa Jawad Khadim

2023A.D

1444A.H

بِسْمِ اللَّهِ الرَّحْمَنِ الرَّحِيمِ

(يَرْفَعِ اللَّهُ الَّذِينَ آمَنُوا مِنْكُمْ وَالَّذِينَ
أُوتُوا الْعِلْمَ دَرَجَاتٍ وَاللَّهُ بِمَا تَعْمَلُونَ خَبِيرٌ)

صدق الله العظيم

« سورة المجادلة: الآية 11 »

This is dedicated to

my family,

&

Dr. Hanaa Jawad Khadim

**For their endless love, support and
encouragement**

Acknowledgments

First of all, I would like to express my thanks and gratitude to Allah Almighty for granting and facilitating this research. Thank you befitting His Majesty and greatness.

Secondly, I would like to thank my family, one by one, for their help, encouragement, and invitations to me in completing my master's thesis.

I would also like to thank the doctor supervising the research, Prof. Dr. Hanaa Jawad Khadim , for his great efforts and his assistance in completing my master's thesis.

I also extend my heartfelt thanks to all my professors who supervised me during my undergraduate studies in the Faculty of Materials Engineering, Department of Polymers and Petrochemical Industries.

I also extend my sincere thanks to all the staff members in the Faculty of Materials Engineering, Department of Polymers and Petrochemical Industries at the University of Babylon, for their great role in overcoming the difficulties in front of the research students by assisting with examinations.

Supervisor Certificate

We certify that we read this thesis entitled " Super hydrophobic natural nano composite based fibers blends for hig Surface protection application by electrospinning technique " as an examination panel examined by the student " Ammar Karim Kazem " in its contents and that , in our opinion meets the standard of thesis for the Degree of Master of Philosophy in materials Engineering

Signature:

Prof. Dr. Hanaa Jawad Khadim

Supervisor

Date: / / 2023

Abstract

The research deals with the study of the physical properties of the produced Nano fibers

1 using AC – HV

2 using DC – HV

The fibers were produced from polyvinylidene fluoride and polystyrene materials and with the influence of various factors, some of which are related to the solution such as (viscosity, conductivity, surface tension) and the other is related to the installation Such as (liquid pumping capacity, voltage value, voltage type) and also added a natural substance extracted from plants, which is argan oil, to the best prepared samples to know its effect on the prepared solutions and the properties of the resulting fibers. Several tests were carried out, including tests for solutions, which include surface tension, viscosity, and electrical conductivity, as well as fiber tests, which include examining the infrared rays of the fibers produced by DC - HV to determine the type of The interaction between the components and knowledge of the resulting bonds and composition, and the wetting angle. Examination to determine whether the prepared fibers are hydrophilic or hydrophobic. The results showed that the wetting angle of the fibers produced by DC - HV is greater than the results of AC - HV. Atomic force microscopy test to know the surface roughness and surface tolerance index. The results showed that the surface roughness of the fibers produced by AC - HV is more than the fibers produced by DC-HV 79.97, scanning electron microscope to study the morphology and distribution of the fibers and the results showed that the fibers produced using DC - HV contain beads and are more regular than the fibers produced by AC - HV. The corrosion test of the coating was studied and the results showed that the corrosion resistance increases 77.29 when the percentage of (PVDF) is increased. The results of adhesion resistance were also studied by pull test, as it increases 93.51 with increasing percentage of PVDF

Table of Contents

| No. | Subject | Page No. |
|--|-----------------------------------|----------|
| | Abstract | V |
| | List of Contents | VII |
| | List of Figs | X |
| | List of Tables | XIV |
| | List of Abbreviations | XV |
| Chapter One: Introduction | | |
| 1.1 | Introduction | 1 |
| 1.2 | Aims | 3 |
| Chapter two: Theoretical Part and literature review | | |
| 2.1 | Introduction | 4 |
| 2.2 | Nano fibers techniques | 4 |
| 2.2.1 | Drawing | 4 |
| 2.2.2 | template synthesis method | 6 |
| 2.2.3 | Phase Separation | 7 |
| 2.2.4 | self assembly | 8 |
| 2.2.5 | Electrospinning | 9 |
| 2.3 | electro spinning set up | 11 |
| 2.4 | Solution Parameters | 13 |
| 2.4.1 | Concentrations | 13 |
| 2.4.2 | Viscosity | 14 |
| 2.4.3 | Surface Tension | 15 |
| 2.4.4 | Electrical conductiityv | 15 |
| 2.5 | Processing Parameters | 15 |
| 2.5.1 | High Voltage Power Supply: (HVPS) | 15 |

| | | |
|---|---|----|
| 2.5.2 | Pumping Rate | 16 |
| 2.5.3 | Electrospinning Distance | 16 |
| 2.5.4 | Capillary Tip Diameter | 17 |
| 2.5.5 | Collector Geometry Shape | 17 |
| 2.6 | Ambient Parameters: heat | 18 |
| 2.7 | For Eliminate of Beads Number in Resultant Nanofibers | 19 |
| 2.7.1 | Concentration | 19 |
| 2.7.2 | adding a salt additive | 19 |
| 2.7.3 | Suitable solvent for electro spun products: | 19 |
| 2.8 | Polystyrene | 20 |
| 2.9 | Polyvinylidene fluoride (PVDF) | 22 |
| 2.10 | Applications of nanofibers | 23 |
| 2.11 | Literature Review | 24 |
| Chapter Three: Experimental Part | | |
| 3.1 | Introduction | 37 |
| 3.2 | Materials used | 38 |
| 3.2.1 | General purpose Poly Styrene (GPPS) | 38 |
| 3.2.2 | Polyvinylidene fluoride (PVDF) | 38 |
| 3.2.3 | N,N-Dimethylformamide (DMF) | 39 |
| 3.2.4 | Argan oil “liquid gold” | 40 |
| 3.3 | Methods | 40 |
| 3.4 | Sample Preparation | 41 |
| 3.5 | Tests | 41 |
| 3.5.1 | Fourier transform infrared spectroscopy (FTIR) Test | 42 |
| 3.5.2 | Surface tension test | 42 |
| 3.5.3 | Capillary viscometer test (Ostwald viscometer) | 43 |

| | | |
|--|--|----|
| 3.5.4 | Scanning Electron Microscope (SEM) | 44 |
| 3.5.5 | Atomic Force Microscopy (AFM) Test: | 46 |
| 3.5.6 | Contact Angle Test | 47 |
| 3.5.7 | Corrosion tester (electrochemical Tafel method) | 48 |
| 3.5.8 | Pull-off adhesion test | 49 |
| Chapter Four: Results and Discussion | | |
| 4.1 | Introduction | 50 |
| 4.2 | FTIR analysis | 50 |
| 4.3 | Effect of solutions parameters on fiber properties | 51 |
| 4.4 | SEM Images of Nanofibers With AC and DC-HVPS | 52 |
| 4.5 | SEM Images of nanofibers under DC-HV (18 KV-21KV) | 55 |
| 4.6 | SEM Images of (68:32)PS:PVDF:AO Nanofibers | 57 |
| 4.7 | AFM Results of Nano fibers under AC and DC-HVPS | 58 |
| 4.8 | AFM Results of Nanofibers under DC-HVPS (18 KV) | 60 |
| 4.9 | AFM Results of (PS:68: PVDF :32)AO Nanofibers | 62 |
| 4.10 | Contact Angles Results of Nanofibers under AC, and DC-HVPS | 64 |
| 4.11 | Contact Angles Results of PS and PS blends Nanofibers under DC-HVPS (18KV) | 67 |
| 4.12 | Resu Contact Angles lts of (PS:68:PVDF:32):AO Nanofibers | 69 |
| 4.13 | Corrosion Behavior Results of Nanofibers under AC and DC-HVPS | 70 |
| 4.14 | The results of the pull-out adhesion test | 73 |
| Chapter Five: Conclusions and Recommendations | | |
| 5.1 | Conclusions | 74 |
| 5.2 | Recommendations | 75 |
| References | | |

List of Figs

| Fig No | Fig | Page No. |
|--------|--|----------|
| 2.1 | Drawing method steps | 5 |
| 2.2 | Obtaining nanofibers by template synthesis Technique | 6 |
| 2.3 | (a) Phase separation process, (b) SEM image of final form nanofiber | 8 |
| 2.4 | Self-assembly process to create Nanofibers | 9 |
| 2.5 | taylor cone formation. Increase the voltage up equilibrium stage between the surface tension and strength of the electrostatic force at step | 11 |
| 2.6 | the diagram of the fiber formation by electrospinning | 11 |
| 2.7 | electro spinning set up with rotating cylinder collector | 13 |
| 2.8 | Collector type in electrospinning technique | 18 |
| 2.9 | Polystyrene structure | 20 |
| 2.10 | Polymerization of polystyrene | 21 |
| 2.11 | Stereochemistry of (a) atactic, (b) syndiotactic, and (c) isotactic polystyrene | 21 |
| 2.12 | PVDF structure | 22 |
| 2.13 | Applications of polymeric nanofibers | 24 |
| 3.1 | Electrospinning set up | 40 |
| 3.2 | IR Affinity-1 Shimadzu device | 42 |
| 3.3 | Surface tension device | 43 |
| 3.4 | ostwald viscometer | 44 |
| 3.5 | SEM | 46 |

| | | |
|------|---|----|
| 3.6 | Atomic Force Microscope (AFM) Device. | 47 |
| 3.7 | Contact Angle Meter (SL200B Optical) device | 48 |
| 3.8 | Corrosion test device (Tafel's device) | 49 |
| 3.9 | Pull-off adhesion device. | 50 |
| 4.1 | FTIR analysis of PS and PS-PVDF blend | 51 |
| 4.2 | shows the SEM images of Nano fibers produced by AC-DC- HV | 55 |
| 4.3 | shows the SEM images of Nano fibers produced by DC- HV | 56 |
| 4.4 | SEM Images of (68:32)PS:PVDF:AO Nanofibers | 58 |
| 4.5 | AFM Results of Nano fibers under AC and DC-HVPS | 59 |
| 4.6 | AFM Results of Nanofibers under DC-HVPS (18 KV) | 61 |
| 4.7 | AFM Results of (PS:68: PVDF :32)AO Nanofibers | 63 |
| 4.8 | Contact Angles Results of Nanofibers under AC, and DC-HVPS | 65 |
| 4.9 | Contact Angles Results of PS and PS blends Nanofibers under DC-HVPS (18KV) | 67 |
| 4.10 | Resu Contact Angles lts of (PS:68:PVDF:32):AO Nanofibers | 69 |
| 4.11 | corrosion resistance blends and composite of Nano fibers produced by 15KV DC-HV | 72 |

List of Tables

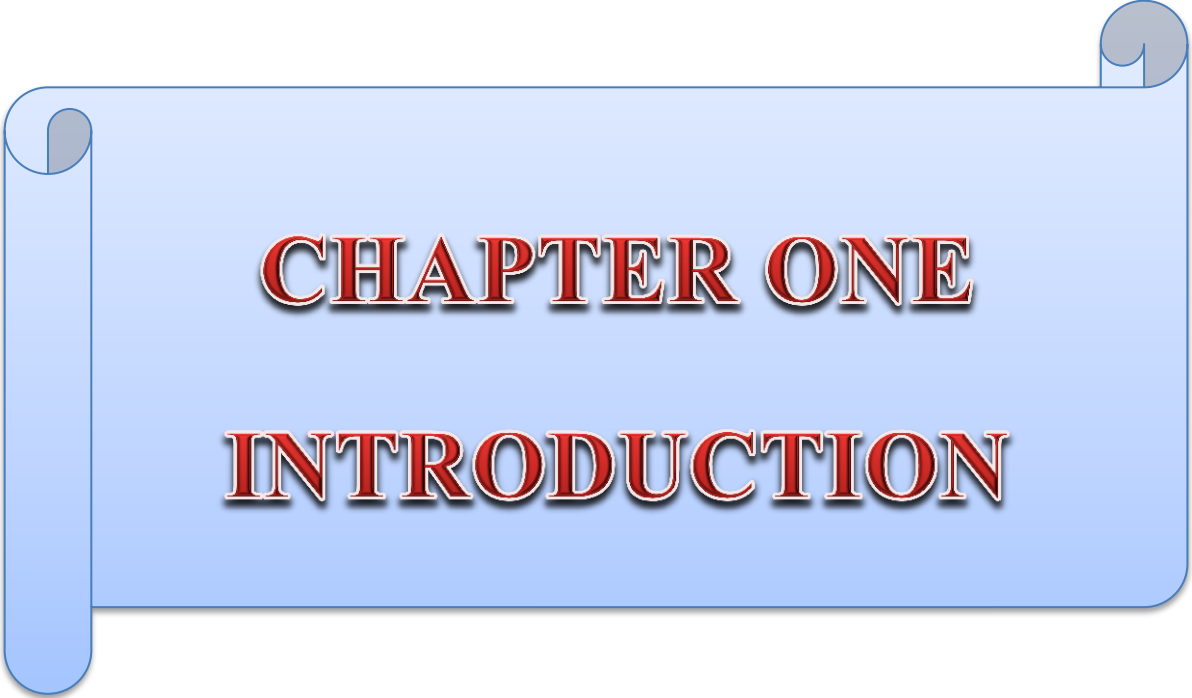
| Table No. | Table | Page No. |
|-----------|--|----------|
| 3.1 | General purpose polystyrene Properties | 38 |
| 3.2 | The Physical properties of PVDF | 39 |
| 3.3 | the physical properties of DMF | 39 |

| | | |
|------|---|----|
| 3.4 | Argan oil content analysis | 40 |
| 4.1 | Effect of concentration of solutions on viscosity, surface tension and conductivity of solutions for all polymer solutions: | 51 |
| 4.2 | shows the surface parameters of PS nanofibers and PS-PVDF blends of nanofibers by AFM | 60 |
| 4.3 | shows the surface parameters of PS nanofibers and PS-PVDF blends of nanofibers by AFM assay | 62 |
| 4.4 | shows the surface parameters of (ps0.68+0.32pvdf) +argan oil of nanofibers by AFM assay | 63 |
| 4.5 | Contact Angles Results of PS and PS blends nanofibers | 66 |
| 4.6 | Contact Angles Results of PS and PS blends nanofibers | 68 |
| 4.7 | Contact Angles Results of PS and PS blends nanofibers | 69 |
| 4.8 | Results of corrosion curves for the first group of samples | 72 |
| 4.9 | Results of corrosion curves for the second group of Samples | 73 |
| 4.12 | shows the adhesive strength of sample | 74 |

List Of Abbreviations

| | |
|-------|--------------------------|
| AC-HV | Alternating high voltage |
| DC-HV | Direct high voltage |
| PS | Polystyrene |
| PVDF | Polyvinylidene fluoride |

| | |
|--------|------------------------------|
| DMF | N, N-Dimethylformamide |
| NFs | Nano Fibers |
| GPPS | General Purpose Poly Styrene |
| Cy.h | Cyclohexane |
| THF | Tetrahydrofuran |
| MW | Molecular weight |
| FTIR | Fourier transforms infrared |
| Sdr | Surface Area Ratio |
| SEM | Scanning Electron Microscopy |
| AFM | Atomic force microscope |
| CA | Contact angle |
| Wt.% | Weight Percent |
| Sci | fluid retention index |
| l.r | Lnjection rate |
| n.d | Needle diameter |
| rpm | Rotate per minute |
| Con. | Concentration |
| Sa | Roughness Average |
| Sbi | Surface Bearing Index |
| Sq | Roughness Mean Square |
| E.corr | Corrosion potential |
| I.corr | Corrosion Current |
| °C | Celsius |
| AO | Argan oil |



CHAPTER ONE
INTRODUCTION

1.1 INTRODUCTION

Nanoscience and nanotechnology research covers a wide range of topics. It is mostly concerned with nanometer-sized objects. Richard F. invented the nanotechnology motif in 1959 [1]. Then, nanotechnology was transformed into a multi-specialized field of applied science and technology, with applications such as self-cleaning surfaces [2], filtration [3-4], denture base [5-6] and other human-related disciplines. For lightweight material applications, polymer nanofibers are an important tool to increase performance and create new jobs [7]. Researchers have recently focused their efforts on the study of super-hydrophobic materials and have achieved tremendous progress [8]. The wetting behavior of materials is divided into two categories: hydrophobic and hydrophilic. The former has a surface that has a strong attraction for water, while the latter repels it [9]. Hydrophobic Surface is the capability of the surface which repel water molecules is high and is determined by knowing the contact angle of the surface , where the contact angle $\theta > 90^\circ$. [10]. when the value exceeds 150° , the surface is defined as a super-hydrophobic surface while, with contact angle less than 90° , the coating behaves as a hydrophilic surface, Hydrophobic surfaces have low surface energy , high efficiency for anticorrosion , anti- icing and repel the water. It has an self-cleaning propertyfor these reason, it play an critical role in different applications [11]. High corrosion resistance, self-cleaning, anti-bacterial growth, and anti-pollution are just a few of the benefits of hydrophobic surfaces [12-15]. Electrostatic spraying [15], spin coating [16], immersion coating [17], and electrospinning coating for nanofibers are just a few of the approaches for creating hydrophobic surfaces [18-19]. Processes including drawing [20], templates assembling [21], phase segregation [22], self-assembly [23], Electrospinning is a simple and effective technique in which natural and synthetic polymers are used in the

CHAPTER ONE INTRODUCTION

formation of nanofibers. Because of the high efficiency of nanofibers, they have been used in several different fields, such as efficient food packaging [24,25] can be used to create polymeric nanofibers. By propelling a polymeric material jet in an electric field, the electrospinning procedure produces nanofibers with diameters ranging from 10 μm to 10 nm [1,2,8,9]. This technique generates a lot of attention since it has the ability to spin a wide range of polymeric fibers and has potential uses in membranes, electrical devices, and nanocomposites [24,25]. Although the electrospinning process has been known for nearly 70 years, polymer nanofibers produced by this method have been a topic of great interest in the past few years. In 1934, the first invention that detailed the electrospinning technique was issued, when Formals revealed a device for producing polymer filaments using electrical repulsion between surface charges [26]. The electrospinning process is described in the literature and patents [26-30]. Electrospun nanofibers provide a very large area/mass ratio result for their small diameter, and thus for nonwovens, with a small use of particle filtration in the sub-separation industry. It can also be used for gas absorption, biological and chemical warfare, protective clothing, biomedical and medical industries as artificial blood vessels, sutures, surgical mask, Wound dressings, drug delivery systems, and fiber-reinforced materials (composite materials). Electrospinning technology can be used to make materials for spray coatings, electrophoresis, plasma deposition, metallurgy, metallurgy, solar cell design, optical mirrors for use in space as well as structural elements in artificial organs. [31] Nanocomposites are materials produced from different nanocomponents with different physical and chemical properties, such as the size of nano-films produced from nanoparticles of different types, yarn or fabrics made of different nanofibers, or nanofibers with nanoparticles. [32-33] Material transformation to the nanoscale results in the creation of nanofibers with novel features that expand the field's use, particularly in the sectors of

advanced technology. The electrospinning process is simple, effective and low cost in the production of nanofiber composites. It is a simple method and the product has many proportion, including the following: [34-35]

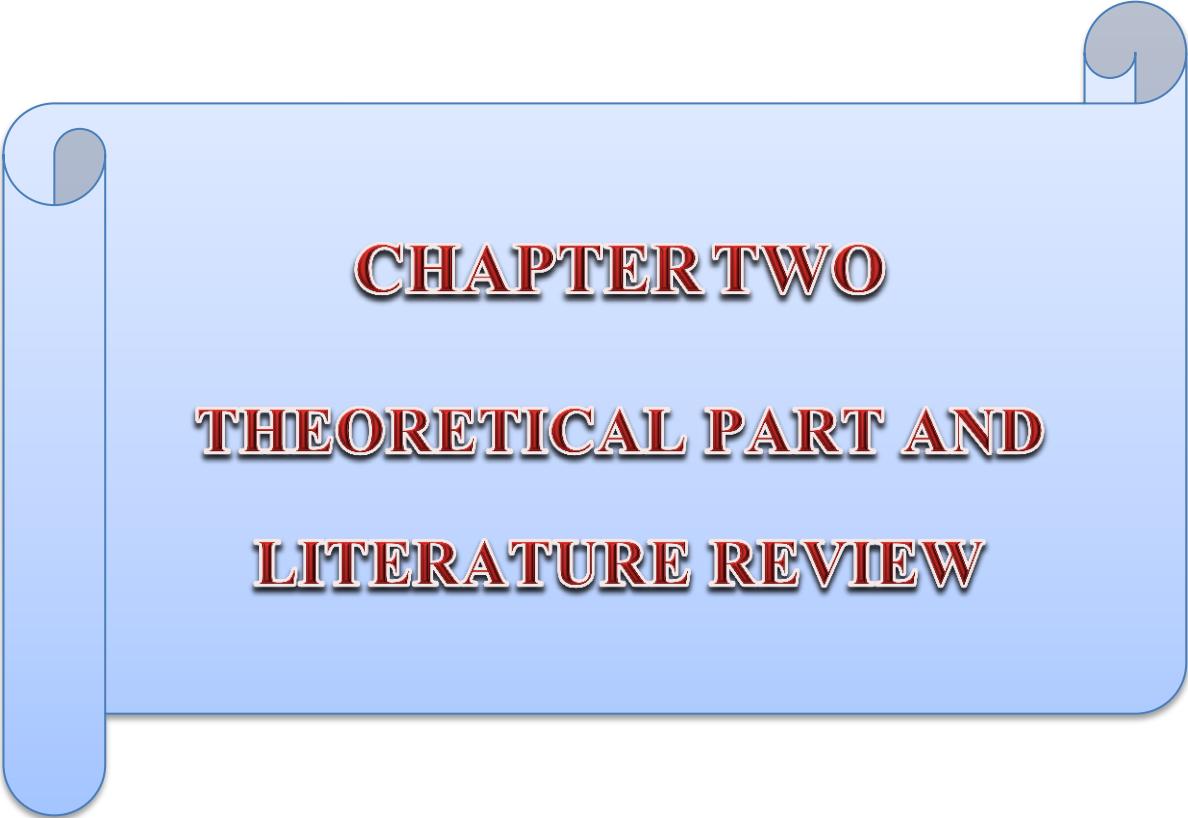
a) The length is excessive. The electro spun nanofibers are extraordinarily lengthy compared to single (1D) nanostructures that are generated or that are synthesized to use other chemical or physical processes. Since electro spinning is an unbroken process, the fibers can exceed several kilometers. [36].

b) A porous structure with a large surface area. Electro spun fibers have a significantly smaller diameter and a greater surface-to-volume ratio than fibers produced using a traditional mechanical extruded or spin method. The interweaving of nanofibers can also lead to the formation of a dense population of pores.

c) At the molecular level, alignment. The solvent evaporates quickly during electrospinning at the rate of an electrified jet. During in the electro spinning process, it is anticipated that the polymers would experience a very significant shear force [37]. Thus there must be a series of crystallization and formation of polymeric nanofibers resulting from different products obtained through solution casting or conventional spinning processes [38].

1.2 Aim of this study

1. Preparation and characterization of nonwoven Nano fiber from PS: PVDF with argan oil by AC and AC _ HVPS electro spinning.
2. Compared the physical properties of Nano fibers produced by the above electro spinning techniques.
3. Studding the effect of Nano fibers produced on corrosion and adhesion resistance.



CHAPTER TWO
THEORETICAL PART AND
LITERATURE REVIEW

2.1 Introduction

Nanomaterials are materials produced from several different physical and chemical properties, such as films, filaments, nanofibres, or nanoparticles mixed with nanofibers. However, electrospinning is the best technique for producing nanofibers compared to other chemical and physical methods for producing nanofibers with the following properties

a) High stretching. Nanofibres (one-dimensional) produced by electrospinning technology because it is a continuous process that can extend nanofibers to several kilometers. [39]

b) The highly porous region of the normal and more complex porous structure . Compared with fibers manufactured using extrusion or a traditional mechanical spinning process, electrospinning nanofibers are thinner in diameter and thus have an increased surface-to-volume ratio. It can also be of high pore density as a result of interlacing nanofibers.

c) The electrospinning process can align the produced nanofibers with a highly aligned polymeric chain, the latter being the result of rapid evaporation of the solvent that produces high shear strength, resulting in crystallized nanofibers. [40]

2.2 Nanofibers techniques

2.2.1 Drawing

Fibers are generated in a certain way. It works similarly to dry spinning. This technique requires only a fine tip or a micro-pipette, which limits its main advantages. In this technique, a thin tip is used to withdraw liquid fibers from a drop of a polymer solution. Due to the large surface area, the solvent gradually evaporates, leaving the liquid fibers to solidify. To solve the problem of volume shrinkage affecting the continuous pulling of

CHAPTER TWO Theoretical Part and literature review

the fibers and the effects on their diameter, hollow cylindrical glass pipettes are used instead of the sharp tip with a fixed dose of polymer, see Fig (2.1) [41]

After being immersed in a droplet of the polymer solution, the micropipette is gently removed from the drop at a low speed (about 10 m/s). As a result, nanofibers are formed by contacting the nanofibers pulled from the substrate and the needle's point, and this process was repeated several times for each drop of the polymer solution [42].

This method can be used to produce continuous nanofibers in any configuration. Moreover, precise control of key drawing parameters such as viscosity and drawing speed can be achieved, allowing for repeatability and control over the measurements of generated fibers [43].

Although this technique is simple, it is limited to the laboratory level because the nanofibers were singly formed. It is a low-throughput discontinuous method, and it can also control the diameter of the fibers. Only viscoelastic materials can withstand pulling tension, and depending on the hole size, only fibers with diameters greater than 100 nm can be formed.

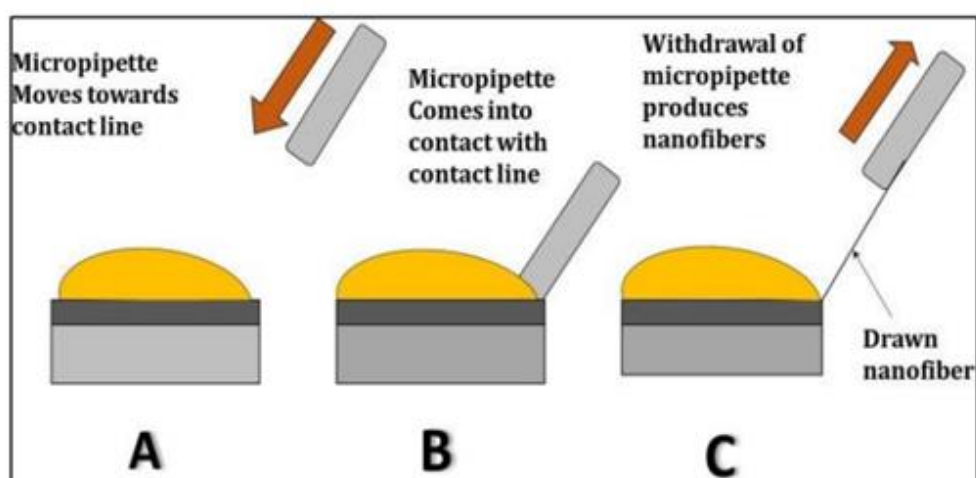


Fig (2.1) Drawing method steps [30]

2.2.2 Template synthesis method

The process produced many polymeric, metallic, semiconductor or ceramic nanofibers by chemical or electrochemical oxidative polymerization also using a porous nano membrane with many cylindrical holes whose thickness ranged from (5-50nm). The method produces nanofibers using a die made of aluminum oxide (AL2O₃) to obtain the final structure. The nanofibers are created by pumping the polymer solution through the holes of nano diameter by the effect of water pressure on one side, which enables the polymer to be extruded and form nanofibers when it comes into contact with the solidification solution as shown in (Fig. 2.2). This method is unable to form large length nanofibers. The method results in a few micrometers of long fibers, and the diameter of the fibers is related to the membrane pore sizes[44-45]. Some of the benefits of using this technology are the ability to produce nanofibers of different diameters using multiple moulds.

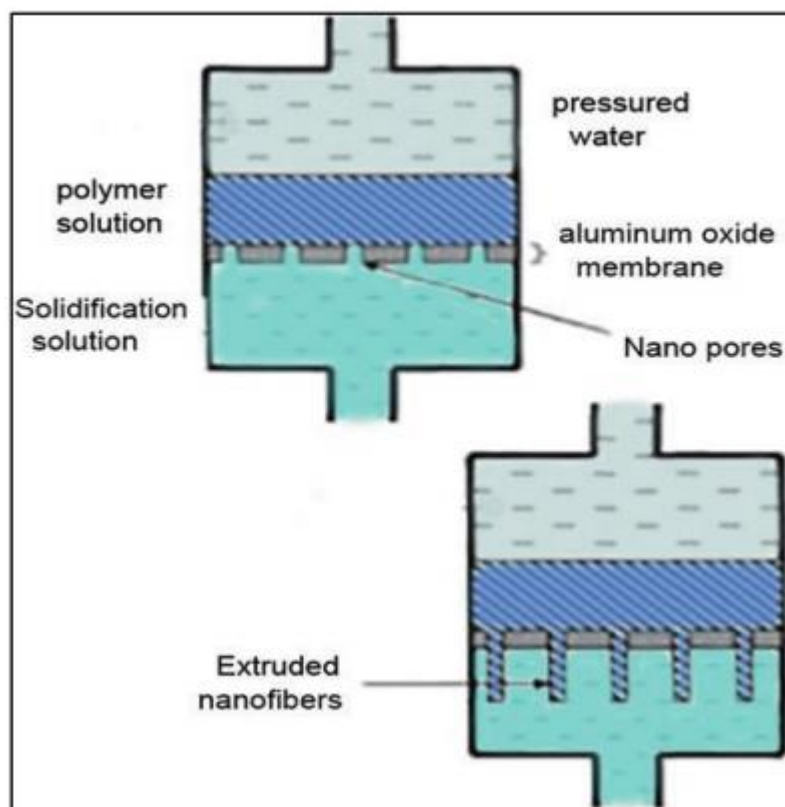


Fig (2.2) Obtaining nanofibers by template synthesis Technique [44-45].

2.2.3 Phase Separation

Phases will separate in this process. The solvent layer is then separated from the solution, leaving behind the other phase. there are four main stages in this method: [46]

- 1- Dissolve the polymer with using convenient solvent a room temperature or upper it.
- 2- Gelation step and it regarded as difficult step because of difficult regulating the porosity of nanofibers.
- 3- Extraction of solvent step to separate and remove the solvent from the produced gel by using water.
- 4- Freezing followed by drying under vacuum step.

The characteristics of nanofiber are determined by the concentration of polymer used; if the polymer percentage rises, porosity of the fiber decreases, and the mechanical properties of the fiber increase [45].

The first step in this method is dissolving the polymer at room temperature to make homogeneous solution, after that removing the gel from the solution by holding it to temperature of gelation, where nanofibrous matrixes are formed due to phase separation, and eventually the solvent will be extracting followed by the matrix drying step, this eventually leads to the formation of nanofibers. As shown in Fig (2.3)

This method requires minimal equipment, it may produce a nanofiber matrix directly, with mechanical properties adjusted by altering the polymer concentration [47].

The phase separation technique has only been utilized to create nanofibers from few polymers, like “polylactide (PLA)” and “polyglycolide” [44]. This technique also cannot create long continuous fibers, and not all

polymers can undergo phase separation and form nanofibers since it needs gelation capacity, which restricts the application of this technology.

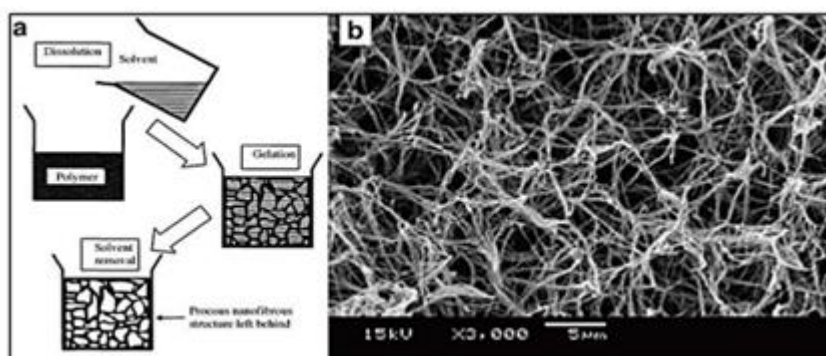


Fig (2.3) (a) Phase separation process, (b) SEM image of final form nanofiber [30]

2.2.4 Self-assembly

This method involves rearranging and reassembling molecules on their own to form different shapes and configurations through non-covalent forces such as hydrogen bonding forces and electrostatic interactions. Fig (2.4)[41].

This method is suitable for fabricating smaller diameter nanofibers with an average diameter of less than 100 nanometers and length in micrometers. The mechanism of his method is to hold the molecules together. The orientation of the particles determines their final shape. The main disadvantages of this method are the complexity, slowness, low production volume, and the complexity in maintaining the diameters of the produced fibers [44,48].

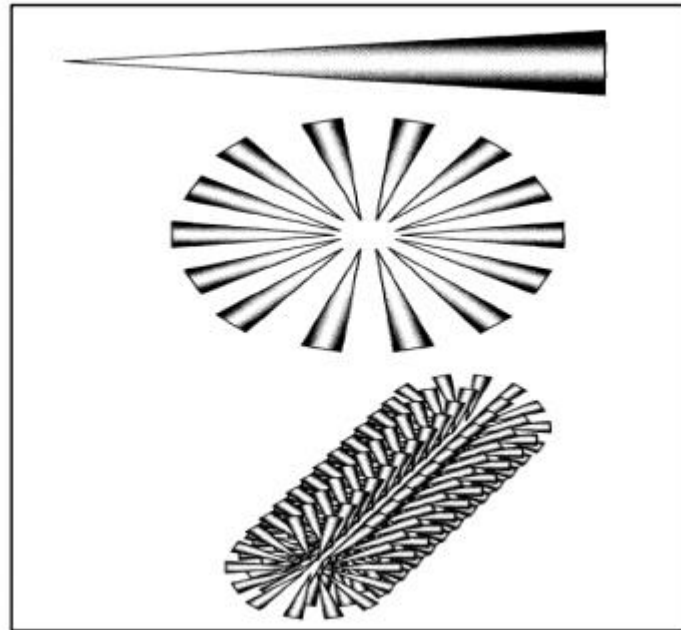


Fig (2.4) Self-assembly process to create nanofibers [30]

2.2.5 Electrospinning

To understand the basic principle of the electrospinning process, consider charged spherical drops of a thin molecular structure liquid that occur in a vacuum where the drop is under two effective forces :

- 1- centrifugal, electric force
- 2- surface tension Which seeks to keep the drop in a spherical shape

When balancing the two forces, describe the follows

formula:

$$\frac{1}{8\pi\epsilon_0} \frac{Q^2}{R^2} = 8\pi\sigma_s R$$

Where

Q is the electric charge present on the droplet's surface,

R is the droplet radius

ϵ : is a dielectric constant of the vacuum

CHAPTER TWO Theoretical Part and literature review

σ_s : is the surface tension factor [49]

With the increase in the strength of the electric field until it the voltage on the top of the droplet rises until it attains a critical point, when the repulsive force exceeds the surface tension. The drop decomposes into small charge droplets. This process is called electrostatic spraying. [49]

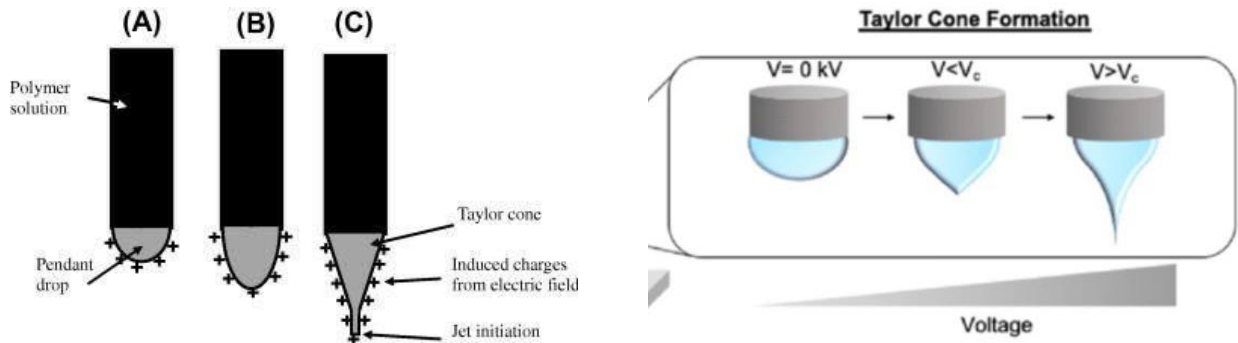
However, for higher molecular weight solution electrospinning occurs with increasing voltage applied to the surface of the liquid resulting in strong electric repulsive forces to overcome the surface tension and droplet extension. This occurs at a critical point on fluid flow. This is known as the eruption point of the Taylor cone. When the jet dries or hardens, the fibers remain electrically charged, [50] The current flow regime changes from ohms to convection when the charge moves to the surface of the fibers while the jet dries in air. Electrostatic repulsion, which starts at tiny bends in the fibers, causes the skin process that lengthens the jet until it is eventually deposited on the ground collector. This bending instability causes the fibers to elongate and soften, which results in the production of homogeneous fibers with nanometer-scale diameters [51]

There are three regions of nanofiber formation by electrospinning technique:

1. Initiation of jetting to extend the flow along the straight line, this region occurs at the beginning of the application of the voltage, the critical value and the formation of the Taylor cone.
2. instability and more prolonged curvature of the plane, allowing it to move in a circular path whose rings rise. This occurs in increasing the applied voltage to reduce the solution's surface tension

CHAPTER TWO Theoretical Part and literature review

3. Plane hardening in nanofibers. This happens when the jet from the needle (in the air) and the effective forces from the ohmic forces are translated into the surrounding forces



Fig(2.5) Taylor cone formation. Increase the voltage up equilibrium stage between the surface tension and strength of the electrostatic force at step

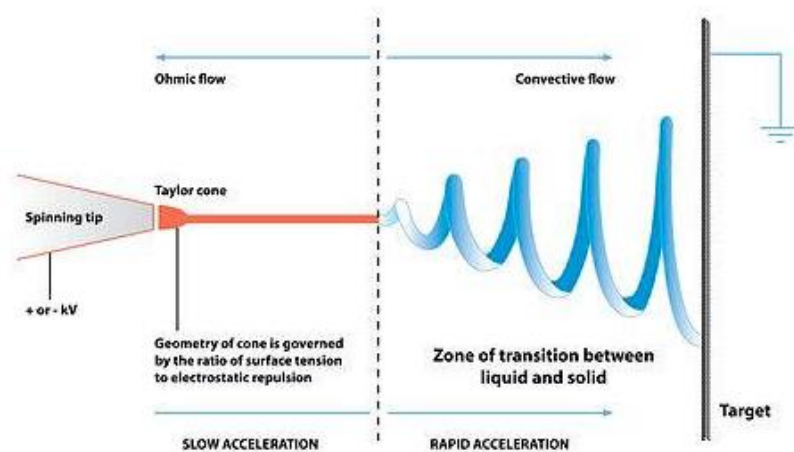


fig (2.6) the diagram of the fiber formation by electrospinning

2.3 Electro spinning set up

There are several experimental setups that have been developed for the production of nanofibers. Every preparation tries to produce woven or non-woven. [52-53]

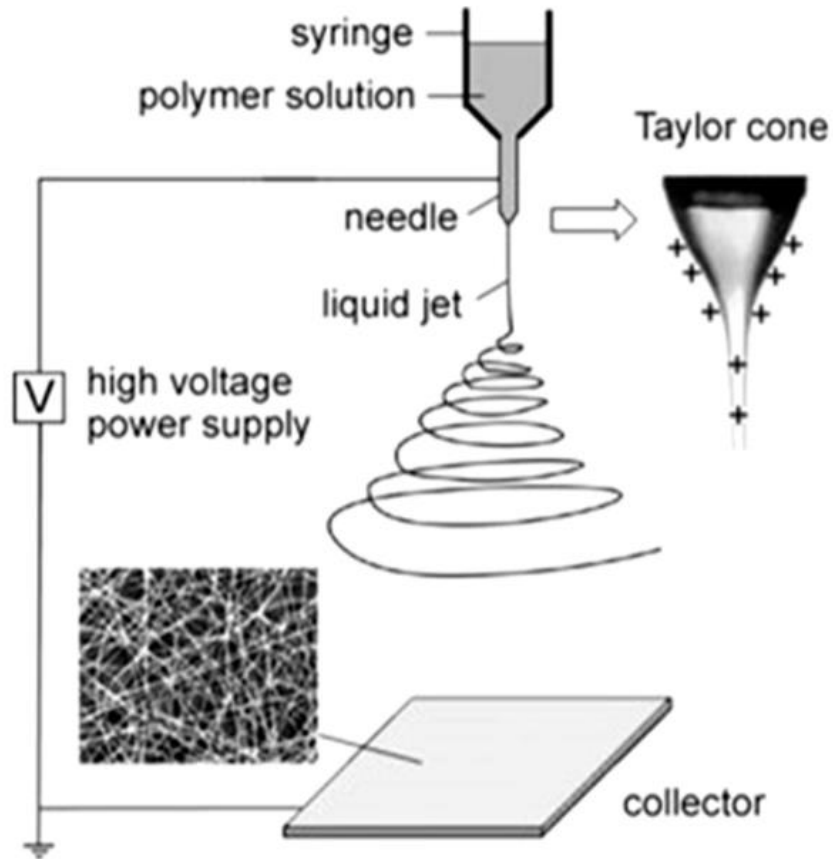
The basic electrospinning setup consists of three

1. high-voltage power components.

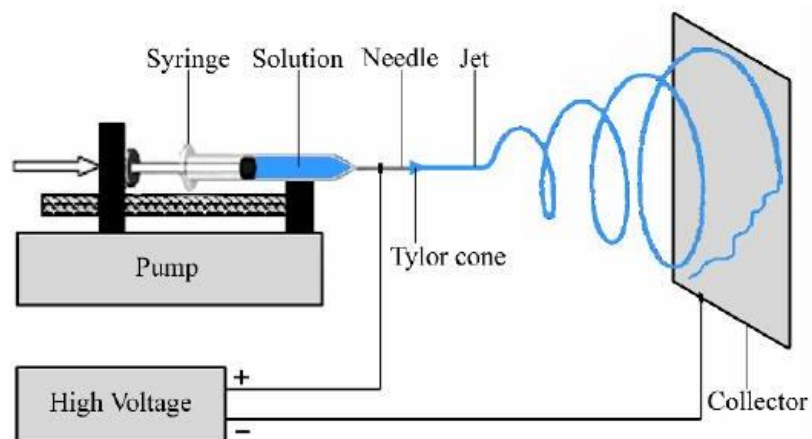
CHAPTER TWO Theoretical Part and literature review

2. Spindle (metal needle). Main: Source and Syringe pump

3. Collector (earthed conductor) as shown in fig

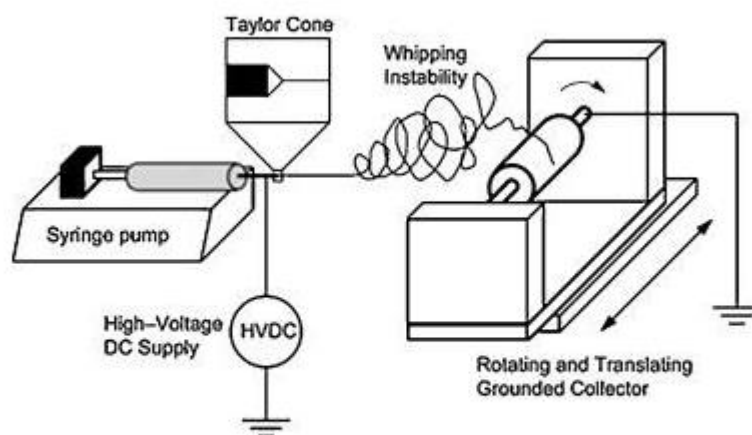


Vertical set up(A)



Horizontal set up(B)

Fig flat plate collector for non_alignment nanofibers



Fig(2.7) electro spinning set up with rotating cylinder collector

A common electrospinning setup is holding the liquid into a medical syringe with a metal needle of tiny diameter. To control the flow of fluids during the electrospinning process, this syringe is connected to a syringe pump.

To control the flow of fluids during the electrospinning process, this syringe is connected to a syringe pump. Typically, it is connected to the positive anode (electrode) of the HVPS, which is connected to the metal needle, and the negative electrode (cathode), which is connected to the metal target, which is connected to the ground [54]

2.4 Solution Parameters

These parameters include concentration, viscosity, surface tension, and electrical conductivity as in the following details:

2.4.1 Concentrations

The concentration of the polymer solution is crucial to the electrospinning process' ability to produce nanofibers. From low to high, there are four significant concentrations to be aware of:

CHAPTER TWO Theoretical Part and literature review

A- If the concentration is too low, micro/(nano) polymeric particles will be obtained.

B- If the concentration is increased to a slightly higher value, a mixture of beads and fibres.

C- can be observed with proper concentration, fine nanofibers can be obtained.

D- With increasing concentration to a very high value, you will notice microscopic fibers, helix, shape and fine streaks [55]

usually. If the solution concentration is suitable for electrospinning, the diameter of the fibers will rise as the solution concentration increases. In addition, the viscosity of the solution and its concentration are very close characteristics, that's why we can also control the viscosity by adjusting the concentration of the solution [55]

2.4.2 Viscosity

In general, the viscosity of the solution can be adjusted by adjusting the polymer concentration of the solution; Solution viscosity is the critical key in determining fiber morphology.

A- At very low viscosity, smooth and continuous fibers cannot be obtained.

B- The very high viscosity results from the difficulty of expelling the jets from the solution, and for this we need a suitable viscosity for electrospinning. [56]

Viscosity also affects the surface tension of a solution . For a low viscosity solution, surface be tension findings in beads; beaded fibres. If the solution has a suitable viscosity, continuous obtained[56]

2.4.3 Surface Tension

Surface tension, as a function of the solvent compositions of a solution, is a very important factor in electrospinning.

Different solvents may contribute to different surface tensions. With constant concentration, which reduces the surface tension of the solution, the bead fibers can be converted into fine fibers.

In addition, they also showed that the surface tension and viscosity of the solution can be reduced by changing the mass ratio of the solvent mixture. [57]

2.4.4 Electrical conductivity

The type of polymer solution, the type of solvent and the conductivity of the salt are mainly determined. In contrast to their synthetic counterparts, weak fibers arise when natural polymers, which are often electrolytes in nature, are exposed to extreme stress under an electric field where the ions increase and the polymer jet's capacity to transport charge [58]. Ionic salts like KHPO_4 , NaCl , etc. can also be added to the solution to boost its electrical conductivity. Ionic salts are used to create nanofibers with tiny diameters. The use of organic acids as solvents can sometimes produce extremely conductive solutions. [59]

2.5 Processing Parameters

2.5.1 high Voltage Power Supply: (HVPS)

(HVPS) represents the first component of electro spinning set up, used for generating high electrical force which is applied on the polymer solution to form the Taylor cone. This forms the Nano fibers diameter after increasing it to critical value and overcome on the surface tension of solution. [60]

In general, the effects of increasing applied voltage on fiber diameter and shape may be summarized as follows:

CHAPTER TWO Theoretical Part and literature review

1. Increasing voltage causes the electro rotating jet to extend further results in a raise in the columbics forces applied by the charges
2. The voltage increase causes the jet acceleration to increase, which reduces the electro spinning jet's flight duration.
3. Fiber diameters can be decreased by increasing voltage.
4. With adequate flight time, solid also grows [61].

AC HV and DC - HV can be used for electric resonance. Increasing the applied voltage causes the polymer jet to discharge with greater electrostatic repulsion, causing it to undergo higher levels of drag stress. The applied voltage will cause charges to accumulate on the droplet's surface, and with the applied electric field, it will result in the formation of a Taylor cone, with a jet of electrospinning solution shooting off from the tip of the cone.

The use of AC-HVPS prevents skin blistering and leads to better alignment of the nanofibers. There is also less problem with the use of alternating current - higher voltages than the DC voltage collector type. [62]

2.5.2 Pumping Rate:

The flow rate of the polymer solution within the syringe is another important process parameter ; The amount of solution available for the ES process will be determined by the feed rate, typically:

- a) Low flow velocity are ideal for giving solutions ample time to polarize.
- b) High flow rates cause an increase in fiber beads with thicker diameters.
- c) A quick drying process before the collector and minimal stretching stresses. [63]

2.5.3 Electro spinning Distance

The production and shape of the resulting Nano fibers appear to be less affected by the distance from the tip of the needle to the collection. [67]

CHAPTER TWO Theoretical Part and literature review

According to this method, the electrospinning range is between 5 and 15 cm; the 5 to 10 cm range has a considerable impact on the diameter and shape of nanofibers, whilst the 10 cm range has little impact. Typically, a short distance results in:

- 1) The solvent's incomplete evaporation accelerates the pace at which the resultant fiber may reach the collector.
- 2) Potential catalyst for the development of beads a nanofiber

With low distance , we increase HVPS value to maximum , form Taylor cone and consequ the formation of Nano fibers.[64]

2.5.4 .Capillary Tip Diameter

The utilizing of smaller diameter results in:

- 1- Reduce the development of beads by collecting less solution at the tip, which results in a smaller fiber diameter.
- 2- Additionally, a smaller droplet is produced by a smaller needle diameter, which results in a higher surface tension. For a fixed voltage, this implies that the fiber will have more time to stretch and elongate it before reaches the collector.

The acceleration of the jet decreases as a result of the increased columbic force needed to generate jet imitation at the same voltage provided, giving the solution more time to stretch and lengthen before it is collected [65].

2.5.5 .Collector Geometry Shape

There are many types of collector discovered for different application such as: wire mesh , pin , grids , parallel or gridded bar , rotating rods or wheel , liquid bath [66] fig the most widely used form of collectors

The Al foil conductor, used to collect the charged nano-fibers. However different application used different collector . [67]

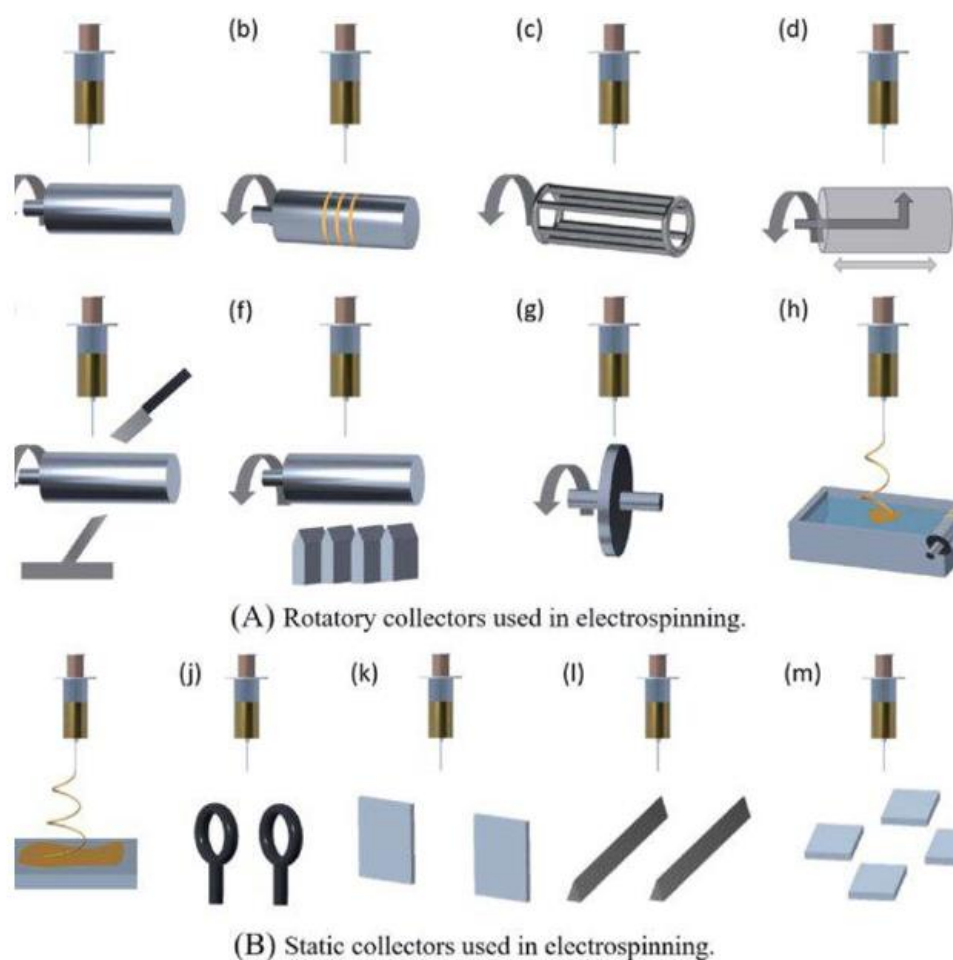


Fig (2.8) Collector type in electrospinning technique

A non - fiber material collector reducing the amount of being deposited with lower packing, but it can be used with AC - HV. Compared to non-porous collector plates, fibers produced using porous collectors have a lower packing density. In comparison to non-porous collector plates, the surface area of porous collector plates is enhanced, causing leftover solvent molecules to evaporate more quickly.

While a flat plate collector leads to a random collection of nanofibers, a cylinder rotational collector leads to nanofiber alignment [68-69].

2.6 Ambient Parameters: heat

The heating with a suitable range (45-60) C during the electrospinning process eliminates beads number in resultant nanofibers, Additionally, the

CHAPTER TWO Theoretical Part and literature review

inverse connection between solution temperature and viscosity is in favor of narrower fiber diameter [70].

2.7 For Eliminate of Beads Number in Resultant Nanofibers :

Beads are considered the main demerit of electro spun nanofibers. There are many factors affecting the occurrence of beads , such as the applied voltage , the viscoelasticity of the solution , charge density , and the surface tension of the solution , etc. [71]

There are three methods for eliminating these beads in electrospinning nanofibers as following:

2.7.1 Concentration:

When the polymer concentration is low, the products contain a lot of beads or microspheres, since because the process becomes electro spraying. Also , by increasing the polymer concentration it might be possible to decrease the numbers of beads and reduces the sizes of it [72]

2.7.2 adding a salt additive

The net charge density carried by the electrospinning jet is an important factor that greatly influenced the morphology of the electrospun products besides the viscosity and the surface tension of the solution. With increasing the net charge density , the beads become smaller and the shape became more spindle - like choosing [73]

2.7.3 Suitable solvent for electro spun products :

There are many possible factors influencing the morphologies in different solvents, such as volatilization rate, solvent polarity, solution conductivity, surface tension coefficient, solution viscoelastic behavior, molecular weight, chain entanglements, or ambient temperature . This shows that the optimal solvent system could be decided to reduce or even eliminate

CHAPTER TWO Theoretical Part and literature review

the by-products in the electro spinning process Additionally, the solvent system was very important to the efficiency in the electrospinning process [74]

2.8. Polystyrene

Polystyrene regarded as an aromatic synthetic polymer synthesized from monomer styrene [75]. Polystyrene may be solid or foamed. General purpose polystyrene is clear, hard, and brittle. Polystyrene regarded as a good barrier to oxygen and water and also has a lower melting point [76]. Structure of polystyrene consist from long hydrocarbon chain made from centered carbon atom with alternated phenyl group as shown in the Fig (2.12) [77].

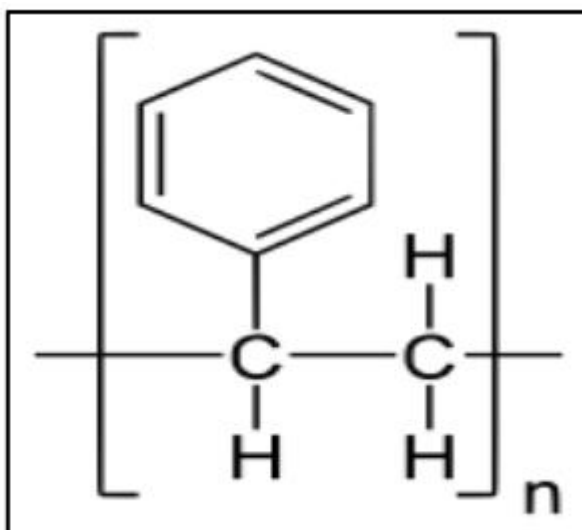


Fig (2.9) Polystyrene structure [77]

Polystyrene produces from the addition polymerization of styrene monomer, in which the carbon-carbon (π -bonds) of the vinyl group will break and form new carbon-carbon (σ -bonds) as shown in the Fig (2.10) .

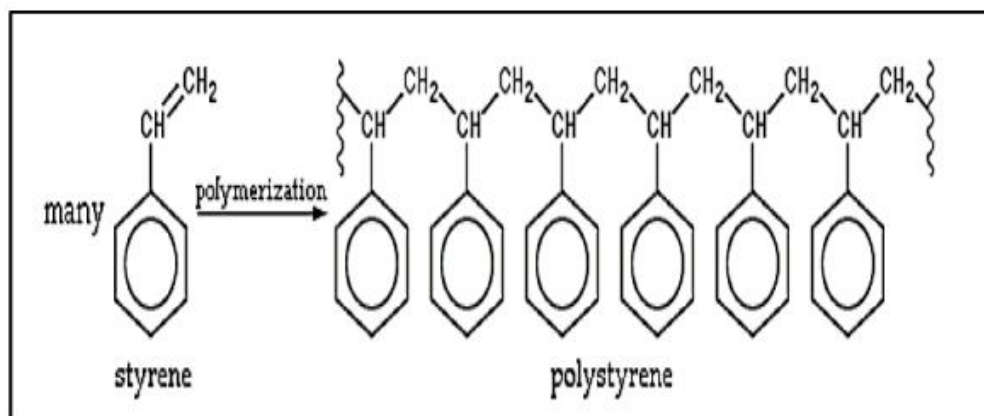


Fig (2.10) Polymerization of polystyrene [78]

According to the position of phenyl group around the carbon chains of polystyrene there are three tacticity structures (the isotactic structure syndiotactic structure atactic structure) as shown in the Fig (2.11), each one of them has different properties from the other types [79].

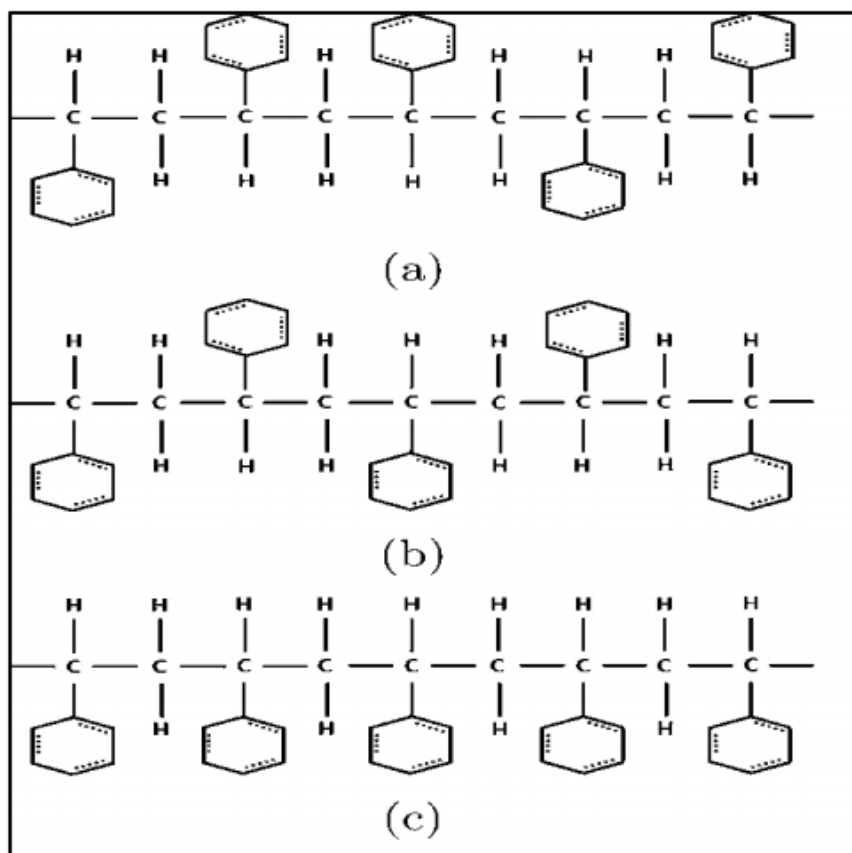


Fig (2.11) Stereochemistry of (a) atactic, (b) syndiotactic, and (c) isotactic polystyrene [80]

CHAPTER TWO Theoretical Part and literature review

Polystyrene has a wide range of applications in our life such as I food packaging, laboratory, electronics, automobile parts, toys, medical uses, petri dishes, egg cartons ...etc.[79].

2.9 Polyvinylidene fluoride (PVDF)

Vinylidene difluoride is converted into polyvinylidene fluoride, often known as polyvinylidene difluoride (PVDF), an actually non thermoplastic fluoropolymer.

In applications needing the utmost purity as well as tolerance to solvents, acids, and hydrocarbons, PVDF is a speciality plastic employed. PVDF has a low density (1.78 g/cm³) when compared to other fluoropolymers, such as polytetrafluoroethylene (Teflon), and its structure is shown in fig. (2.12) [81].

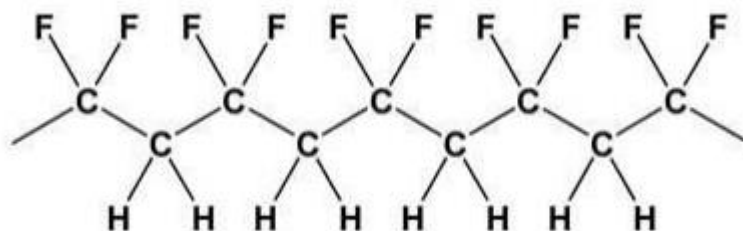


Fig (2.12):PVDF structure [81].

And there are several uses of PVDF such as [82].

- 1) A semi-crystalline polymer with around 50% amorphous material. Its structure is extremely regular, with relatively few monomer units connected head-to-head and the majority of PVDF units attached head-to-tail.
- 2) PVDF has the highest heat dispersion temperature under load while having the lowest boiling temperature of the commercial fluorothermoplastics.

CHAPTER TWO Theoretical Part and literature review

3) PVDF has a comparable tensile properties but lower impact strength. It also has a lower modulus but higher flexibility and specific stiffness.

The application of (PVDF) can be clarified as [82].

1- Electrical and electronic devices are utilized in the aviation and electronics industries for wire insulation and cable jacketing, industrial control system systems, high temperature wiring, etc.

2- PVDF is utilized extensively in filtering and separation machinery (filters, membranes, housings).

3- Piezoelectric plates are very responsive transducers with a wide range of uses. These films may be shaped into distinctive shapes, are robust, light, and flexible, and can be attached with common adhesives.

4- Corrosive material resistance is required by energy-intensive sectors, automotive, military aviation, and petrochemical industries. These industries all use PVDF-based seals, gaskets, and linings.

2.10. Applications of nanofibers

There are many different applications of polymeric nanofibers in many fields such as applications found in cosmetics, military, filtration, industrial, sensors. as shown in Fig (2.13).

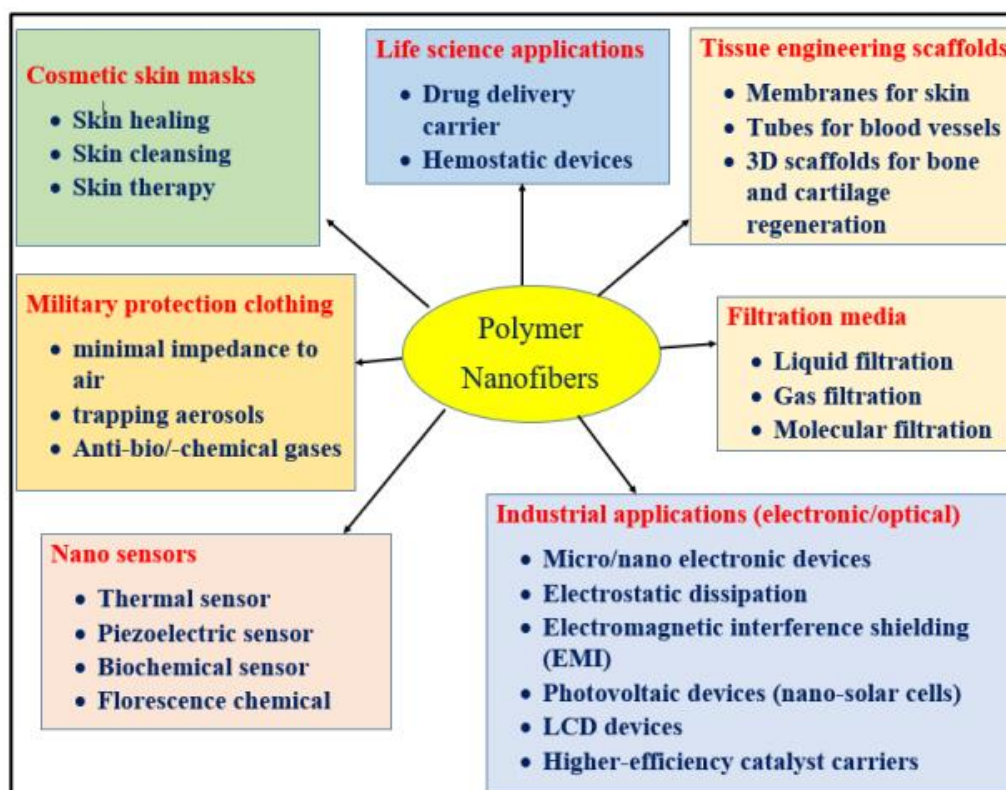


Fig (2.13) Applications of polymeric nanofibers [47]

2.11 Literature Review

goes back to the beginning of the process of electrospinning in the fifteenth century AD when Gilbert observed that when an appropriately charged piece of amber was approached near a drop of water, it formed a conical shape and a small drop came out, from the end of the conical hook although the term "electro spinning" ', derived from "electrostatic spinning", was used relatively recently (around 1994), but its basic idea dates back more than 60 years. From 1934 to 1944, formallas published a series of patents, after 1950 this process developed and expanded greatly, and many studies appeared on the nature and factors affecting it [83] - [90].

In 2004, Qingbiao Y.et al. The . Experimentally observed the effect of different solvents on the shap and morphology of micro/nano poly(vinylpyrrolidone) (PVP) fibers that were prepared by electrospinning, these different solvents, included ethanol, dichloromethane (M C and N, N-

CHAPTER TWO Theoretical Part and literature review

dimethyl formamide (DMF)). PVP fibers made from MC and DMF solvents have a bead-on-chain form when manufactured using 4 wt% PVP solutions. In contrast, ethanol was used to create smooth PVP nanofibers, despite the fact that the fibers' size dispersion was somewhat increased. The tactic of exploiting mixed experimental findings may be employed to create PVP nano-fibers with tiny diameters and narrow size distributions. Results indicated that when the ratio of DMF to alcohol was 50:50 (w/w), regular cylinder PVP secondary fibers with a diameter of twenty nm were created. These tiniest nanofibers were produced as a result of the interaction between the charge distribution of the polymer jet, the viscosity of the ethanol solution, and the DMF solvents. Additionally, intriguing helical fibers were produced by combining a 50:50 (w/w) solution of 20% PVP with ethanol. [97] By using scanning and scanning electron microscopy (SEM) methods,

Chdchaok.M., et al. (2004) investigated the effects of solution factors such as viscosity, surface tension, and conductivity on the morphology and average size of PA-6 fibers. The diameter of nanowires and the shape of the fiber were discovered to be significantly influenced by these variables. Solution viscosity was determined to have the most impact out of these three factors. Beadless fiber production required suitably viscous solutions, or solutions with high concentrations. When m-cresol and formic acid were combined to function as a given solution for 6-PA, the solutions' viscosity increased, causing the fiber diameters of the 6-PA fibers with greater molecular weights to look bigger in diameter. [98]

Xiaoyan y.et.al.(2004) Bisphenol-polysulfone (PSF) nanowires were created by electrospinning PSF solutions at high voltages in a solution of acetone and N,N dimethylacetamide (DMAC). The quantity of acetone inside the mixed solvents and the percentage of PSF electrospun fibers inside the polymer solutions both had an impact on the form and size of the

CHAPTER TWO Theoretical Part and literature review

electrospun fibers, according to the results of electron microscopy. The input power, fluid velocity, and needle-collector distance were crucial processing variables for regulating the shape of the electronically spun PSF fibers. By electrospun a solution of PSF DMAC/acetone 20 (wt%) (1: 9 = DMAC: acetone) at a voltage of 10-20 KV for an hour, capillaries - the screen distance was 10 cm, and PSF nanowires with a size of 300-400 nm may be produced [99].

In 2005, Zhang C. et. al. The . Poly(vinyl alcohol) (PVA) fiber mats were prepared by electrospinning of aqueous PVA solutions at a concentration of 6-8%. SEM was used to study the morphology of nanofiber diameter, impacts of work factors such as voltage, goal terminal distance, flow rate, and solution parameters focusing on electrospun PVA fiber shape. The findings demonstrated that the tip-target distance did not significantly affect the fiber morphology when employing PVA with a high level of hydrolysis (DH) of 98%, but that the morphology may be marginally modified by varying the solution flow rate. The electrospun Pvp fibers showed a broad diameter dispersion at high voltages exceeding 10 KV. The morphology changed from stitched fibers to regular fibers with an increase in solution concentration, and the fiber diameter grew from 87 + 14 nm to 246 + 50 nm. Additionally, it was discovered that due to the variable conductivity of the solution, the surface tension, and viscosity, the additions of table salt and ethanol had a substantial impact on the size of the fibers and the production of electrically spun PVA fibers [100].

Huang et. al. The in 2006 Electrospinning was used to create nylon-4,6 nanofibers with sizes between 1 nm and 1 m. Changing the amount of the polymer solution altered the fibers' diameter. Electrical tape-like fibers with a band width of around 850 nm were created by electrospinning a concentrated solution of up to 20 weight percent nylon and 4.6 weight

CHAPTER TWO Theoretical Part and literature review

percent formic acid. The lightest Nylon 4.6 nanofibers, with widths of 1.6 nm or less, are produced at a semi-dilute level of 2% Nylon - 4.6 by weight. To prevent the production of awl nanofiber, a little quantity of pyridine was added to the electrospinning solution. using low-concentration electrospinning. nano fiber sizes were determined using scanning and transmission electron microscopy [101].

Also, J. Hana et.al. (2006) and others. Nylon 6 Nano filters were created using nanofibers with a diameter of 80-200 nm, and the filtration effectiveness and pressure drop across the filter were assessed. These conditions were researched and adjusted for nanofiber manufacture in the year (2006) utilizing 6 Nylon. When the concentration is increased to 24 wt.%, the diameter progressively thickened to 200 nm, but there are no beads, whereas 80 nm was obtained with a 15. wt% dosage, but there are numerous beads. Thinner nanofibers are created and more fibers are gathered in the complex at the shortest spinning distance. Six nylon filters have a 99.993% efficiency. [102]

Goki E. et.al. The in 2007 He looked at the grain-to-fiber transition, or morphological shift, of electrospun polystyrene, which has a molecular weight range of 19300 to 1877000 g/mol. To investigate the impact of solvent characteristics on morphological variety, tetrahydrofuran, N, and N-dimethyl formamide were utilized as solvents. The morphology of the granules and the nanofibers was significantly influenced by the solvent characteristics and polymer molecular weight. The distribution and diameter of the fibers revealed that the effects of solvent and molecular weight could be independent. As predicted, the critical concentration at which primary and full fibers could be seen showed a considerable decline with increasing molecular weight. For solutions of medium to high molecular weights (>100000 g/mol), the influence of solvents on these make content was less

CHAPTER TWO Theoretical Part and literature review

pronounced. During electrospinning, the quick hardness of the plane that was anticipated to happen with concentrated forms may be crucial to the development of stable fibers. [103]

The Jianfen Zed et. al. Through electrospinning, he investigated the control of a few factors on PVDF nanofibers. Electrospinning was used to create fibrous PVDF films with fiber diameters ranging from 100 nm to several μm , and it also allowed for the simultaneous modification of the crystalline of the electrospun PVDF fibers. PVDF fibril films comprising mostly α -, β -, or γ -phase may be effectively manufactured by regulating electrode materials parameters such as solvent, electrode heat, feed rate, and tip-to-collector distance. [104]

Haitao z.et al. published The in 2008. In order to create secondary polyurethane (PU) fibers, electrospinning is used. The authors extensively monitored and investigated process variables such as applied voltage, feed rate, and solution concentration. The findings shown that the ultrafine diameters of the nanofibers made from electrospun PU/N,N-dimethylformamide (DMF) solutions range from 700 to 50 nm. Additionally, it was discovered that the process parameters had a considerable impact on the diameters and shape of natto fibers. Particularly, the diameters grew as solution concentrations rose. In the end, it is determined that uniform PU nanofibers free of beads or crimping may be created by electrospinning when proper process parameters are followed, such as 5.0–7.0 weight of PU/DMF solutions, 10-15 KV applied voltage, and 0.06–0.08 mm/min feeding rates. [105]

Additionally, Tan J. et. al. produced polymer micro/nano fibers using conventional and electrophoretic modified techniques (2008). The micro chord forms of electrically spun micro/secondary fibers have been studied using scanning electron microscopy (SEM), and micro/nano fibers produced

CHAPTER TWO Theoretical Part and literature review

by conventional electrospinning are often gathered in the form of nonwoven mats without structural orientation. But simply altering the electrospinning setup's collector, the produced polymer fibers displayed more or less aligned topologies. This study discovered that the alignment of the micro/nano fibers is significantly influenced by the electrostatic force generated by the discrete electric field. [106]

M. Dhanalakshmi (2008) has successfully created NATO nylon 11 fiber mats using electrospinning from a formic acid solution. Scanning electron microscopy (SEM) analysis of the shape and diameter of the resultant nanofibers revealed that secondary fibers with uniform diameter were created at a polymer concentration of 10% w/v, whereas tapes were formed at a greater concentration. X-ray analysis (XRD) of the nanofiber mats' crystal structure revealed that the mats 1 crystallized, as shown in Fig 7. Differential scanning calorimetry (DSC) was used to study the subsequent crystallization, and it was discovered that the electrophoretic spun fibers that were seen had formed on top of the liquid crystallized samples. The spun electrode fibers' crystallinity, however, was lower compared to the solution-crystallized sample (Fig.) [107].

In (2009), Lilia M. Guerrini, et.al , Poly(vinyl alcohol) (PVOH fibers) were studied by electrospinning. Non-woven films (mats) were produced from secondary PVOH fibers by electrospinning PVOH solutions in water with and without aluminum chloride. When using SEM to analyze mat morphology, a 12.4% PVOH/water solution concentration was utilized. (DSC) previously Wide angle X-ray diffraction was used to assess the thermal characteristics, degree of crystallinity of the nanofibers, and crystal structure of the mats. By electrospinning a PVOH/water mixture with aluminum chloride at (45% w/v, 3.0 KV/cm applied voltage), the best nanofibers were produced. It was discovered that the average lengths of the

CHAPTER TWO Theoretical Part and literature review

nanofibers decreased as a result of the introduction of aluminum chloride and an increase in the applied electric field. Mats devoid of aluminum chloride exhibited greater melting points and levels of crystallization than mats containing salt. It was discovered the monoclinic mats' crystal structure. The mats did not exhibit a high degree of crystallinity, nor were they strongly orientated. [108]

Solvent mixtures, Marcia C. et. al. The . In 2009, two different types of chloroform/dimethylformamide (DMF) and chloroform/acetone, at concentrations of 40/60 V/V, were used to form electrospun poly (D,L-lactic acid) (PDLLA). The effect of solvent type, solution concentration, morphological treatment conditions and properties of electrospun mats were studied. The resultant nanofibers were examined using wide-angle X-ray diffraction (WAXD), wide-angle X-ray diffraction (SEM), and DSC. The lowest diameters of nanofibers (5 wt%/vol.1.0, PDLLA KV/cm) were achieved from both mixes of electric field solutions. In general, the diameters of the nanofibers produced by the chloroform/DMF mixture were smaller than those produced by the chloroform/acetone mixture. The latter were porous, whereas chloroform/DMF combination nanofibers were not. Irrespective of the solvent composition, all PDLLA nanofibers have a very low crystallinity and are made up of very tiny, crooked a3 and a3 crystals. [109]

In 2010, Muhammad C. et. al. The . studied the ultra-fine 6 Nylon nanofibers produced by electrospinning of nonwoven nylon 6 mats that were generated from a solution of different concentrations. The effect of (viscosity, surface tension, electrical conductivity of the polymer solution, applied electric field and aggregation distance) was studied, and it was proved that the diameter of the electrically spun fibers was affected by the parameters of theses. Smaller diameter nylon 6 nanofibers can be produced

CHAPTER TWO Theoretical Part and literature review

with a lower concentration of polymer solution (15 wt%), but no uniform/punched fibers were used due to the increased concentration of the solution (20 wt% - 25% wt), then viscosity exceeding the critical value led to the formation of Smooth fibers with larger diameters (924 nm to 1071 nm). The applied voltage (12 KV to 18 KV) yields thinner fibers (1211 nm). Advice for assembly distance and flow rate also affected the production of uniform fibers. Thinner fibers with a larger distance (900 nm) and hydrated short-range fibers with a flat cross-section were obtained. The higher flow rate (0.300 ml/hr) resulted in the production of large diameter nanofibers. The concentration of the polymer solution is 20 by weight. %, applied voltage is 15 KV, volume feed rate is 0.20 ml/hr and rotation distance is 8 cm. These optimal parameters can produce uniform 924 nm diameter Nylon-6 nanofibers. [110]

In 2010 Kheybari S. et .al. The . Silver nanoparticles (NPS) were prepared by chemical reduction for antibacterial applications.. UV spectroscopy is used to examine the formations of silver NPs. The antibacterial activity of silver NPS was evaluated by determining the minimum inhibitory concentration (MIC) against Gram-positive (Staphylococcus Aureus and Staphylococcus Epidermisis) as well as Gram-negative (Escherichia Coli and Pseudomonas aeruginosa), the results indicated the production of (NPS) of 50 Nanometer is a very effective anti-bacterial for both types. [111]

Danielle M. (2011) also created two types of anti-microbial and bio-fouling nanofibers for water filtration and compared (PVA) and (PAN) fibers with silver nanoparticles (morphology). scattered electron images revealed that silver nanoparticles in PVA nanofibers are more evenly distributed. These measurements included silver nanoparticle content, physical distribution of silver nanoparticles, and levels of platinum leaching from of

CHAPTER TWO Theoretical Part and literature review

the fibers throughout water, which can imply toxicity and, most importantly, antimicrobial efficacy. However, PAN nanofibers have a larger percentage of silver nanoparticles than do comparable non-PAN nanofibers. Energy-dispersive X-ray (EDX) study proved this. Silver nanoparticle-containing PVA and PAN nanofibers show outstanding antibacterial properties. There are also two types of nanofibers that do not leak from a substance other than silver to water. [112]

In 2011, Hong, S. et al. produced composite nanofibers by spinning nano particles in a nylon solution using an electric spindle. They next examined the various characteristics of the electronically spun fibers. They discovered that adding silver nanoparticles was a good way to enhance the antibacterial properties of the composite nylon fibers. When variables like solution concentration and silver nanoparticle quantity was altered, it had a substantial influence on the average fiber length and fiber shape. They might utilize the hybrid fibers they created as filter membranes. [113]

In 2012, Sencadas et. al. The investigated the electrospinning technique used to create nanofiber mats from chitosan. In this study, trifluoroacetic acid and dichloromethane solutions were used to make electric chitosan mats, which helped to alleviate the concerns mentioned above. We were able to create mats with sub-micron homogeneous fibers. Without beads. Additionally, the solution's impact on various process parameters' effects on the average fiber diameter and the breadth of the fiber size dispersion were assessed. In this investigation, the applied voltage, travel characteristics, and solvent installation needle diameter were all taken into account. [114]

Additionally, the effect of salt production during polycondensation reaction on electrospinning super-aramid fibers was investigated by Hyun j.et al. The. (2012) in addition to creating a spider web-like structure in the mat. The addition of a salt (CaCl₂) increased the amide epitaxial solution's

CHAPTER TWO Theoretical Part and literature review

electronegativity and resulted in the development of a matting structure resembling a spider web. The influence of the solutions and the voltage on the development of the fibrous structure resembling a spider web was investigated. According to the SEM photos, the mats' thick, spider-like strands were present throughout. Analysis in [115] revealed CaCl₂.

In 2013, z.li et.al. increase the li tre of the carpet working parameter on the resulting Nanafabers • Electrospinning. These parameters can be divided into molecular weight, viscosity, tension parameters of the solution (surface charge), process parameters; Voltage, collectors, flow rate, syringe distance and ambient parameters including (humidity) and these parameters, through appropriate control of these parameters, can affect the shapes of electrically spun fibers with spun shapes and diameters. [116]

In 2014, Ngadiman et. al.review effect coefficients by electrospinning technique concentration, spin distance, applied voltage, and volumetric flow rate, to the diameter of the nanofibers during the electrospinning process.It was concluded that the volume flow rate of the fibers is proportional to the fibers' diameter while there was no agreement in reports on other parameters. [117]

In addition, during 2014, new therapies such as the use of intentional liquid to improve the diameter of nanofibers emerged, Deng – GuangY. et.al. The Some solvents are deliberately used as liquids in electrospun ethyl cellulose (EC). With 24 EC % w/v in ethanol as the electrode core liquid and pure solvents including methanol, ethanol, N and N-dimethylformamide (DMF) as sheath fluids, EC nano-fibers were produced by the modified processes. The redesigned procedure was successful in enhancing the grade of nanofibers in term of nanofiber sizes, distributions, and structural homogeneity, as shown by the observations made using a FESEM microscope. The careful selection of jackets solvents appropriate for the

CHAPTER TWO Theoretical Part and literature review

procedure of drawing out the principal EC fluid throughout electrical circulation was essential to the improved axial process. Using a sensible coating solvent choice that takes into account the boiling point of the solvents, the diameters of nanofibers D (EC, nm) may be handled. [118]

In a work that was inspired by the "lotus effect," Zhou et al. published in 2016, they combined electrospinning and weaving technologies to create nanofiber textiles made of polyvinylidene fluoride (PVDF), polyethylene glycol (PEG), and silicon dioxide (PVDF/PEG/SiO₂). Hierarchical nanotube surfaces in Polypyrrole and PVDF/PEG/SiO₂ nanofiber textiles are produced by hydrolyzing PEG and doping using SiO₂ nanoparticles, and are comparable to the surface structure of a lotus leaf. Using field emission scanning electron microscopes (FESEM), FTIR spectra, and thermogravimetric analysis, the mechanical properties and wettability of these three fabrics are examined (TGA). The findings show that after water scrubbing, the SiO₂ nanoparticle-doped PVDF/PEG composite nanofiber has a fiber structure made up of many balls, which are produced by the Nanoparticles embedding inside the polymer. The "ball" also resembles the "hill" of a lotus leaf surface and the "small thorn" on the "hill" due to the distractions and interruptions of SiO₂ nanoparticles on its surface. The ultimate tensile strength and breakdown strain of the PVDF/PEG/SiO₂ nanotube fabric are 92.12 MPa and 18.98%, respectively. The PVDF/PEG/SiO₂ nanotube fabric is very hydrophobic, with a contact angle with water of 173.2° [119].

In order to increase the mechanical properties of PS, Yoon et. al. carried out a study in 2017 that combined polyamide 6 (PA6) with PS utilizing multi-jet electrospinning. The blend internet's content ratio was determined via confocal microscopy analysis and chemical immersion testing. Each syringe included the same quantity of fiber that was required for PA6 and

CHAPTER TWO Theoretical Part and literature review

PS, respectively. It was investigated how content ratio affected web form, heat resistance, tensile behavior, permeability to air and water, and surface hydrophilicity. Investigations were also done into how the ambient humidity affected the electrospinning process' three-dimensional (3D) web structure. Larger cracks and corrugations could be seen on the PS web's surface that was produced with more humidity. Surface porosity and roughness were shown to promote hydrophobicity [114].

In 2018, Altan, et al. produced composite nanofibers from zein and poly (lactic acid) (PLA) by incorporating carvacrol at three different concentrations (5, 10 and 20%) using electrospinning. The field emission scanning electron microscope (FE-SEM) images showed that bead free fibers were obtained from zein and PLA polymer solutions containing carvacrol at different concentrations. The Fourier transform infrared (FTIR) spectroscopy, thermogravimetric analysis (TGA), Antioxidant activity, and antimicrobial test. The results showed that carvacrol was encapsulated in nanofibers from zein and PLA. The antioxidant activity of carvacrol loaded zein fibers ranged from 62 to 75%, while antioxidant capacity of PLA fibers varied from 53 to 65% for 5 to 20% carvacrol content. The composite nanofiber from zein and PLA at 20% carvacrol content inhibited 99.6 and 91.3% of the growth of mold and yeast. Carvacrol- loaded nanofibers with antioxidant and antimicrobial properties can be used to extend the shelf life of fresh foods as a new approach to electrospun fibers in food applications [115].

In 2018, Yue et al. produced nanofibers from solution of carboxymethyl chitosan and polyoxyethylene (CMCS/PEO) by using electrospinning technology. The purpose of this study is to explore the potential application of electrospun (CMCS/PEO) nanofiber membranes in fruit preservation. The microstructure, antibacterial activity, hydrophilic, and air permeability of the nanofiber membrane have been tested. For compared, the fresh-keeping

CHAPTER TWO Theoretical Part and literature review

effects of typical conventional coatings and CMCS/PEO nanofiber membranes on strawberries' rotting rate and weight loss were studied. The CMCS/PEO nanofiber membrane exhibited antibacterial capability to both *Escherichia coli* and *Staphylococcus aureus*. The measured gas permeability was on a scale of 40–50 mm s⁻¹ in the 200 Pa for nanofiber. These results showed that the CMCS/PEO nanofiber membrane might be used as a fruit packaging material. Compared with typical conventional coatings. Additionally, the composite 43(CMCS/PEO) nanofiber membrane is non-toxic and edible, making it suitable for application in the food industry [116].

A research on the electrospinning method for making Poly Monomer (PS) Nano filters for cleaning sand water from dumps and keeping the quality of the generated water was published in 2019 by Jawad et. al. A 4 m thickness filter was produced by electrospinning an 18% con. of (PS + methyl formamide DMF) liquid on a metal surfaces for 10 hours. Testing on this filter has included scanning electron microscopy, thickness measurement using a digital micrometer, and contact angle measurement with a contact angle shape drop analyzer. The water sample is also tested for viscosity, surface tension, volume, PH number, etc sample weight after the wastes have been removed from it by creating a nano filter. The produced filter has a hydrophobic characteristic, according to the results [117].

In 2019, Alehosseini et al. produced nanofibers from protein such as (gelatin and zein) loaded curcumin by electrospinning to make an effective coating for food packaging. Green Tea Extract (GTE) has been added to formulations to evaluate its effects on the stability, protective ability and release properties of curcumin from the fibers. Due to the low solubility of curcumin in aqueous solutions, it is combined with liposomes to facilitate incorporation into gelatin fibres. The addition of GTE resulted in strong interactions with proteins, and in the case of gelatin in particular., it

CHAPTER TWO Theoretical Part and literature review

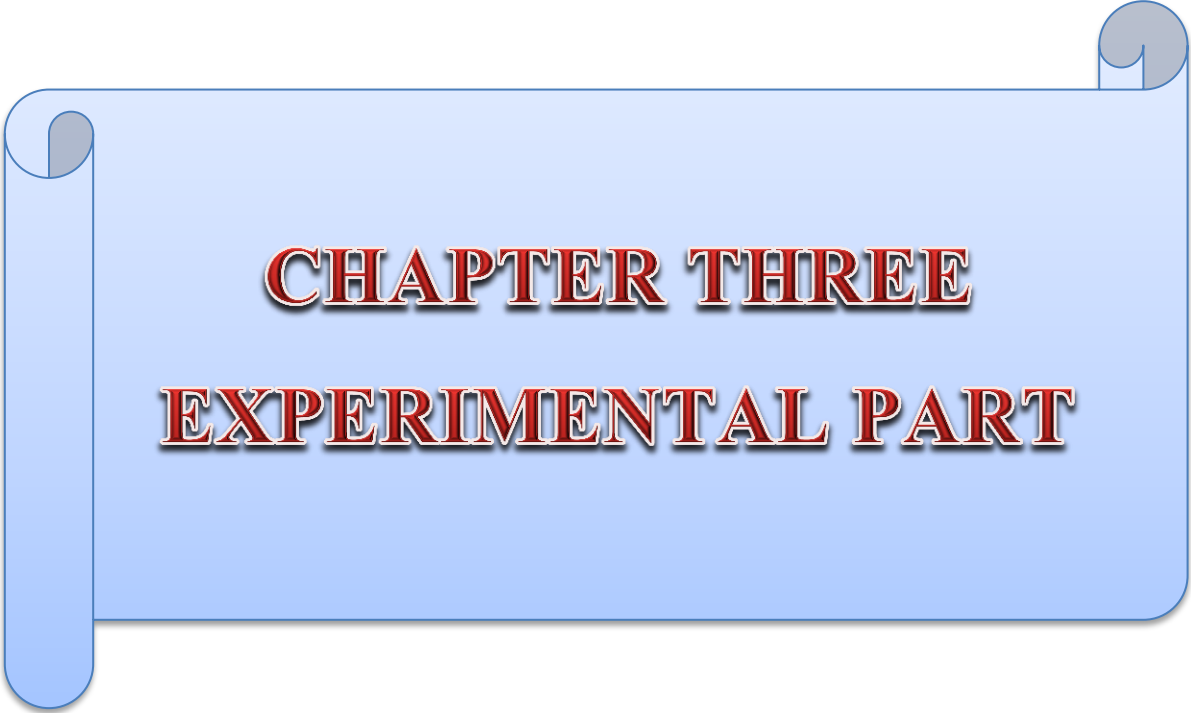
improved the protective effect and slowed down the curcumin release from the fibers, although it did not prevent their collapse in water. the incorporation of GTE into the zein structures did not produce any significant improvements. The higher stability of the zein fibers in water and their better release performance in the polar food simulant. Were studied using by scanning electron microscopy (SEM), Fourier transform infrared (FTIR), Small angle X-ray scattering (SAXS), thermal gravimetric analysis (TGA), and transmission electron microscopy (TEM). The results showed the developed gelatin coatings a promising release behavior in contact with fatty food, and zein-based coatings would be more adequate for packaging of high water content food products. The coatings can be optimized for packaging structures in contact with more hydrophilic or hydrophobic food products by selecting the suitable protein matrix [118].

In 2019, Somsap et al. produced antibacterial nanofibers by the electrospinning method of polymeric solutions from chitosan (CS), cellulose acetate (CA), and gelatin (G) were blended at a volume ratio of 4: 1: 5, with the incorporation of eugenol at different concentrations of 0–10% v/v into the mixed polymers solutions. Scanning electron microscopy (SEM) showed that the average diameter after entering the eugenol ranges from $(152.32 \pm 41.48 - 288.92 \pm 77.69 \text{ nm})$. the diameter increases with the increase in the eugenol concentration, were using Differential scanning calorimetry (DSC) analyses, release of the eugenol from nanofiber and Antibacterial test. The results showed that the release of eugenol was related to eugenol diffusion through the polymer and/or erosion of the polymer, and Thermal analysis proved better thermostability when the concentration of eugenol was less than 5.0% (v/v). The CS/CA/G electrospun nanofiber mats with incorporated eugenol were better in controlling *Salmonella typhimurium* and *Staphylococcus aureus*. This approach may effectively extend the shelf- life

CHAPTER TWO Theoretical Part and literature review

of food with potential applications in active food packaging and others products [119].

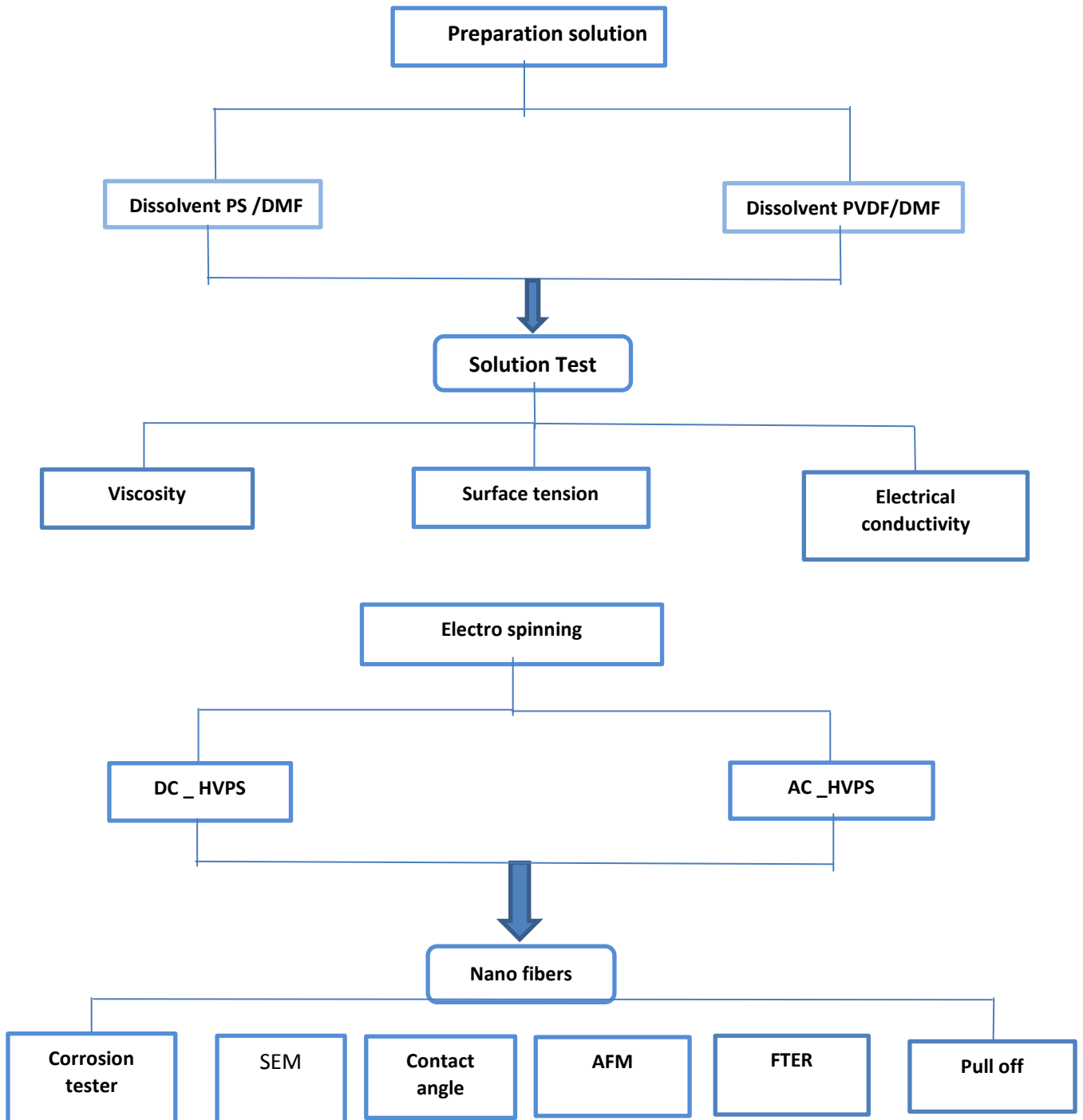
In 2021, Wang et al. produced nanofibers from gelatin/zein (G/Z) loading with different ratios of perillaldehyde (P) by using electrospinning method. The morphology showed that the G/Z/P film had a uniform microstructure and a nano diameter at a weight ratio of 5:1:0.02 (G/Z/P). The results of FTIR and XRD indicated that these three ingredients had good compatibility and strong interaction via hydrogen bonding. water contact angle results showed that the G/Z/P films gradually change from hydrophilic to hydrophobic with the increase of perillaldehyde. Thermal analysis indicated that the G/Z/P (5:1:0.02) film has good thermal stability. Antibacterial and storage analysis indicated that G/Z/P (5:1:0.02) film is effective to inactivate *Staphylococcus aureus* and *Salmonella enteritidis*, and obviously reduces the increasing rate of total bacteria counts and volatile basic nitrogen of chicken breasts. The results tests for the stability, morphology, and antibacterial activity of the different prepared films indicated that G/Z/P (5:1:0.02) has a potential application in antibacterial food packaging [120].



CHAPTER THREE
EXPERIMENTAL PART

Experimental Part

3.1 Introduction: The experimental program for this thesis is depicted in the diagram below:



3.2 Materials used**3.2.1 General purpose Poly Styrene (GPPS)**

Polystyrene grains with a purity of 99% were obtained from American polymers services Inc. (APS) made in the USA, general properties of polystyrene illustrated in table (3.1). according to cas.no. [9003-53-6]

Table (3.1) General purpose polystyrene Properties.[77]

| no | Property | Information |
|----|-----------------------------------|--|
| 1 | Melting point | 180-260 °C |
| 2 | Density | 1.04 - 1.05 g mL ⁻¹ |
| 3 | Thermal conductivity | 0.35 W/m.K |
| 4 | Tensile strength break at 23 c | 47MPa |
| 5 | Solvents | Benzene, toluene, DMF, Chloroform, cyclohexane, THF |
| 6 | Volume resistivity | > 6 * 10 ¹⁵ |
| 7 | Dielectric strength | 2.1 - 3.5 V/mm *10 ⁴ |
| 8 | Dielectric constant | 2.20 – 2.35 n/a |
| 9 | Processing temperature | 170 – 240 °C |
| 10 | Continuous service Temperature | -73 – 82 °C |
| 11 | Molecular Weight(MW) | 290,000 |

3.2.2 Polyvinylidene fluoride (PVDF)

Vinylidene difluoride is converted into polyvinylidene fluoride, a semi-crystalline thermoplastic fluoropolymer that is stable. The PVDF starting material employed in this investigation is a powder that is white in color. Table provides details on the physical characteristics of PVDF (3.1) according to cas.no.[24937-79-9]

Table (3.2) The Physical Properties of PVDF [121]

| Property | Value |
|--|----------------------|
| Melting point (T _m) | 177 C |
| Glass transition temperature (T _g) | -40 C |
| Molecular weight (M _w) | -534.000 g/mol |
| Density | 1.74 g/ml at 25 C |
| Bell indentation hardness | 110N/mm ² |
| Thermal conductivity | 0.19 W/(K.m) |

3.2.3 N,N-Dimethylformamide (DMF)

Polyvinylidene fluoride (PVDF) is dissolved in an organic substance known as DMF to create a homogeneous PVDF solution. Sigma-Aldrich (SCR) produced DMF solvent, which had a 99% purity level. DMF attributes are displayed in Table (3-2) according to cas.no. [68-12-2]

Table (3.3) the physical properties of DMF (122)

| Properties | Value |
|------------------|----------------------------------|
| Color and shape | Colorless liquid |
| Molecular Weight | 73.09 g/mol |
| Density | 0.94 g/cm ³ |
| Chemical Formula | C ₃ H ₇ NO |
| Boiling Point | 153 C |

3.2.4 Argan oil “liquid gold”

An oil extracted from the almonds of the argan tree, which is a rare Tree that is found very widely in Morocco, especially in the Souss region,

CHAPTER THREE Experimental Part

and is more than 200 years old. It is an oil widely used in the traditional cuisine of this region, and is also used for its cosmetic and therapeutic properties. according to cas.no. [223747-87-3]

Table (3.3) argan oil content analysis

| Element | Value |
|---------|-------|
| N | 3 |
| P | 0.4 |
| K | 0.04 |

3.3 METHODS

Nanofibers consisting of PS and PS-PVDF were produced by electrospinning. There was a metallic needle linked to the positive high-voltage power source, and the negative power supply was connected to an earthen metallic collector. The electro spinning solution was put into a syringe and linked to a using a peristaltic pump to control fluid flow. The ideal electro spinning process configuration is shown in Fig(3.1)

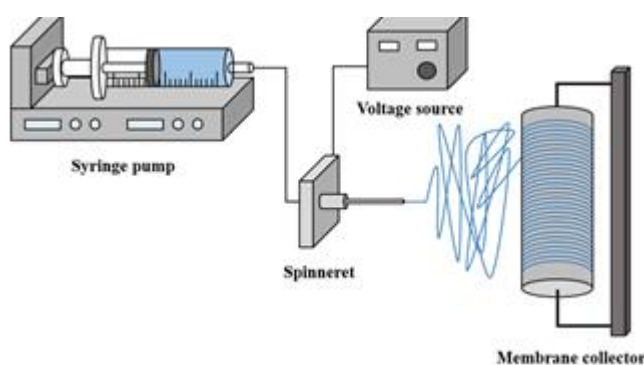


Fig 3 (a) Electrospinning set up Dc-HV,

(b) Electrospinning set up Ac-HV

3.4 Sample Preparation

Using a magnetic mixer at 50 ° C, a concentration of 0.12 wt. polystyrene (PS) dissolved in di methyl formamide (DMF) and a concentration of 0.1 g/ml polyvinylidene fluoride (PVDF) dissolved in DMF were created. To obtain homogeneous solutions of these polymers, the

CHAPTER THREE Experimental Part

solution was mixed for two hours for each solution. Then, using a hot plate magnetic stirrer at 50 ° C, different quantities of PS solution dissolved in DMF and PVDF solution dissolved in DMF were combined in the volume ratios using a hot plate magnetic stirrer. The viscosity, surface tension, and electrical conductivity of the prepared solution were all examined, the prepared solution was pumped using an electro spinning apparatus.

3.5 Tests

3.5.1 Fourier transform infrared spectroscopy (FTIR)

FTIR test is done by utilizing IR Affinity-1 Shimadzu –Japan Fig (3.7).

To know the type of interaction between components and bonds types of it



Fig (3.2): IR Affinity-1 Shimadzu device

3.5.2 Surface tension

The surface tension of the solutions was measured with a TEN202 Surface Interfacial Tensiometer using a pt ring immersed in a solution mounted in a cylindrical petri dish and the surface tension value of the solutions was measured in mN/m. Fig (3.5).



Fig (3.3) Surface tension device

3.5.3 Capillary viscometer test (Ostwald viscometer)

The instrument has to be calibrated using substances with known viscosities, such pure (deionized) water. As demonstrated in fig, one may determine the viscosity of some other liquid from the value of one liquid's viscosity (3.4)

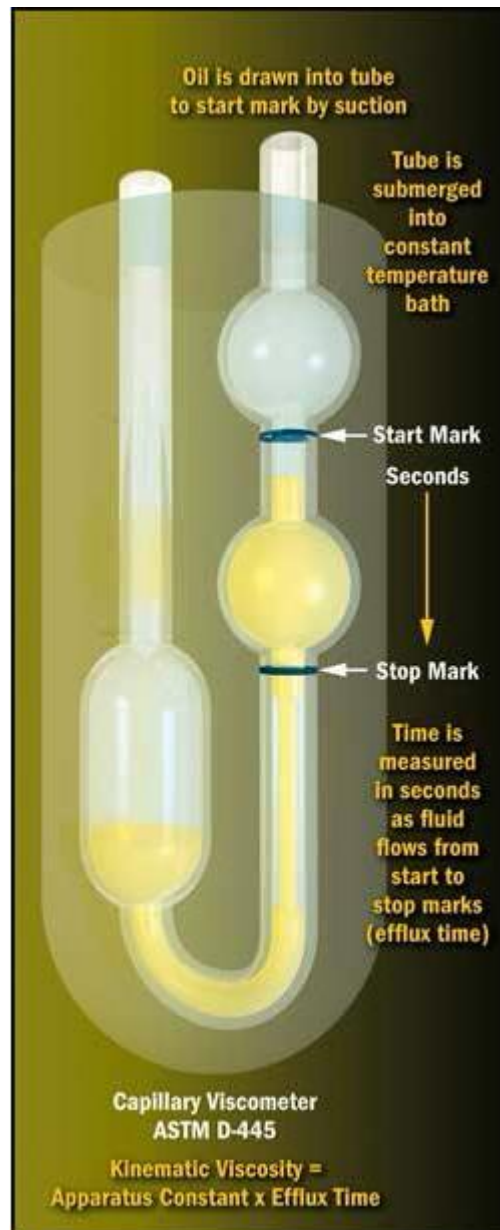


Fig 3.4 ostwald viscometer

3.5.4 Scanning Electron Microscope (SEM)

We can view incredible stereoscopic pictures thanks to scanning electron microscopy. It is sufficient to spray the sample with a thin metallic coat of a high atomic material, such as gold, to boost the electrons radiated rather than cutting the sample in slices in need to see it. The metallic paint is pushed to release a barrage of electron towards a fluorescent screen or photo plate when a packet of electrons is delivered down to the specimen's surface, creating a bigger picture of the object's surface. The magnification power of

CHAPTER THREE Experimental Part

scanning transmission electron microscopy can reach 100,000 times. Means the acquisition of an integer package of accelerated electrons with a probe segment. The analysis ability depends on the size of the probe obtained using the acceleration and induction system. The probe moves to scan all parts of the model and the physical effects of the electron beam reaction are detected.

The microscope is used to examine the internal structure of the thin models at high magnification, but the scanner is used to examine the outer surface of the thick and large model and at a greater extent of access.

In an electron microscope, samples may be seen under a variety of circumstances, including high vacuum, low vacuum, moist environments, and a wide range of really low or high temperature. The detection of backscattered electrons released from atoms stimulated by the electron beam is the method of scanning electron microscope (sem that is used the most frequently. The sample topography is one factor that affects how many secondary electrons may be found. The picture displaying the surface topography is produced by scanning the sample and gathering the secondary electrons released using a specialized detector.



Fig (3.5) SEM

3.5.5 Atomic Force Microscopy (AFM)

AA3000 Scanning Probe Microscope is a very well device designed for use in research and industry, in which the inspector may do quick, easy analysis. Because the tip is placed into the base, there is no risk of being damaged by handling. tapping mode, contact mode, lateral force microscopy, all possible with the AA3000 Scanning Probe Microscope.

The main function of the standard unit is to see the area of samples prepared up to 10 microns by 10 microns. The device can be adjusted to inspect larger areas of the sample. With the existing “digital signal processor (DSP)” in the system, the device can treat more complex tasks effectively. The device is shown in Fig (3.6)



Fig (3.6) Atomic Force Microscope (AFM) Device.

3.5.6 Contact Angle

Contact angle (circle fitting mode) was used to evaluate the wettability of the Nanocomposite samples using “SL200B Optical Dynamic / Static Contact Angle Meter” as shown in Fig (3.7).

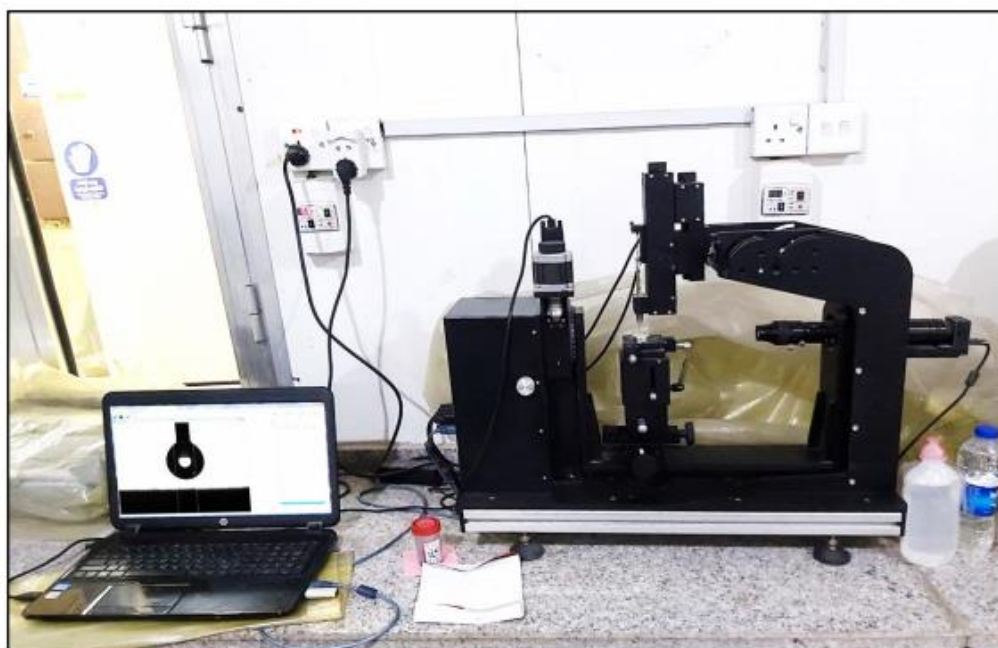


Fig (3.7): Contact Angle Meter (SL200B Optical) device

3.5.7 Corrosion tester (electrochemical Tafel method)

The corrosion tester was used to determine the corrosion resistance through the electrochemical method used. The device consists of the measuring cell and its electrodes. The cell is made of glass and has a spherical capacity of one liter and contains different holes for placing the electrodes. The cell consists of three electrodes are the electrode, together, an auxiliary electrode (auxiliary electrode), another electrode and the electrode is the main electrode that contacts the platinum », experiments in aqueous solution where (400 ml) of water was placed in the measuring cell and the electrodes were filled The auxiliary electrode and the reference electrode were carried out with the cell solution, and the main electrode was prepared, washed with alcohol and then dipped in the measuring cell. Then the circuit is opened and the curves are drawn with the endoscope and the back polarization by the computer connected to the stationary device (Potentianstat), where we use the (Bank - Elechtignies) program to draw these curves. This device is of the type (Mlah Potentistat Bansh Elektronik GMP 200), which is located in the College of Materials Engineering / Department of Mineral Materials, shown in Fig (3.8). Corrosion currents curves for all studied samples are fixed in Annex 1.



Fig (3.8) Corrosion test device (Tafel's device)

3.5.8 Pull-off adhesion test

The device that uses hydraulic pressure to measure the adhesion strength of a certain diameter of the coating, displays the pressure results on an LCD screen along with their values, and accounts for the good adhesion of the coating on the surface treatment. Prior to the test, it must be ready and primed for all weights (primer) and the coating's surface. Then, it must be adhered with a beautiful adhesive (epoxy glue), but it must be epoxy, placed on a bond basis (4–2 ml), bonded to the surface ready for the test, and gently pushed to remove it. The glue is outdoors, where it has been allowed to dry. The pressure values are shown on the screen that reach the highest value after duly separated. The test is carried out both on the surface coated with pure Ps and ps + pdf in different proportions in the College of Materials Engineering, Department of Polymer and Petrochemical Industries in Fig. (3.9) .



Fig

(3.9) Pull-off adhesion device.



CHAPTER FOUR
RESULT AND DISCUSSION

4.1 Introduction

This chapter includes and discusses the results of all prepared samples, including coating morphology, FTIR, contact angle results for all samples, AFM results, corrosion resistance results for samples, and coating adhesion strength for samples.

4. 2 FTIR analysis

Fig(4.1) shows an FTIR analysis of PS and a PS-PVDF combination produced by Dc-HV. In electro spun fibers, The C-H asymmetrical stretch vibration is thought to be responsible for the distinctive peak at 2824 cm⁻¹. The ring's C–H bending vibration has a peak at 1028 cm⁻¹, while the PS segments' benzene ring's C–H out-of-plane bending vibration has two peaks at 752 cm⁻¹ and 640 cm⁻¹. This is agree with Wang et al. 2020 [123]. The FTIR diagram for PS/PVDF blend is comparable to that of polystyrene, with the C-F stretching bond observed at 1188 cm⁻¹, and the C-F bending bond observed at 840 cm⁻¹ , which is attributable to the presence of PVDF within the mixture's composition . It also can see by a rise in the intensity of the rest of the combination's absorption peaks, which indicates that the mixture was homogeneously mixed using the electro spinning process, which agrees with Daems et al 2018 [124].

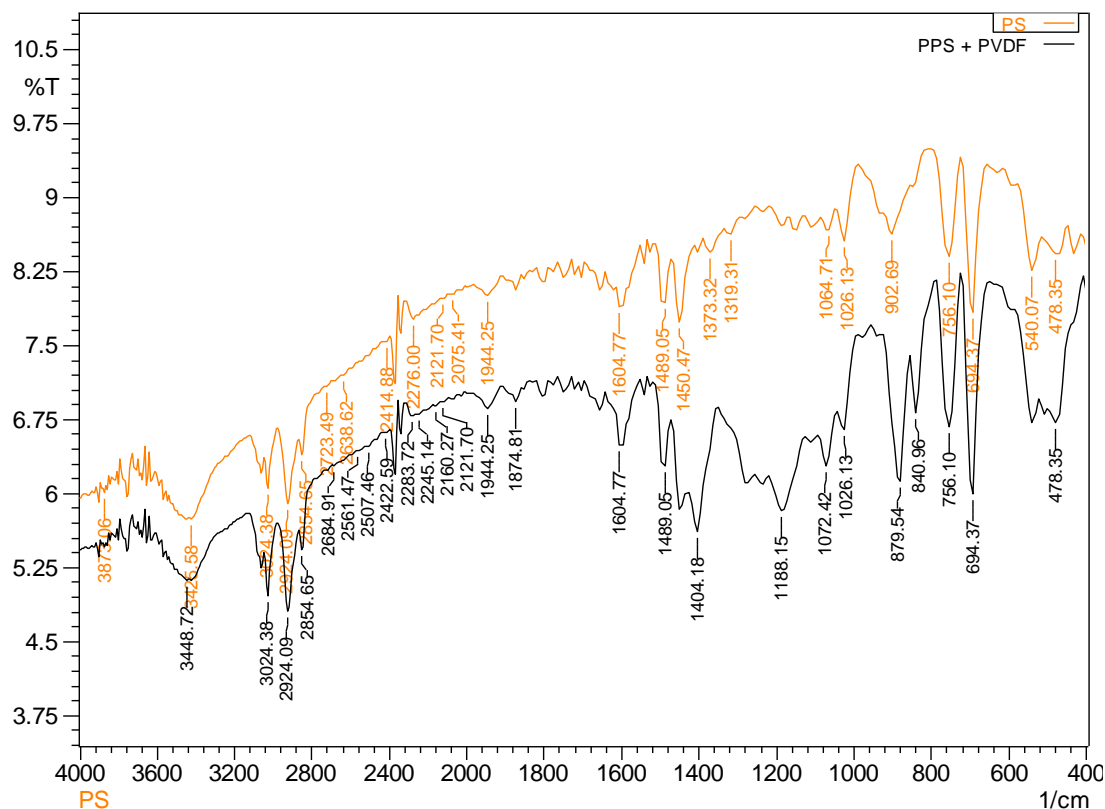


Fig 4.1 FTIR analysis of PS and PS-PVDF blend

4.3 Effect of solutions parameters on fiber properties

The solutions' viscosity and surface tension increase with the increase in the concentration of the solution. Solution concentration and surface tension are closely related, because a higher concentration means an increase in the number of polymer chains in the solution and this may lead to an increase in viscosity and surface tension and vice versa.

Table (4.1): Effect of concentration of solutions on viscosity, surface tension and conductivity of solutions for all polymer solutions:

| (PS:PVDF) % | Relative Viscosity η_{rel} | Surface Tension MN/m | Electrical conductivity $\mu\text{S/cm}$ |
|----------------|------------------------------------|-------------------------|---|
| Pure PS | 14 | 30 | 1.6 |
| 84: 16 | 20 | 30 | 1.8 |
| 74: 26 | 30 | 31 | 1.9 |
| 68: 32 | 40 | 30 | 3 |
| Argan oil | 12 | 26 | 1.4 |

4.4 SEM Images of Nanofibers With AC and DC-HVPS

SEM results of nanofibers SEM images of pure polystyrene fibers and polyvinylidene fluoride - polystyrene blends are shown in Fig 4.2. The pure polystyrene fibers in Fig 4.2 have large cross - sections due to the failure to completely pump the solution in the form of fibers and the presence of some polymeric droplets on the target with a heterogeneous distribution for the resulting fibers on the target. This is due to the instabilities of the flow rate , the low intensity alternating voltage used, and the low electrical conductivity of the solution. As demonstrated in Fig 4.2, adding polyvinylidene fluoride to the PS/DMF solution at a (weight ratio) of 24 by increases flow rate and was a reason for the electrospinning process' stability, which resulted in more homogeneous fibers than pure polystyrene fibres. This is due to the fact that adding PVDF to a PS / DMF solution boosts the solution's conductivity and pumping ability. Fig 4.2 shows a blend of nanofibers (68 PS: 32 PVDF). By increasing the (weight ratio) of PVDF in blends of (PS: PVDF) solution to 32 (wt%) we find microfibers as a result of the electro spinning process' unsuitability. This is owing to a large increase in viscosity with a constant applied voltage , as seen in table 1. This is with . [124-126]

SEM results for nanofibers show images of pure polystyrene fibers and polyvinylidene fluoride-polystyrene blend in Fig. 4.2. The pure polystyrene fibers in Fig 4.2 contain a large number of beads. This is due to the instability of the pumping process,As shown in Fig 4.2 the addition of polyvinylidene fluoride to the PS/DMF solution in a (weight ratio) of 16 by increasing the volume of the pumping process caused the electrospinning process to be stabilized, resulting in more homogeneous fibers than pure polystyrene fibers. This is due to the fact that the adding of PVDF to the PS/DMF solution enhances the conductivity of the solution and the pumping capacity. Fig 4.2 shows a mixture of nanofibers (76 PS: 24 PVDF). By

CHAPTER FOUR Results and Discussion

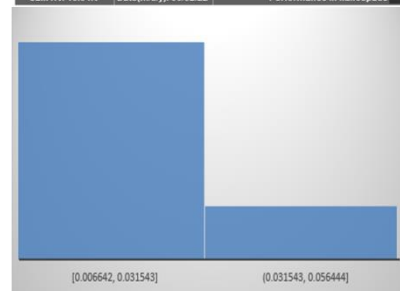
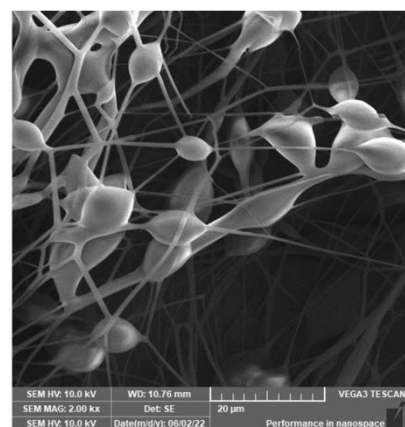
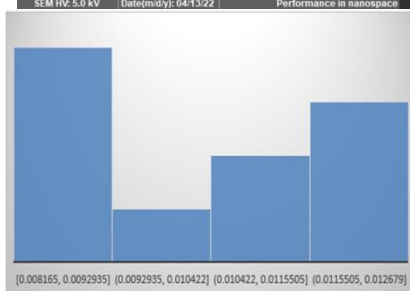
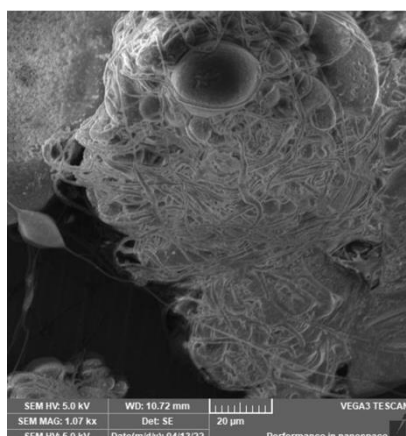
increasing the (weight ratio) of PVDF in (PS: PVDF) solution mixtures to 32(wt%), The microfibers as a result of the inappropriateness of the electrospinning process are found. This is due to the large increase in viscosity with a constant applied voltage. We note that with the increase in the (weight ratio) of in solution mixtures to 32, The microfibers as a result of an increase due to an increase in conductivity and an increase in viscosity and this can be found , as shown in Table 1. [124-126]

1- The fibers produced using DC-HVPS are much softer and less grainy than the branched fibers using AC-HVPS, because the AC voltage has different values at each inconsistent point. This leads to the production of irregularly shaped microfibrils with more beads of different shapes as in the previous ones, and there is also axial instability that occurs with AC HVPS-, and this leads to more beads.

2- AC-HV leads to reduced dermal process and increased microfiber alignment. This is achieved [130-131]

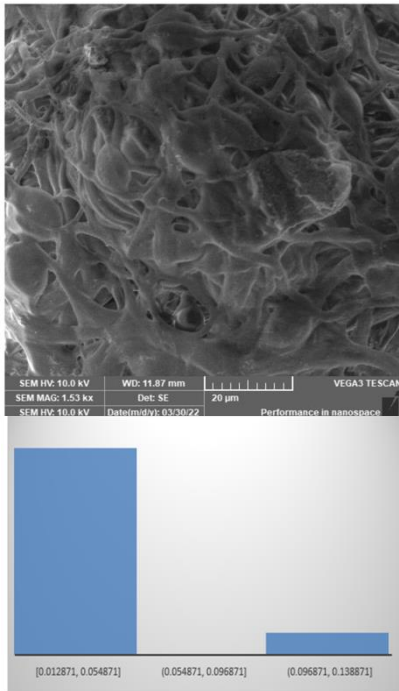
collector: Two types of accumulators are used:

- 1- flat aluminum collector using AC-HV
- 2 - stainless steel (rotating cylinder) collector using DC-HV

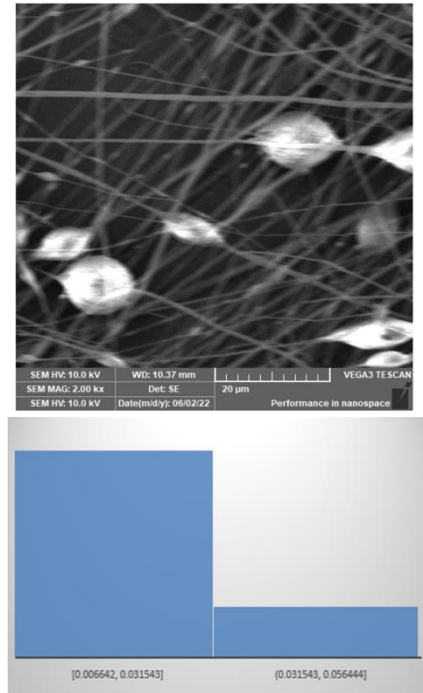


CHAPTER FOUR Results and Discussion

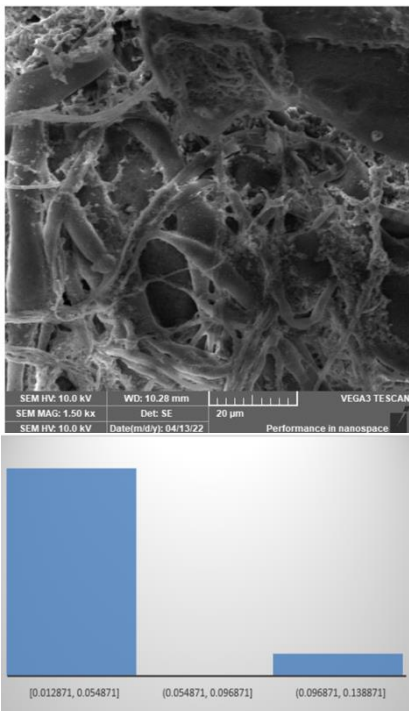
Pure PS



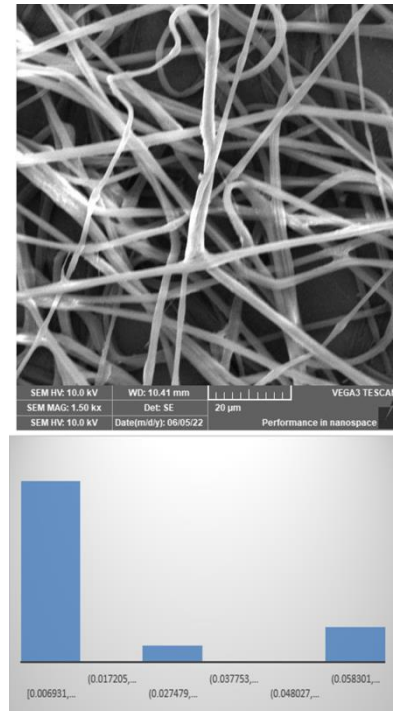
Pure PS



76:24 PS:PVDF



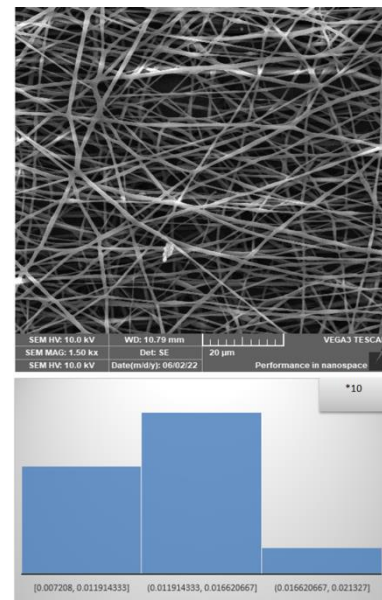
76:24 PS:PVDF



68:32 PS:PVDF

SEM- Imges AC-HV

68:32 PS:PVDF



84:16 PS:PVDF

SEM Images DC-HP

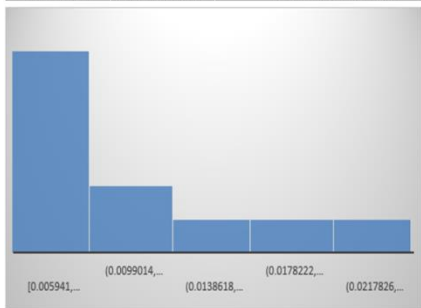
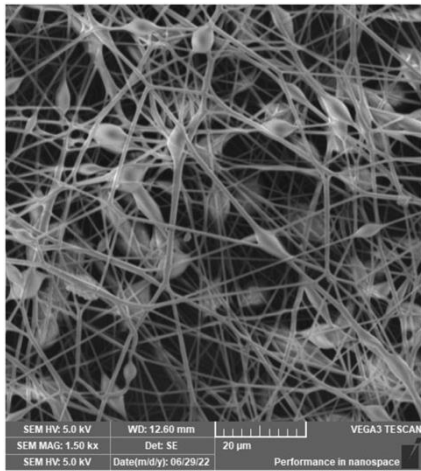
Fig(4.2) shows the SEM images of Nano fibers produced by AC-DC- HV

4.5 SEM Images of nanofibers under DC-HV (18 KV-21KV)

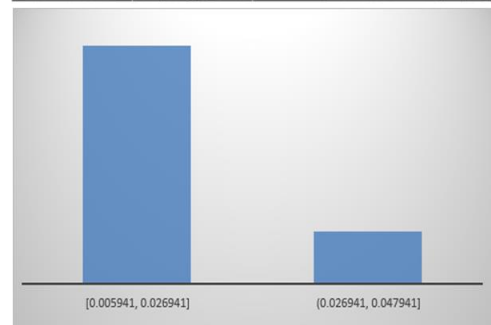
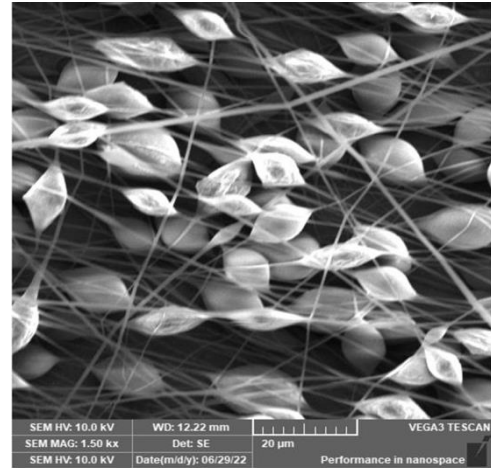
Effect of applied voltage on Pure polystyrene fibers and polyvinylidene fluoride – polystyrene blends With different voltage applied to DC (18,21) KV Figs (4.3) show when applying a voltage of (18KV) the decreased diameter of fibers(PS) as the applied voltage increases because higher voltages The electrostatic repulsion force on the charged plane, the narrowing of the fiber diameter, the higher voltage induces a higher repulsion strong which helps the formation of the thinner fibers. This is satisfied with the reference. [101] Also when applying a voltage of (18KV) we some beads in (4.3) This is due to the morphology of the fibers due to the presence of axial instability of the plane through the process of electrospinning, which results from the conduction instability mainly governed by the electrical conductivity of the jet is subject to several modes Different from the instability, if the applied voltage is too high, however, the increased mass flux can lead to increased bead formation. [102]

CHAPTER FOUR Results and Discussion

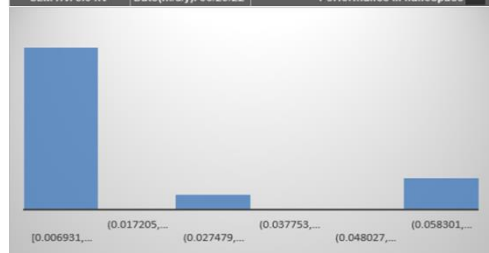
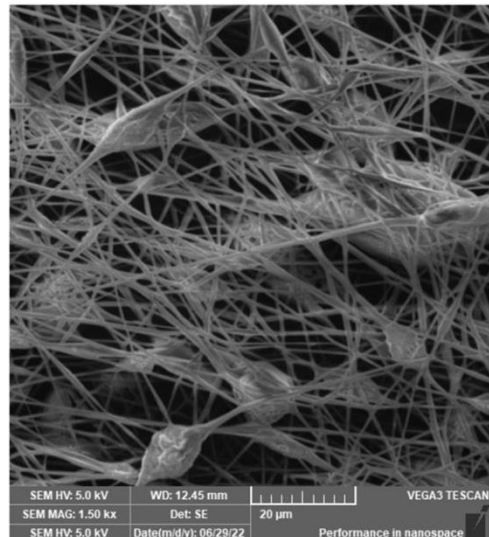
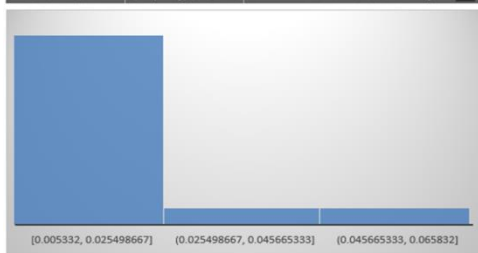
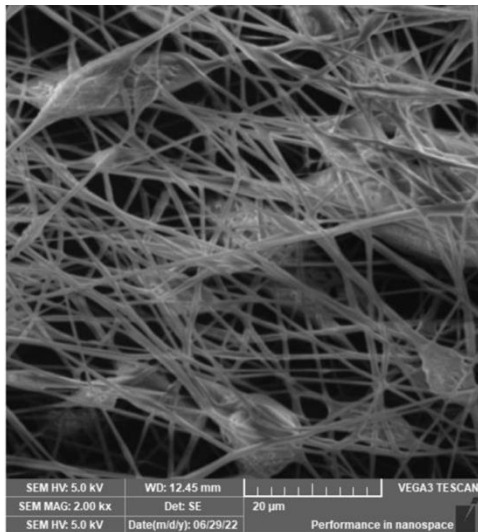
increase in voltage, and also at voltages(21KV) we did not get any results, whether Pure PS or PS+ PVDF at any ratio.



PS:PVDF NF (84:16) : 18 KV



pure PSNF : 18 KV

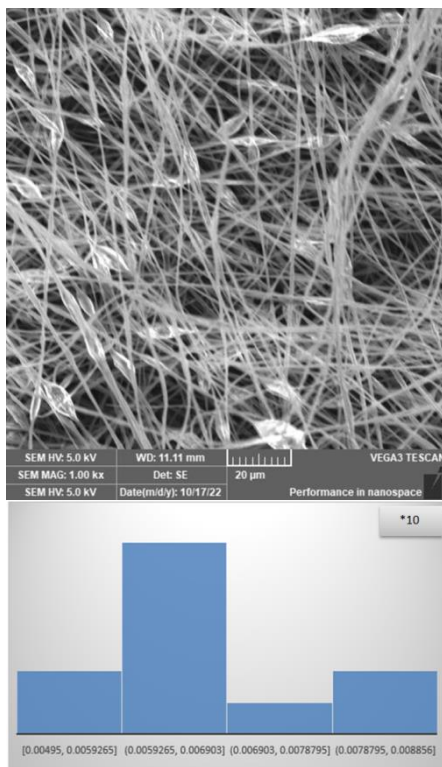


PS: PVDF NF (68:32) : 18 KV PS: PVDF NF (76:24) : 18 KV

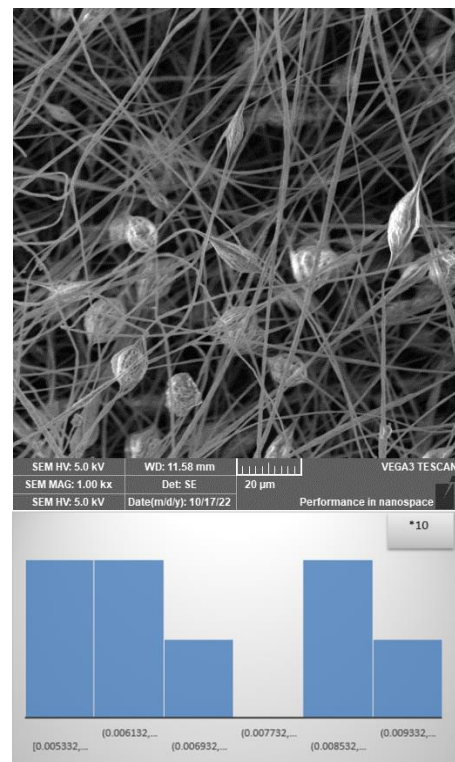
Fig(4.3) shows the SEM images of Nano fibers produced by DC- HV

4.6 SEM Images of (68:32)PS:PVDF:AO Nanofibers

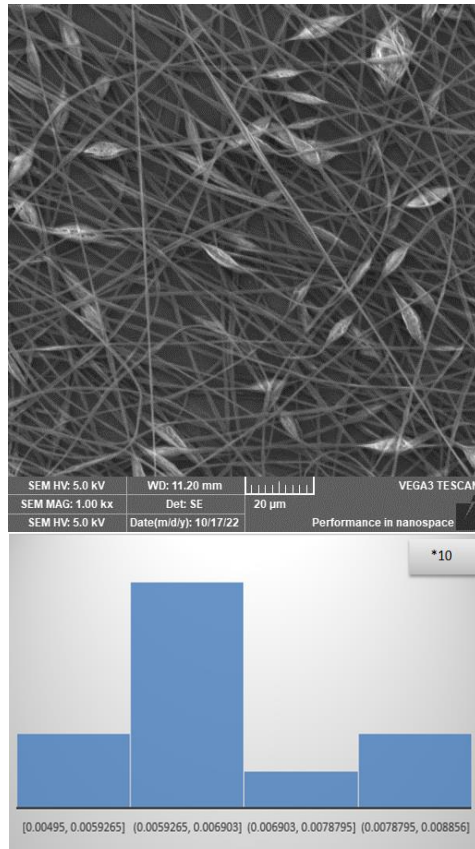
Fig (4.4) shows a mixture of nanofibers(PS:68: PVDF:32) wt % mixed with a natural substance, which is AO in the ratio of 0.0292, 0.0584 and 0.0876, respectively, where the weight of one drop is 0.0292. on a number of beads as a result of the unsuitability of the electro spinning process. This is due to a significant increase in viscosity with a constant applied voltage, as shown in Table 1. This corresponds to.[124-126]



(68:32:0.0584) PS:PVDF:AO Nanofibers



(68:32:0.0292) PS:PVDF:AO Nanofibers

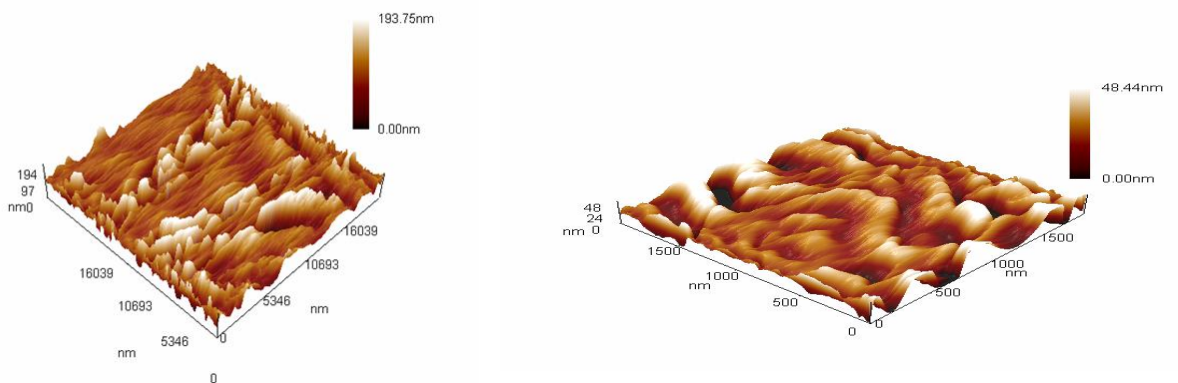


(68:32:0.0876) PS:PVDF:AO Nanofibers

Fig(4.4) SEM Images of (68:32)PS:PVDF:AO Nanofibers

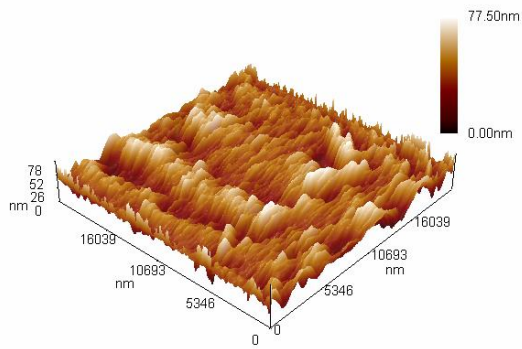
4.7 AFM Results of Nano fibers under AC and DC-HVPS

for nanofibers Fig 4.5 depicts AFM images for PS and PS/PVDF blending nanofibers,

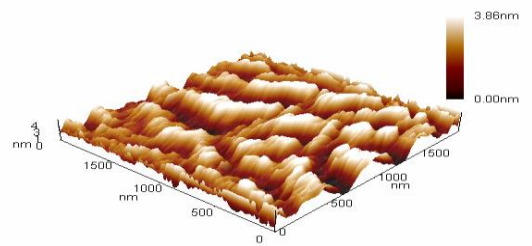


CHAPTER FOUR Results and Discussion

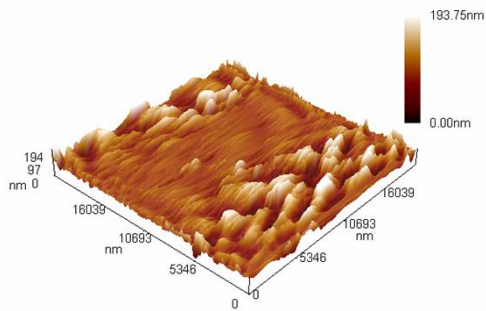
pure PSNF : 15KV



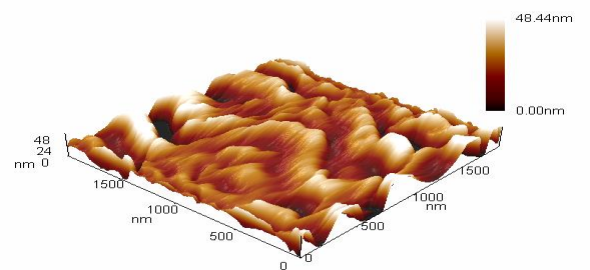
pure PSNF : 15 KV



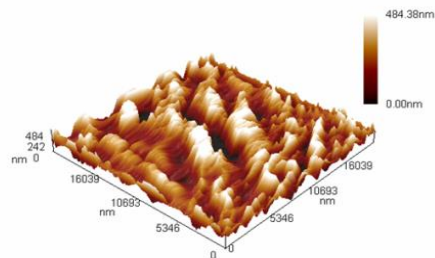
PS: PVDF NF (84:16) : 15 KV



PS: PVDF NF (76:24) : 15 KV



PS: PVDF NF (76:24) : 15 KV



PS: PVDF NF (68:32) : 15 KV

PS: PVDF NF (68:32) : 15 KV

Fig(4.5) AFM Results of Nano fibers under AC and DC-HVPS

CHAPTER FOUR Results and Discussion

. Table(4.2). shows the surface parameters of PS nanofibers and PS-PVDF blends of nanofibers which studied by AFM

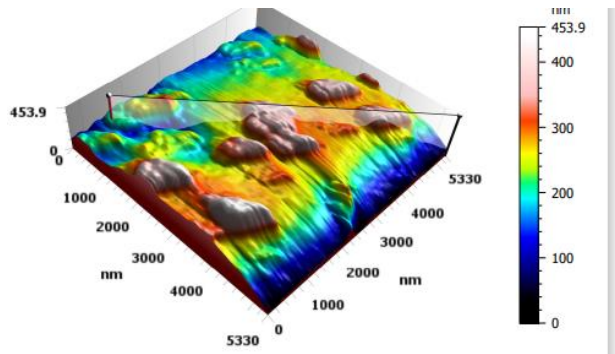
| Sample No. | Contents PS:PVDF | Roughness average nm | Sdr(Surface area ratio) | Bearing index | Sci(fluid retention) index |
|--------------|------------------|----------------------|-------------------------|---------------|----------------------------|
| AC-HV | | | | | |
| 1 | PS | 6.8 | 14.9 | 1.33 | 1.53 |
| 2 | 76:24 | 0.863 | 0.15 | 4.07 | 1.56 |
| 3 | 68:32 | 8.53 | 6.51 | 1.55 | 1.51 |
| DC-HV | | | | | |
| 1 | Pure PS | 8.87 | 0.619 | 0.601 | 1.59 |
| 2 | 84+0.16 | 22.8 | 3.35 | 0.747 | 1.6 |
| 3 | 0.76+0.24 | 20.6 | 3.25 | 0.644 | 1.59 |
| 4 | 0.68+0.32 | 95.5 | 14.5 | 2.37 | 1.6 |

Fig 4.5 and Table(4.2) show that sample No. 2 (76: PS: 24: PVDF) has the highest surface bearing index ratio (4.07), lowest surface roughness (0.863 nm), and lowest surface area ratio (0.15). This is because sample 2 (76: PS:24:PVDF) has a more homogeneous nanofibers morphology than the other samples, as shown in SEM image Fig4.4 and this is due to the electrospinning process's stability Fig 4.4 Table(4.2) show that sample No. 4(68:PS:32:PVDF) has the highest surface bearing index ratio (2.37), highest surface roughness (95.5), and highest surface area ratio (14.5). This is because sample 4(68: PS:32: PVDF) has a more homogeneous nanofibers morphology than the other samples, as shown in SEM image fig and this is due to the electrospinning process's stability.

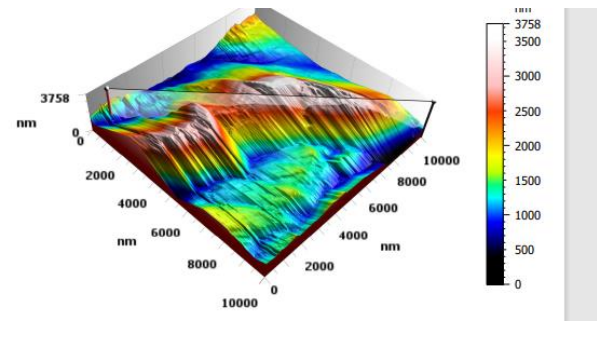
CHAPTER FOUR Results and Discussion

4.8 AFM Results of Nanofibers under DC-HVPS (18 KV)

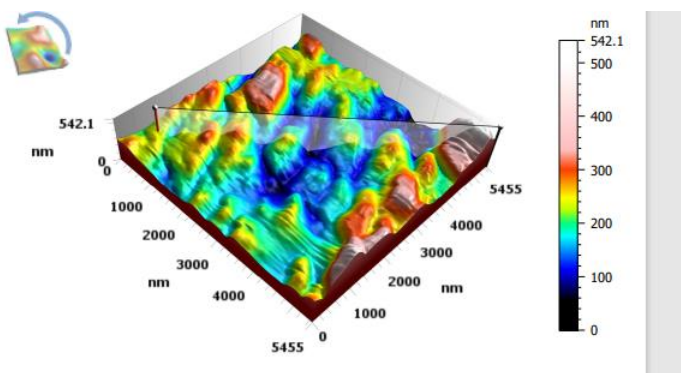
for nanofibers Fig 4.6 depicts AFM images for PS and PS/PVDF blending nanofibers



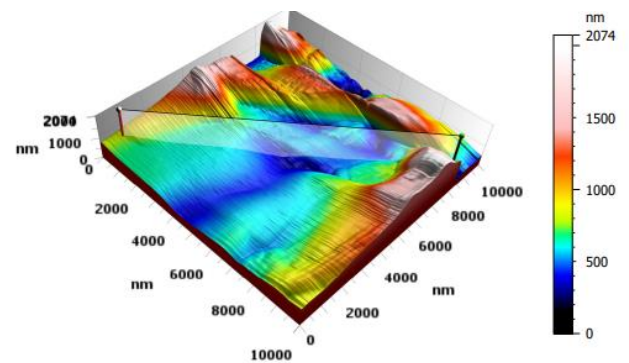
pure PSNF : 18 KV



PS: PVDF NF (84:16) : 18 KV



PS:PVDF NF (68:32) : 18 K



PS: PVDF NF (76:24) : 18 KV

Fig(4.6) AFM Results of Nanofibers under DC-HVPS (18 KV)

CHAPTER FOUR Results and Discussion

| Sample no | Contents PS:PVDF | Roughness average nm | Sdr(surface area ratio(| Bearing index | Sci(fluid retention index(|
|-----------|---------------------|----------------------------|----------------------------|------------------|----------------------------------|
| 1 | PS Pure | 99.68 | 6.240 | 0.4333 | 1.383 |
| 2 | 16:84 | 441.3 | 95.31 | 0.4395 | 1.682 |
| 3 | 76:24 | 200.5 | 23.72 | 0.4617 | 1.821 |
| 4 | 68:32 | 59.6 | 6.188 | 0.4666 | 1.623 |

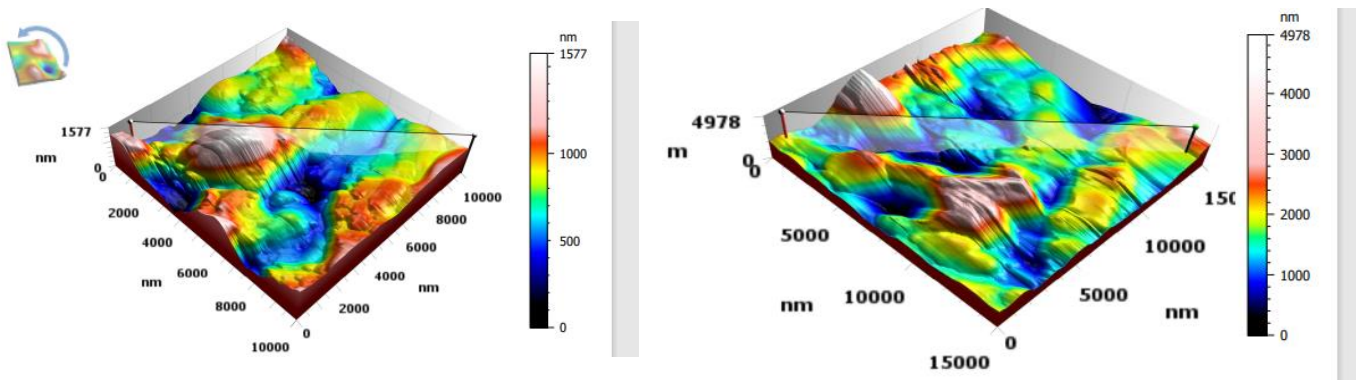
Table(4.3). shows the surface parameters of PS nanofibers and PS-PVDF . blends of nanofibers by AFM assay

Fig 4.6 and Table (4.4) show that sample No. 4 (68 PS:32 PVDF) has the highest surface tolerance index (0.466), the lowest surface roughness (59.6 nm), and the lowest surface area ratio (6.188) This is because sample 4 (68 PS:32 PVDF) has a more homogeneous nanofiber morphology than the other samples, as shown in SEM image and this is due to the stability of the electrospinning process

4.9 AFM Results of (PS:68: PVDF :32)AO Nanofibers

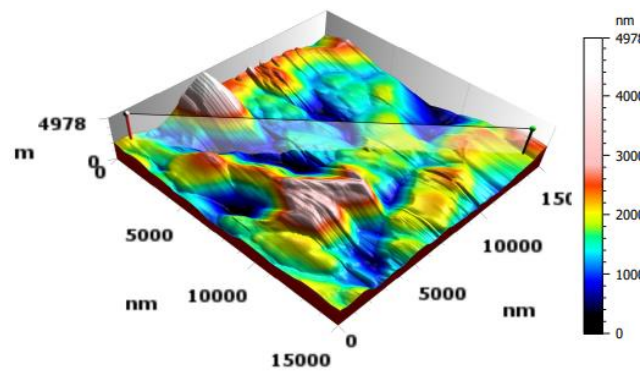
for nanofibers Fig 4.7 depicts AFM images of nanofibers (PS:68 :32:PVDF) with droplet, droplet and three drops that mix the nanofibers.

CHAPTER FOUR Results and Discussion



(68:32:0.0292) PS:PVDF:AO

(68:32:0.0584)PS:PVDF:AO



(68:32)PS:PVDF:AO

Fig(4.7)AFM Results of (PS:68: PVDF :32)AO Nanofibers

| Sample no | Contents PS:PVDF:AO | Roughness average Nm | Sdr(surface area ratio) | Bearing index | Sci(fluid retention index) |
|-----------|---------------------|----------------------|-------------------------|---------------|----------------------------|
| 1 | (68:32:0.0292) | 168.0 | 11.57 | 0.9475 | 1.277 |
| 2 | (68:32:0.0584) | 133.8 | 11.0 | 0.4038 | 1.465 |
| 3 | (68:32:0.0876) | 435.4 | 49.32 | 0.4614 | 1.501 |

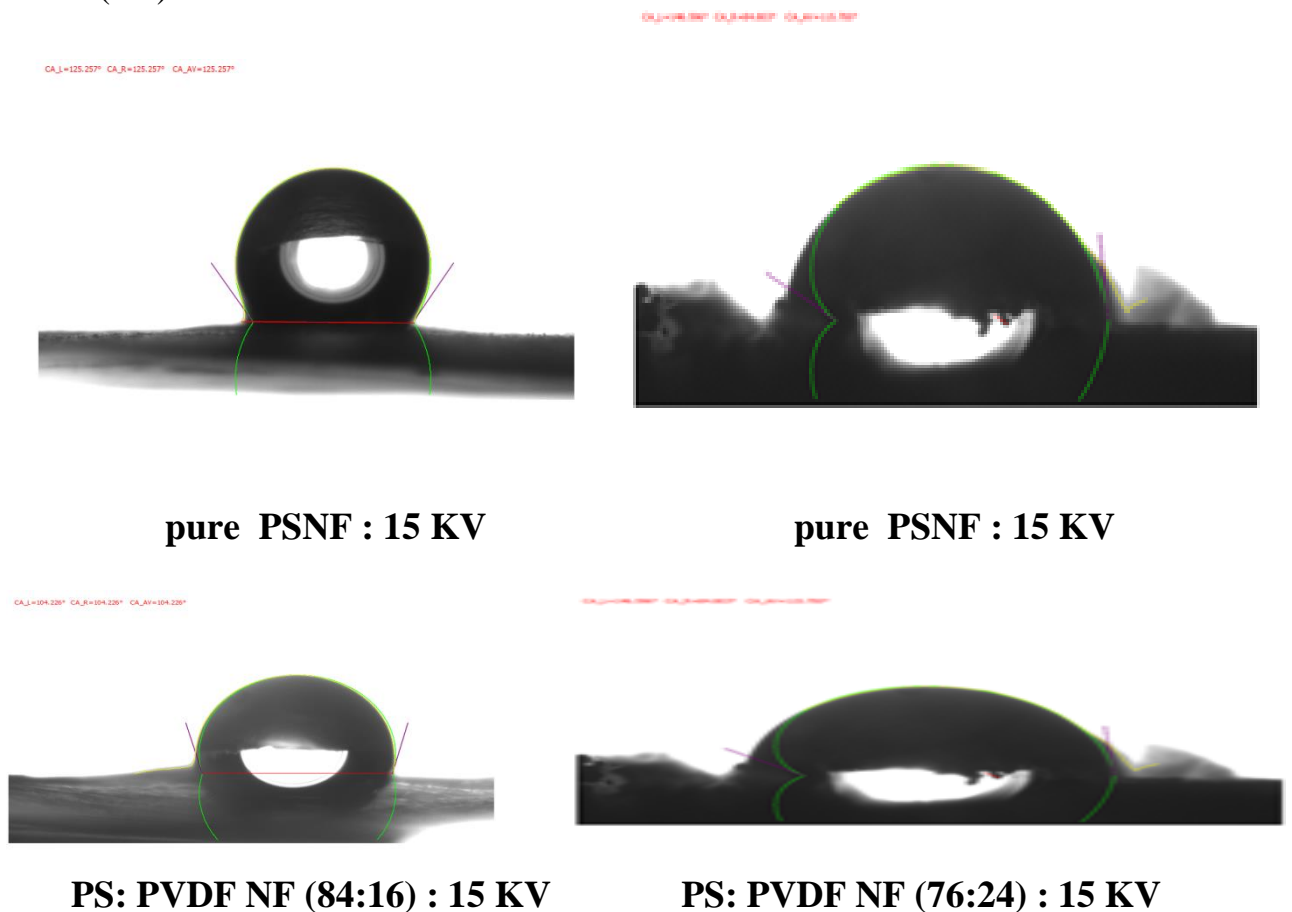
Table(4.4). shows the surface parameters of (ps0.68+0.32pvdf) +argan oil of nanofibers by AFM assay

CHAPTER FOUR Results and Discussion

Fig 4.7 and Table (4.5) show that Sample No. 1 (68 PS:32 PVDF) + one drops of argan oil has the highest surface tolerance index. (0.9475) average surface roughness (168.0) and average surface area ratio (11.57) This is because Sample 1 (68 PS:32 PVDF):0.0292AO has a more homogeneous nanofiber morphology than the other samples, as shown in the form of SEM image and this is due to the stability of the electrospinning process

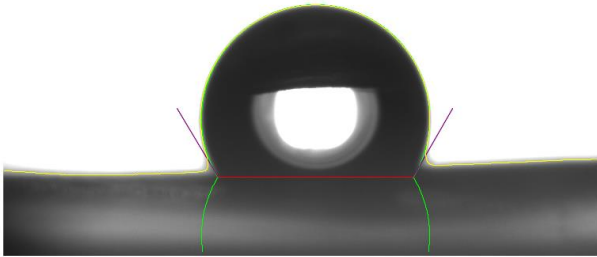
4-10 Contact Angles Results of Nanofibers under AC, and DC-HVPS

The contact angles of electro spun PS fibers and their mixes with PVDF electro spun fibers with varied volume ratios are shown in Figs 4.8 and table(4.6).



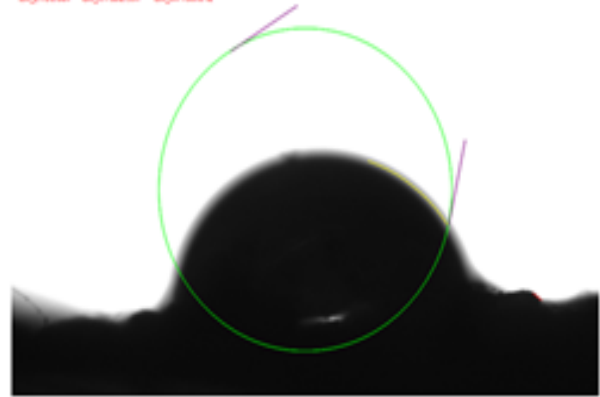
CHAPTER FOUR Results and Discussion

CA_L=120.759° CA_R=120.759° CA_AV=120.759°



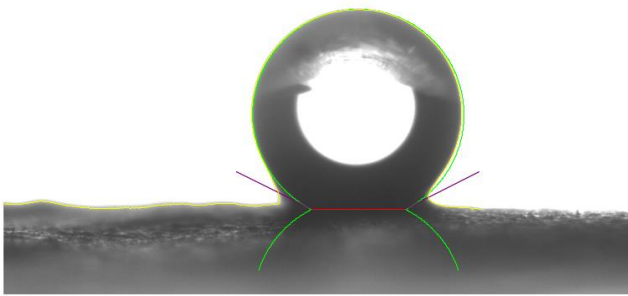
PS: PVDF NF (76:24) : 15 KV

CA_L=115.987° CA_R=102.907° CA_AV=106.847°



PS:PVDF NF (68:32) : 15 KV

CA_L=153.926° CA_R=153.926° CA_AV=153.926°



PS:PVDF NF (68:32) : 15 KV

Fig (4-8) Contact Angles Results of Nanofibers under AC, and DC-HVPS

CHAPTER FOUR Results and Discussion

| Contents | Contact angle of Ac-HV nanofibers | Contact angle of Dc-HV nanofibers |
|-----------------|-----------------------------------|-----------------------------------|
| Pure PS | 115 | 125 |
| PS0.84+0.16PVDF | 105 | 104 |
| PS0.74+0.24PVDF | 103 | 153 |
| PS0.68+0.32PVDF | | 120 |

Table(4.5). Contact Angles Results of PS and PS blends nanofibers

The water contact angles of PS fibers and their mixes with various PVDF volume ratios were 115°, 105°, and 103°, respectively. PS is chemically hydrophobic, as is well known. As a result, its water contact angle is greater than that of other polymers in its blend. As a result, it is plausible to conclude that electro spun mats with varied PS fiber morphologies can be created with good hydrophobicity by combining the hydrophobic behavior of PS with the unique characteristics of the electrospinning technology. As the amount of PVDF was increased, the CA value declined. To our knowledge, the electro spun mat's surface structure has a major influence in determining hydrophobicity. Furthermore, electro spun fibers with a bead, porous, and protuberant structure add to the overall performance. PS and PVDF are hydrophobic due to their nonpolar polymers, which prevent them from reacting with water.[132] The aqueous contact angles of PS fibers and their mixtures with different PVDF size ratios were 125, 104 and 153, and 120 and 128 respectively. PS is chemically hydrophobic, as is well known. As a result, its contact angle with water is larger. As a result, it is reasonable to conclude that electrospun mats with diverse shapes of PS fibers can be generated with good hydrophobicity by combining the hydrophobic behavior of PS with the unique properties of the electrospinning technique, the electrospun surface composition mat has a

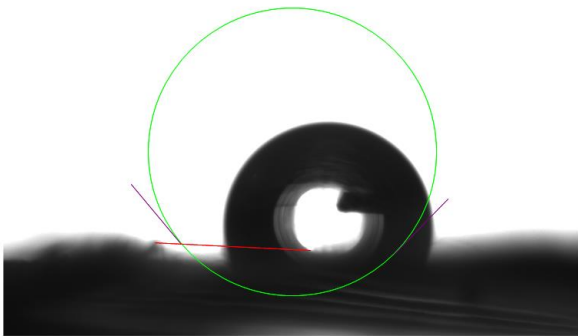
CHAPTER FOUR Results and Discussion

significant influence in identification with its hydrophobicity. Moreover, with the increase of the ratio to reach (0.76+0.24), we notice an increase in the value of this CA due to the surface structure of the electrical spun mat as shown in the results, SEM above, how much surface abrasion coefficients also play a role in this increase as shown in the above AFM results. Electrospun fibers with a granular, porous and prominent structure add to the overall performance. PS and PVDF are hydrophobic due to non-polar polymers, which prevents them from reacting with water. [131]

4.11 Contact Angles Results of PS and PS blends Nanofibers under DC-HVPS (18KV)

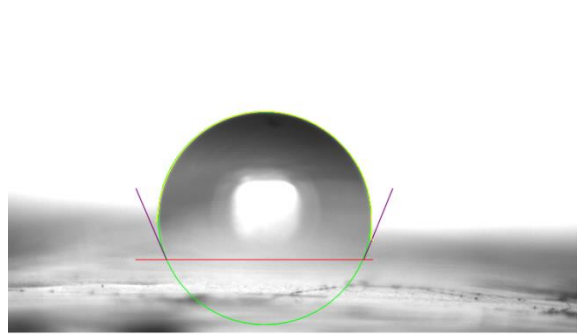
The contact angles of electro spun PS fibers and their mixes with PVDF in Fig (4.9) and table(4.7).

CA_L=129.665° CA_R=135.028° CA_AV=132.346°



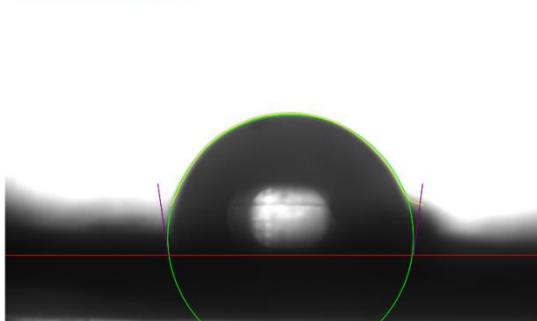
pure PSNF : 18 KV

CA_L=112.688° CA_R=112.688° CA_AV=112.688°



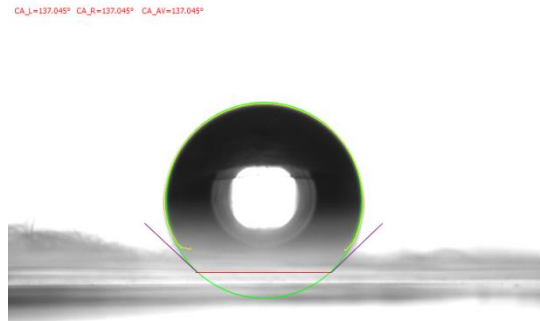
PS:PVDF NF (84:16) : 18 KV

CA_L=97.957° CA_R=97.957° CA_AV=97.957°



PS:PVDF NF (76:24) : 18 KV

CA_L=137.045° CA_R=137.045° CA_AV=137.045°



PS: PVDF NF (68:32) : 18 KV

Fig(4.9) Contact Angles Results of PS and PS blends Nanofibers under DC-HVPS (18KV)

CHAPTER FOUR Results and Discussion

| Sample no | Contents | Contact angle |
|-----------|---------------|---------------|
| 1 | Pure PS | 112 |
| 2 | P:84:16:PVDF | 132 |
| 3 | PS:76:24:PVDF | 97 |
| 4 | PS:68:32:PVDF | 137 |

Table(4.6) CONTACT ANGLES Results of PS and PS blends nanofibers

The German contact angles of PS fibers and their mixtures with different PVDF size ratios were 112, 132, 97 and 137, respectively. Is added the ps contact angle increased when is increased the PVDFmaterial and when the voltage to 18 and this is due to the shape of the resulting fibers, as with the increase in voltage, the diameter of the fibers decreases and becomes softer and this is shown in the SEM results. In addition to the mixtures of PS andPVDF it is noticed the decrease in the contact angle when the ratio of PVDF increases. This is due to the electrostatic structure of the spun mat surface. It has a significant effect on its hydrophobicity. The increase in the contact angle when the ratio increases from (16 :84) to (24 :76) is also due to Electrospun mat surface as indicated by SEM above, how much surface abrasion coefficients also play a role in this increase as shown in the above AFM results. Electrospun fibers with a granular, porous and prominent structure add to the overall performance. PS and PVDF are hydrophobic due to non-polar polymers, which prevents them from reacting with water [131].

CHAPTER FOUR Results and Discussion

4.12 Resu Contact Angles Its of (PS:68:PVDF:32):AO Nanofibers

The contact angles for (PS:68:32PVDF) fibers added to it 0.0292, 0.0584 and 0.0876AO are shown in Figs 4.10 and Table (4.8).



Fig(4.10) Resu Contact Angles Its of (PS:68:PVDF:32):AO Nanofibers

| Sample no | Contents | Contact angle |
|-----------|-------------------------|---------------|
| 1 | (PS:68:32PVDF:0.0292AO | 98 |
| 2 | (PS:68:32PVDF:0.0584AO) | 86 |
| 3 | (PS:68:32PVDF:0.0876AO) | 71 |

Table(4.7) Contact Angles Results of PS and PS blends nanofibers

CHAPTER FOUR Results and Discussion

The water contact angles for (PS68:32PVDF) fibers were added by one, two and three drops of 98, 86 and 71 drops of AO, and we observed a decrease in the CA value. Because of the effect of AO on the surface structure of the electric spindle mat, it has a significant impact on identifying its permeability as shown in the results. SEM above, the amount of surface wear coefficients also plays a role in this decrease as shown in the above AFM results, Electrospan fibers with a granular, porous and prominent structure add to the overall performance. PS and PVDF are hydrophobic due to the non-polar polymers, which prevents them from reacting with water [131].

4.13 Corrosion Behavior Results of Nanofibers under AC and DC-HVPS

The Figs in the Figs (4.11) show the corrosion currents for group of the samples according to Tafel curves, including: (PS+PVDF) with different percentages and how many (PS84:16PVDF) (PS76:24PVDF) (PS 68:32 PVDF).The results of the corrosion curves for this group have been fixed in Table (4.9) A note from Table (4.9), and we note that the pure PS samples did not show the results of any sample failure in the examination. A note from the confirmed results in Table (4.9) clearly reduces the corrosion, With increasing concentration of PVDF due to the water resistance and lower surface energy of the coating which prevents the formation of an oxidation layer and insulates the surfaces. Corrosive media. This is in agreement with [132] 2014. Su et al.

On the other hand the corrosion rates of sample (2) present an increasing rate this is because pitting corrosion effect. The numbers in (Appendix 2) show the corrosion currents for the second group of samples according to Tafel curves, and they include: (PS68:32PVDF) added to it 0.0292,0.0584, and 0.0876 of AO. The results of the corrosion curves for this group are fixed

CHAPTER FOUR Results and Discussion

on the table (4.10) . A note from the results shown in Table (4.10) that the corrosion rates decrease significantly, with an increase in the concentration of AO, due to the water resistance. [66] 2014 and the low surface energy of the coating, which prevents the formation of an oxidation layer and insulates surfaces. Who et al. The numbers in (Appendix 2) show the corrosion currents for the second group of samples according to Tafel curves, and they include: (PS68:32 PVDF) added to it 0.0292, 0.0584, and 0.0876 of AO. The results of the corrosion curves for this group are fixed on the table (4.10) . A note from the results shown in Table (4.10) that the corrosion rates decrease significantly, with an increase in the concentration of AO, due to the water resistance. [66] 2014 and the low surface energy of the coating, which prevents the formation of an oxidation layer and insulates surfaces. Who et al.

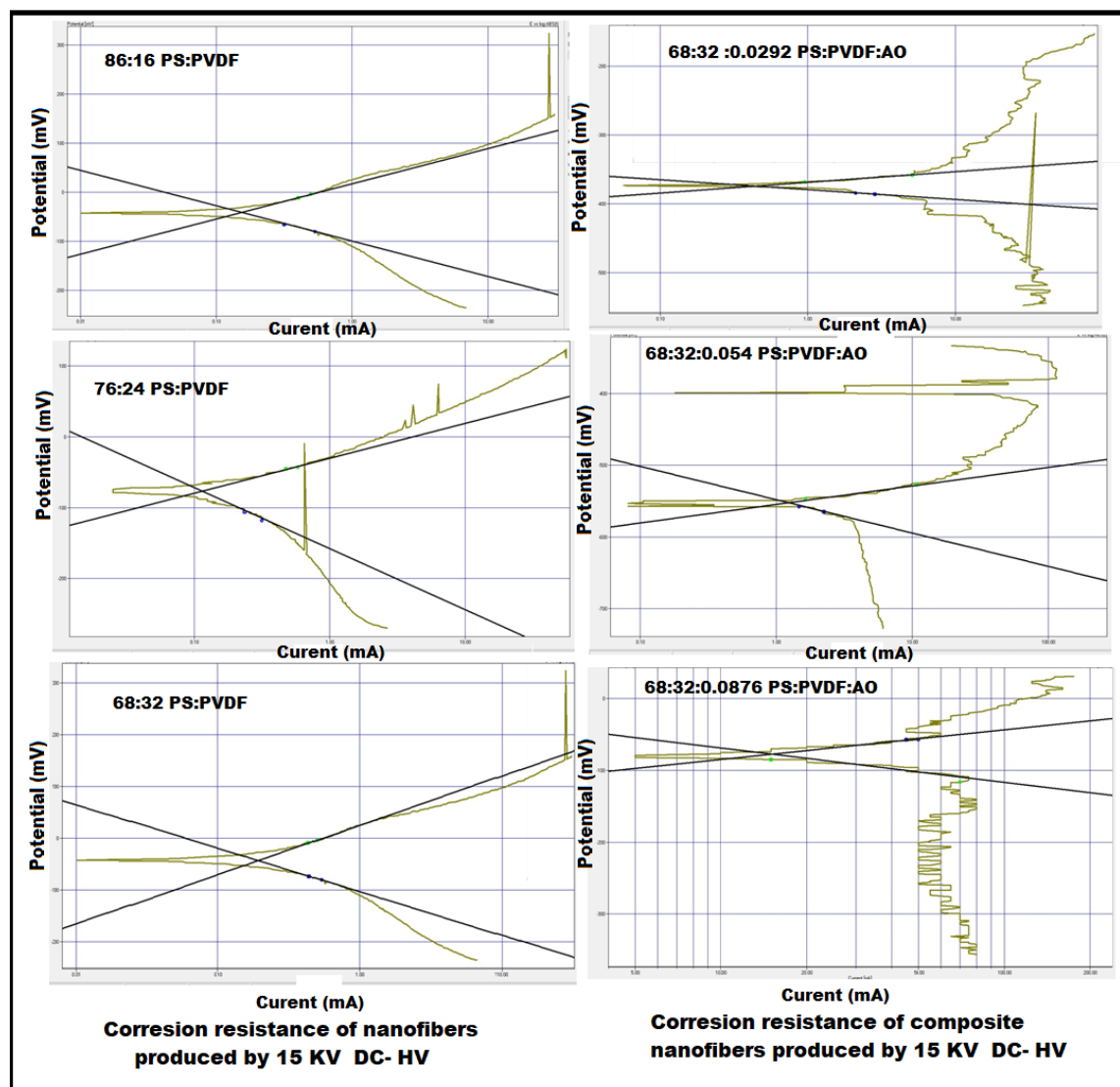


Fig (4.11)corrosion resistance blends and composite of Nano fibers produced by 15KV DC-HV

| Contents | E corr. | I corr. | J corr = I corr /A |
|-------------|---------|----------|-----------------------|
| PS84:16PVDF | -40.7 | 154.21nA | 1.927 |
| PS76:24PVDF | -70.6 | 114.65nA | 1.433 |
| PS68:32PVDF | -43.0 | 192.48nA | 2.406 |

Table (4.8) Results of corrosion curves for the first group of samples

CHAPTER FOUR Results and Discussion

| (PS:PVDF :AO) % | E corr. | I corr. | J corr = I corr /A |
|----------------------------|---------|--------------|-----------------------|
| (PS68:32PVDF:0.0 292AO) | -374.3 | 442.07 μA | 4.42 |
| (PS68:32PVDF:0.0 584AO) | -552.3 | 1.23 μA | 0.0123 |
| (PS68:32PVDF:0.0 876AO) | -77.5 | 15.14 nA | 0.15 |

Table (4.9) Results of corrosion curves for the second group of samples

4.14 The results of the pull-out adhesion test:

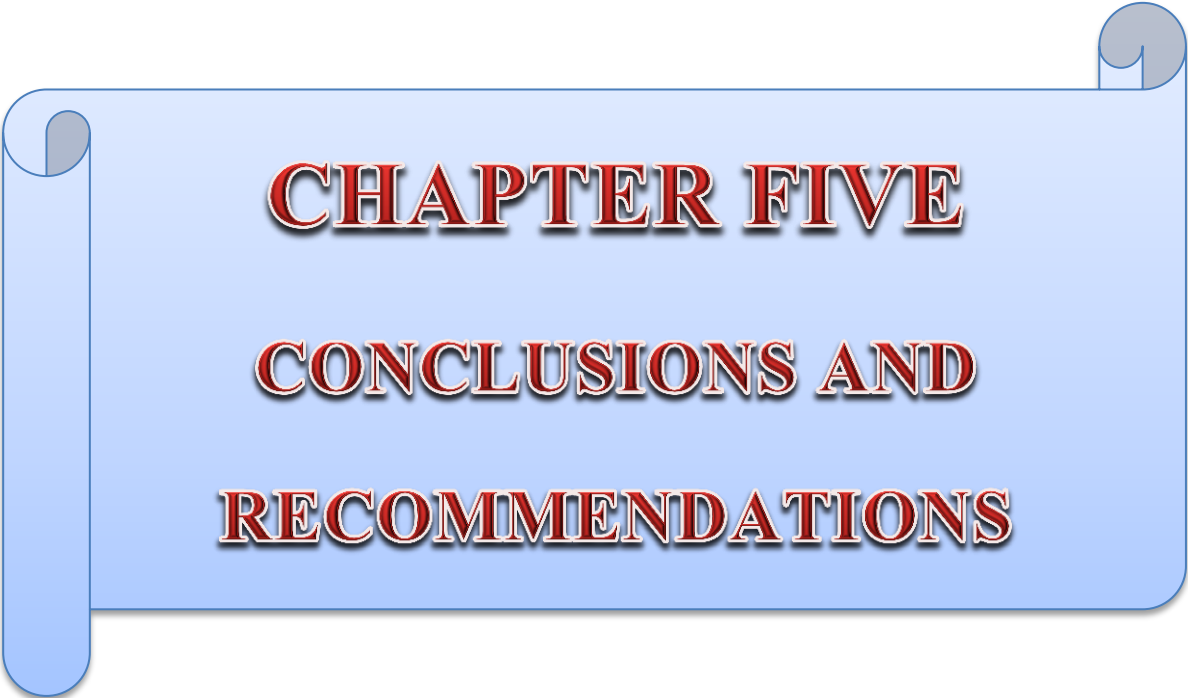
Table (4.12) shows the results of the adhesive forces that were tested in this research. The adhesion strength of the first sample which is (pure ps) and we see an increase in the adhesion strength of the second sample after adding PVDFby(PS16:84 PVDF)and with an increase in the percentage of PVDFwe notice an increase in the adhesion strength of the third sample which is (PS 76:24 PVDF) and with the increase of the ratio we notice an increase The adhesion force of the fourth sample which is (PS 68:32 PVDF) and it is noticed an increasein the adhesion strength of the fourth sample by adding a drops of AO as well as an increase in the adhesion strength of the fifth sample by adding 0.0584 of AO as well as an increase in the adhesion strength of the sixth sample by adding three drops of AO the highest adhesion strength is in the samples as shown in the table below,

CHAPTER FOUR Results and Discussion

| Sample | Contents | Adhesive Strength Mps |
|--------|-----------------------|-----------------------|
| 1 | Pure PS | 0.12 |
| 2 | PS84:16PVDF | 0.16 |
| 3 | PS76:24PVDF | 0.42 |
| 4 | PS68:32PVDF | 0.94 |
| 5 | PS68:32PVDF: 0.0292AO | 1.18 |
| 6 | PS68:32PVDF:0.0584AO | 1.52 |
| 7 | PS68:32PVDF:0.0876AO | 1.83 |

Table 4.10. shows the adhesive strength of sample

And it is concluded that the coating strength increases with the increase in the percentages of nanoparticle weight as shown in Table (4-12). believes that the rough surface may increase the interaction between the coating and the stainless steel, and nanoparticles enhance this effect and thus provide more opportunities for mechanical crosslinking between the coating and the stainless steel surface, and this is in agreement with 2006. Zbai et al and Mukesh et al. 2017 [133-134].



CHAPTER FIVE
CONCLUSIONS AND
RECOMMENDATIONS

5.1 Conclusions

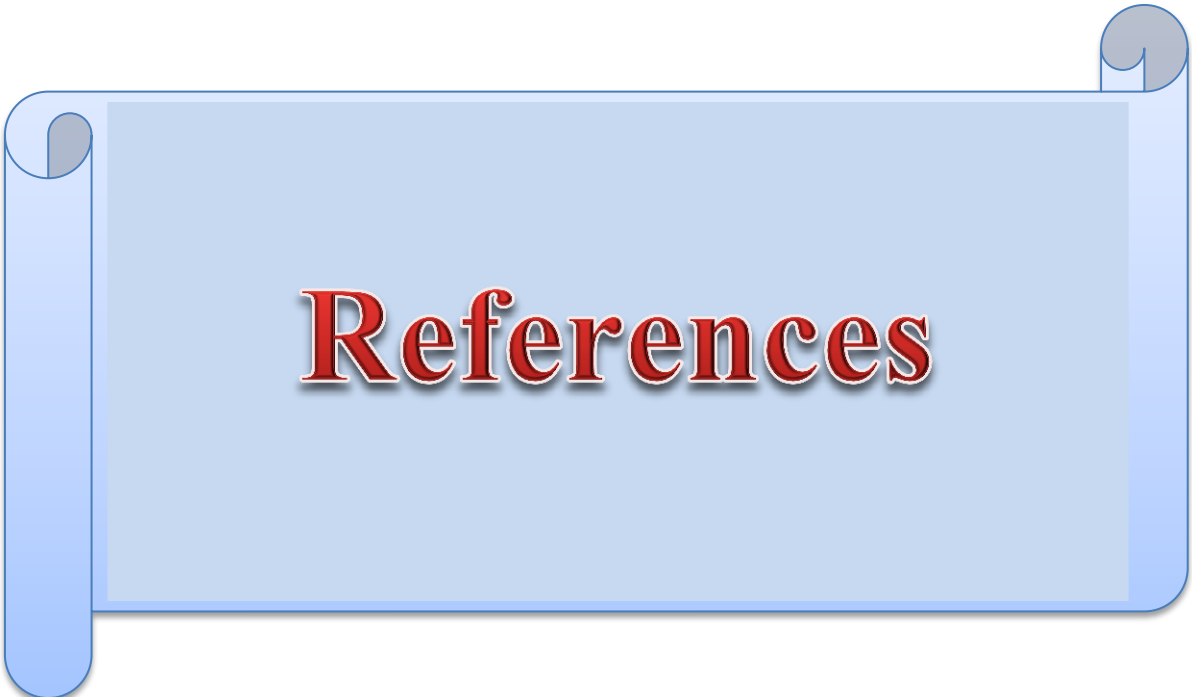
From this study, we conclude:

- 1- Using DC- high voltage power source leads to more nanofibers with a smaller diameter than AC- high voltage power supply .
- 2- AC-HV is suitable for manufacturing PS nano-fibers from DC-HV, as it leads to the manufacture of branch nano fibers which is suitable for filter media
- 3- Adding of the material (PVDF) to the solution leads to increasing pumping ability process it caused the electrospinning process to be stability and increases the electrical conductivity and thus the production of fibers containing less A number of finer beads
- 4- The addition of material (PVDF) also leads to an increase in the hydrophobic property
- 5- The addition of material (PVDF) also increases the abrasion resistance as it increases the resistance Corrosion as the percentage of the material increases
- 6- The addition of the material (PVDF) leads to an increase in the adhesion strength, as the adhesion strength increases as the percentage of the material increases .
- 7- Adding the natural substance, which is Argan oil, to the best sample, which is (PS0.68 + 0.32PVDF) leads to an improvement in the properties such as corrosion resistance, as well as an increase in the strength of adhesion.

CHAPTER FIVE Conclusions and Recommendations

5.2 Recommendations

- 1- Using other polymer with PS as PVA , PEG
- 2- Using other types of natural product as olive oil.
- 3- Studying the effect of ultraviolet - RAD rays on the properties of nanocomposites coatings.
- 4- Studying the morphology of the samples after cross-corrosion test SEM



References

REFERENCES

- 1 Kadhim, H.J., Al-Dabbagh, B.M., Salih, R.M., Ahmed, D.S. Nano composites films for food packaging applications. AIP Conference Proceedings, 2021, 2372, 100002
- 2 Jaafar, H.T., Aldabbagh, B.M.D. Investigation of superhydrophobic/hydrophobic materials properties using electrospinning technique. Baghdad Science Journal, 2019, 16(3), pp.632–638
- 3 Barbooti, M.M., Al-Dabbagh, B.D., Hilal, R.H. Preparation, characterization and utilization of polyacrylic acid–kaolin composite in the removal of heavy metals from water. International Journal of Environmental Science and Technology, 2019, 16(8), pp. 4571–4582
- 4 Al Dabbagh, B.M. Al Shimary, H.J., Salih, R.M. Separation of oil/water system by polymeric the super hydrophobic material for civil application. International Journal of Mechanical and Production Engineering Research and Development. 8 (2). 2017 , pp 1221-1226
- 5 Hameed, T.M., Al-Dabbagh, B.M., Jasim, R.K. Effect of Natural Sisal Fibers on Mechanical Properties of Heat Cured Acrylic Resin. Macromolecular, 2022, 401(1), 2100345.
- 6 Hameed, T.M., Al –Dabbagh, B.M., Jasim, R.K. Mechanical Properties of Heat Cured Acrylic Resin Reinforced with Natural Sisal Fibers Powder. Journal of Physics: Conference Series, 2021, 2114(1), 012023
- 7 Al Dabbagh, B.M., Kadhim, H.J., Salih, R.M. Studying the effect of Polyamide 6 Nanofibers on Physical and Chemical Properties of Unsaturated Polyester Reinforced by Glass fibers Composites. IOP Conference Series: Materials Science and Engineering, 2020, 757(1), 01200
- 8 Mohammed, D.B., Talal, J.H., Jawad, K.H. Fabrication of Hydrophobic Nanocomposites Coating Using Electrospinning Technique for Various Substrate. Journal of Physics: Conference Series. 1 (1032) , 2018
- 9 Alesa, H.J., Aldabbag, B.M., Salih, R.M. Natural pigment -poly vinyl alcohol nano composites thin films for solar cell. Baghdad Science Journal, 2020, 17(3), pp. 832–840 .

REFERENCES

- 10 Diao, B.M., Jaafar, H.T. Superhydrophobic nanocomposites coating using electrospinning technique on different materials. *International Journal of Applied Engineering Research*. 12 (24), 2017. PP. 16032-16038
- 11 Aldabbagh B M, Al Shimary H . SiO₂/ Polyamide Nanocomposite Textile for Super Hydrophobic Coating By Electrospinning Technique. *Int. J. Res Sci*. 2016; 2 (4): 6-10
- 12 Aldabbagh BM, Alshimary HJ (2017) Polyamide nanofibers coating by electrospinning technique for anti corrosion behavior. *J Eng Technol* 35(10):987–991
- 13 Talal H Al dabbagh B M. Kadhim H J. Contact Angle Hysteresis on Glass Using Silicone Rubber As Hydrophobic Nanocomposite Coating. *Nanotechnology and Advanced Materials Research Centre. ICNAMA 6* (2018) 000–000 , PP: 162-170
- 14 Salam Abdullah AL-Badri Hanaa Jawad Kadhim, Asra Ali Hussien . Preparation of anti biotics and self- cleaning polymer coatings. *Test engineering and management*. 83(4). 2020
- 15 Jabbar Z and Jawad H Hameed O. Preparation and studying of Nanofiber Membranes for Heavy Metals Absorption and Antibacterial Application. *Journal of Engineering and Applied Sciences*. 13 (10) , 2018
- 16 Xu, Lebo; Karunakaran, Raghuraman G.; Guo, Jia; Yang, Shu (2012). Transparent, Superhydrophobic Surfaces from One-Step Spin Coating of Hydrophobic Nanoparticles. , 4(2), 1118–1125. doi:10.1021/am201750h
- 17 Volkov, Konstantin (2018). Heat Transfer - Models, Methods and Applications || Techniques for the Fabrication of Super-Hydrophobic Surfaces and Their Heat Transfer Applications. , 10.5772/intechopen.71737(Chapter 14), -. doi:10.5772/intechopen.72820
- 18 Khadhim H J , Salih R M Preparation and Study of some Physical Properties of (Polystyrene/Ethel vinyl acetate) Blend Nanofibers. *Journal of Babylon University/Engineering Sciences*. 25 (4) , (2017) . PP 1267-1274

REFERENCES

- 19 Jaafar H T, Aldabbagh B M. Weathering Effect on Surface Characteristics of Superhydrophobic/Hydrophobic Nanocomposites Coating. *Engineering and Technology Journal*. 37 (3), 2019. PP 92-98.
- 20 Ondarcuhu T., & Joachim C. "Drawing a single Nano fibers over hundreds of microns." *Europhys Lett* ; 42 (2) PP (215-220), 1998.
- 21 Ma PX, Zhang R. "Synthetic Nano-scale Fibrous extracellular matrix." *J Biomed Mat Res*; 46, PP (60-72). 1999
- 22 Nadhim, B.A. and Habeeb, S.A., 2021. Studying the Physical Properties of Non-Woven Polyacrylonitrile Nanofibers after Adding γ -Fe₂O₃ Nanoparticles. *Egypt. J. Chem.*, 64(12), pp.7521-7530.
- 23 Whitesides G. M., Grzybowski B., "Self-assembly at all scales." *Science*. 2002
- 24 Liu, H., Gough, C. R., Deng, Q., Gu, Z., Wang, F., & Hu, X. (2020). Recent advances in electrospun sustainable composites for biomedical, environmental, energy, and packaging applications. *International Journal of Molecular Sciences*, 21(11), 4019.
- 25 Habeeb, S., Rajabi, L., & Dabirian, F. (2019). Comparing Two Electrospinning Methods in Producing Polyacrylonitrile Nanofibrous Tubular Structures with Enhanced Properties. *Iranian Journal of Chemistry and Chemical Engineering (IJCCE)*, 38(3), 23-42.
- 26 Formhals A., "Process and Apparatus for Preparing Artificial Threads US Patent 1,975,504, October 2, 1934."
- 27 Formhals A. US patent 2,160,962
- 28 Formhals A. US patent, 2,187,306, 1940.
- 29 Formhals A. US patent, 2,323,025, 1943.
- 30 Formhals A. US patent, 2,349,950, 1944
- 31 Tung University . Nano fibers "Institute of Applied Chemistry of NCTU , National Chiao
- 32 Jaworek A. , Krupa A. , Lackowski M. , Sobczyk A.T. , Czechl T. Ramakrishna S. , Sundarajan S. , & Pliszka D. ," Electro spinning and Electro spraying Techniques for Nano composite Non - Woven Fabric

REFERENCES

Production " , Fibers & Textile in Eastern Europe , Vol. 17 , No. 4 (75) , 2009..

33 " Nanotechnologies Terminology definitions for Nano objects - Nanoparticle , Nano fiber and Nano plate. "Nanotechnology Task Force. Berlin: Federal Institute for Materials Research and Testing. 2011.

34 Katarzyna M., Perena G.,” Electrospun Composite Nano Fibers Nanoparticle Research, vol.8, Issue 6, pp (769-781). 2006

35 Seeram R. , Kazotoshi F. Wee Eong T. , Teik - Cheng L., & Zuel M., "An Introduction to Electro spinning and Nano fibers" World Publishing Co. Pte. Ltd. , 2005.

36 Frenot A. and I. S. Chronakis, "Polymer Nano fibers Assembled by Electro spinning". Curr . Open. Colloid Interface Sci . , 8, PP (64-75). 2003 .

37 Pedicini, A. Farris, R. J. "Mechanical Properties of Electro spun Polyurethane", Polymer, vol. 44, PP (6857-6866). 2003

38 Lin D. Y., Martin D. C., “Orientation Development in Electro spun Liquid - Crystalline Polymer Nano fibers,” Chem. Society 226: U429 U429 490 - Poly.Part, 2003.

39 Hosseini A. & Pan S., "Morphological Characterization of Individual Polyacrylonitrile Nano Fibers", Current Nano science, Vol. 7, pp. (415-419). 2011.

40 Pankaj G., “Processing-Structure-Property, Studies of Submicron Fibers Produced by Electrospinning”, PhD. Thesis , Virginia Polytechnic Institute and State University ; ISBN: 9780496122301.2004

41 V. Beachley and X. Wen, “Polymer nanofibrous structures: Fabrication, biofunctionalization, and cell interactions,” Prog. Polym. Sci., vol. 35, no. 7, pp. 868–892, 2010.

42 P. Kumar, “Effect of collector on electrospinning to fabricate aligned nanofiber.” 2012

43 W. E. Teo and S. Ramakrishna, “A review on electrospinning design and nanofibre assemblies,” Nanotechnology, vol. 17, no. 14, p. R89, 2006.

44 X. Zhang and Y. Lu, “Centrifugal spinning: an alternative approach to fabricate nanofibers at high speed and low cost,” Polym. Rev., vol. 54, no. 4, pp. 677-701, 2010

REFERENCES

- 45 P. Kumar, "Effect of collector on electrospinning to fabricate aligned nano fiber." 2012.
- 46 I. Alghoraibi and S. Alomari, "Different methods for nanofiber design and fabrication," *Handb. nanofibers*, pp. 1–46, 2018.
- 47 El Fawal, G. F. (2020). Polymer nanofibers electrospinning: A review. *Egyptian Journal of Chemistry*, 63(4), 1279-1303.
- 48 P. Gupta, "Processing-Structure-Property Studies of: I) Submicron Polymeric Fibers Produced By Electrospinning and II) Films Of Linear Low Density Polyethylenes As Influenced By The Short Chain Branch Length In Copolymers Of Ethylene/1-Butene, Ethylene/1-Hexene & Ethylene/1-Octene Synthesized By A Single Site Metallocene Catalyst." Virginia Tech, 2004.
- 49 Natalia H. Vargas, "Aligned Cellulose Nanofibers Prepared by Electrospinning," Ms.c. Thesis, Lulea University of Technology, 2010.
- 50 Ji - Huan H. , Yong L. , Lu - Feng M. , Yu - Qin W. and Lan X. , " Electrospun Nanofibers and Their Applications " , Typeset by iSmithers Printed and bound by Lightning Source Inc. 2008
- 51 Fong, H.; Reneker D. H., "Electrospinning and the Formation of Nano Fibers"; Hanser Gardner Publications: NY. 2001
- 52 Didem R., & Mehmet M., "Effects of Electrospinning Setup Process Parameters on Nanofiber Morphology Intended for the Modification of Quartz Crystal Microbalance Surfaces", *Jour. of Eng . Fibers and Fabrics*, Vol. 7. 2012
- 53 Steffi W., "An Investigation of Process Parameters to Optimize the Fiber Diameter of Electrospun Vascular Scaffolds through Experimental Design," PhD. Project . ENGR 462. 2010
- 54 Prijo H., "Nanostructured Fiber Composite, and Materials for Air Filtration," P.h.D thesis, Tamper University of Technology.2008 University College
- 55 Zeynep K., "Electrospun Nanostructured Composite Fibers for Hydrogen Storage Applications Ph.D Thesis, London England. 2011
- 56 Paulo H. S. Piccianil , Eliton S. Medeiros , William J. Orts and Luiz H. C. Mattoso , " Advanced in Electroactive Electrospun Nanofibers " www.intechopen.com

REFERENCES

57 Mohammad Ch. and George S. , Effect of Experimental on Parameters the Morphology of Electrospun Nylon 6 fibres" , International Journal of Basic & Applied Sciences IJBAS - IJENS Vol : 10 No : 06.2010

58 Wang C. , Chien H. S. , Yan , K. W. , Hung, C. L. , Hung, K. L. and S. Ts. Jai, Jhang, H. J.; "Correlation between Processing Parameters and Microstructure of Electrospun Poly (D, L-lactic acid) Nanofibers," Polymer 50, pp (6100-6110). 2009

59 Huang C., Chen S., Lai C. , Reneker Darrell H. , Qiu H. , Ye Y. , Hou H. , " Electrospun polymer nanofibres with small diameters " , Nanotechnology 17 (6) , pp. (1558-1563). 2006

60 Sener, A.G. , "Effect of voltage on morphology of electrospun Electronics Engineering (ELECO), nanofibers," Electrical and International Conference on . IEEEpp (324-328). 2011

61 Sundaray B., Subramanian V., Natarajan T. S., Xiang R-Z, Chang C., Fann W-S. , " Electrospinning of continuous aligned polymer fibers". Appl Phys Lett 84 (7), pp (1222-1224). 2004

62 Royal K., John F., Gary T., "The use of AC potentials electrospaying and electrospinning processes", Jour. of Polymer, Vol. 45, Iss. 9, pp (2981-2984). 2004

63 Quynh P. PHAM, Upma Sh. , and Antonios G. MIKOS, "Electrospinning of Polymeric Nanofibers for Tissue Engineering Applications: A Review," TISSUE ENGINEERING Volume 12, Number 5, Mary Ann Liebert, Inc. 2006

64 Zhao, Z.Z. , Li, J.Q. , Yuan , X.Y. , Li , X. , Zhang , Y.Y. , and Sheng, J. "Preparation and properties of electrospun poly (vinylidene fluoride) membranes". J. Apple . Polym. Sci. 97, 466, 2005.

65 Javier M. , Alexis M.1 , Roman R. , Tom E. and Anxiu K. , " Effect of needle diameter on nanofiber diameter and thermal properties of electrospun poly (methyl methacrylate) " , Polymers for Advanced Technologies Volume 18 , Issue 3, pages 180-183, March 2007

66 Nuno M. Neves , Rui C. , Adriano P. , José C. Francisco M. , and Rui R. , " Patterning of polymer nanofiber meshes by electrospinning for biomedical applications " , I nt J Nanomedicine." Sep; 2 (3): PP (433 438). 2007

REFERENCES

67 Kim, K. W., K. H. Lee, M. S. Khil, Y. S. Ho, and H. Y. Kim, "The effect of molecular weight and the linear velocity of drum surface on the properties of electrospun poly (ethylene terephthalate) nonwovens. *Fibers and Polymers* 5 (2): pp (122-127). (2004).

68 R. Jiri, P. Marek, V. Vladimir, "Aligned nano-fiber deposition onto an apattered rotating drum collector by electrospinning", Brno, Czech Republic, EU, (2011)

69 Cuiru, Z. Jia, J. Liu, ZhihaiXu, Zhicheng Guan L. Wang, "Guiding surface electric field of collector on deposited Electrospinning fibers," *IEEE Transaction on Dielectrics and Electrical Insulation* Vol. 16, (2009)

70 B. Ahmad, E. Stride , S. Stoyanov, E. Pelan, and Mohan Edirisinghe, "Electrospinning of Ethyl Cellulose Fibers with a Heated Heated Air Using a Co-axial Needle: a Comparison", *Journal of Medical and Bioengineering (JOMB)* Vol. 1, No. 1 , September. 2012

71 Yong L., Ji-Huan H., Jian-yong Y., & Hong-mei Z., "Controlling numbers and sizes of beads in electrospun nanofibers", *Polym Int* 57, pp. (632- 632). 636). 2008. [87] Ki C. S., Kim J. W., Hyun JH, Lee KH, Hattori M, Rah DK, Park Y. H., "Electrospun threedimensional silk fibroin nanofibrou s scaffold " . *Jour. App . Poly . Sci.* 106 (6), pp. (3922-3928). (2007)

72 Lee K. H., Kim H. Y., Khil M. S., Ra Y. M., and Lee D. R., "Characterization of nano-structured poly (e-caprolactone) nonwoven mats via electrospinning," *Polymer*, vol. 44 , no . 4 , p. (1287-1294). 2003.

73 Hsu C. & Shivkumar S., "Nano-size beads and porous fibers of poly & -caprolactone produced by electrospinning", *Journal of Materials Science*, 39, 9, 3003.2004

74 Zuo W., Zhu M., Yang W., Yu H., Chen Y., and Zhang Y., "Experimental study on the relationship between jet instability and formation of beaded fibers during electrospinning," *Polymer Engineering and Science*, vol . 45 , no . 5, pp (704-709), 2005.

75 John Scheirs; Duane Priddy (28 March 2003). *Modern Styrenic Polymers: Polystyrenes and Styrenic Copolymers*. John Wiley & Sons. p. 3. ISBN 978-0-471-49752-3

76 *Common Plastic Resins Used in Packaging*". *Introduction to Plastics Science Teaching Resources*. American Chemistry Council, Inc. Retrieved 24 December 2012.

REFERENCES

- 77 American Polymers Service Inc.APS
- 78 A. G. Adeniyi, S. A. Abdulkareem, J. O. Ighalo, D. V. Onifade, S. A. Adeoye, and A. E. Sampson, "Morphological and thermal properties of polystyrene composite reinforced with biochar from elephant grass (*Pennisetum purpureum*)," *J. Thermoplast. Compos. Mater.*, no. July 2021, 2020, doi: 10.1177/0892705720939169.
- 79 C. L. Huang, Y. C. Chen, T. J. Hsiao, J. C. Tsai, and C. Wang, "Effect of tacticity on viscoelastic properties of polystyrene," *Macromolecules*, vol. 44, no. 15, pp. 6155–6161, 2011.
- 80 K. Grigoriadi, J. B. H. M. Westrik, G. G. Vogiatzis, L. C. A. van Breemen, P.D. Anderson, and M. Hütter, "Physical Ageing of Polystyrene: Does Tacticity Play a Role?," *Macromolecules*, vol. 52, pp. 5948–5954, 2019.
- 81 Liling Y., Wang, K., and Ye, L. (2003). Super hydrophobic property of PVDF/CaCO₃ nanocomposite coatings. *Journal of Materials Science Letters* ,Vol. 22,p.1713–1717.
- 82 Leivo, E., Wilenius, T., Kinos, T., Vuoristo, P., and Mäntylä, T. (2004) Properties of thermally sprayed fluoropolymer PVDF, ECTFE, PFA and FEP coatings. *Progress in Organic Coatings*, Vol.49, p.69–73.
- 83 Berry J. P. US patent 4965110, 1990.
- 84 Khalil A. K., H. Fouad, T. Elsarnagawy, Fahad N. "Preparation and Characterization of Electrospun PLGA/silver Composite Nano Fibers for Biomedical Applications," *Int. J. Electrochem. Sci.* , 8, PP (3483-3493). 2013
- 85 Dzenis Y. A. Hierarchical, "Nano-/micromaterials based on electrospun polymer fibers," predictive models for thermo mechanical behavior. *J Computer - Aided Mater* ; 3, PP (403-8). 1996
- 86 Fang X, Reneker D. H., "DNA fibers by electrospinning." *J Macromolecular Sci - Phys* . ; B36, PP (169-73). 1997
- 87 Fong H, Chun 1, Reneker DH. "Beaded Nano fibers formed during electrospinning". *joe. of polymer* ; 40, PP (4585-4592). 1999
- 88 Fong H., Reneker D.H. Elastomeric Nano fibers of styrene butadiene-styrene triblockcopolymer. *J Polym Sci: Part B Polym Phys*; 37 (24), PP (3488-3493). 1999

REFERENCES

- 89 Buchko C. J., Chen L. C., Shen Y., DC. "Processing and microstructural characterization of porous biocompatible protein polymer thin films." *Polymer*; 40, PP (397-407). 1999
- 90 Bergshoef M. Nanocomposites with ultrathin, electrospun Nylon - 4.6 fiber reinforcement. *Adv Mater* ; 11 (16). 1999.
- 91 Qingbiao Y., Zhenyu L., Youliang H , Yiyang Z., Shilun Q., Ce W., & Yen W., "Influence of Solvents on the Formation of Ultrathin Uniform Poly (vinyl Pyrrolidone) Nano Fibers with Electrospinning", *Jour. of Poly. Sci. Part B: Polymer Physics*, vol. 42, Issue 20, pp. (3721 3726) 2004
- 92 Chidchanok M., Nithitanakul M., Supaphol P., "Ultrafine electrospun polyamide - 6 fibers: Effect of Solution Conditions on Morphology and Average Fiber." diameter". *Macromol Chem Phys* 205 (17), pp (2327-2338). 2004
- 93 Xiaoyan Y., Zhang Y., Dong C., Sheng J., "Morphology of Ultrafine Polysulfone Fibers Prepared by Electrospinning". *Poly . Int .* 53 (11). 2004
- 94 Zhang C., Yuan X., Wu L., Han Y., Sheng J., "Study on the morphology of electrospun poly (vinyl alcohol) mats." *Eur Polym J* pp. (423-432). 2005
- 95 Huang C., Chen S., Lai C., Reneker Darrell H, Qiu H, Ye Y., Hou H., "Electrospun Polymer Nanofibres with Small Diameters *Nanotechnology* 17 (6), pp. (1558-1563) 2006
- 96 Y.C. Ahn, S.K. Park, G.T. Kim, Y.J. Hwangb, C.G. Lee, H.S. Shin & J.K. Leeb, "Development of High Efficiency Nanofilters Made of Nano Fibers", *Jou. 6 of Current App. Phy. VOL. ,* pp. 1030 1035. (2006)
- 97 Goki E. & Satya S., "Bead-to-Fiber Transition in Electrospun Polystyrene," *Jour. of App.Poly. Sci.* vol. 106, pp. (475-487). 2007.
- 98 Jianfen Z., Aihua H., Junxing L., & Charles C., "Polymorphism Control of Poly (vinylidene Fluoride) through Electrospinning", *Macromolecular Rapid Communications.* vol. 28, pp. (2159-2162). 2007
- 99 Haitao Z., Jinlian H., Shaojun C., & Lapyan Y., "Preparation of Polyurethane Nano fibers by Electrospinning", *Jour. of App. Poly. Sci.* Vo.109, pp. (406-411). 2008
- 100 Tan J. , Long Y. , & Li M. , "Preparation of Aligned Polymer Micro/Nanofibres by Electrospinning", *Chinese Phys. Let .* 25 3067 . 2008

REFERENCES

101 Dhanalakshmi M. & Jog J. P., "Preparation and Characterization of Electrospun Fibers of Nylon 11", Express Polymer Letters vol.2, No.8, pp® (540-545). 2008

102 Lilia M., Maurício P., D. Oliveira, Marcia C. B., Tassiana A. Custódio & Rosario E., "Thermal and Structural Characterization of Nano fibers of Poly (vinyl alcohol) Produced by Electrospinning," Jour. of App . Poly . Sci. Vol . 112, pp (1680-1688). 2009

103 Marcia C. Tassiana A., Lilia M., Luc A. & Rosario E., "Characterization of Nano-Structured Poly (D, L-lactic acid) Nonwoven Mats Obtained from Different Solutions by Electrospinning," Jour. Mac . Sci. , Part B: Phys. , Vol. 48. 2009

104 Mohammad C. & George S., "Effect of Experimental Parameters on the Morphology of Electrospun Nylon 6Fibres", International Jour. of Basic & App . Sci. IJBAS - IJENS Vol.10 . 2010

105 kheybari S. , Samadi N. , Hosseini S.V. , Fazeli A. , Fazeli M.R. "Synthesis and antimicrobial effects of silver Nanoparticles produced by chemical reduction method", DURU Jour. of Pharm. Sci. , 18(3), pp (168-172). 2010

106 Danielle M., "Fabrication and Characterization of Anti-microbial and Biofouling Resistant Nano Fibers with Silver Nanoparticles and Immobilized Enzymes for Application in Water Filtration", MSc. Theses, Stellenbosch University. (2011)

107 Hong S. Tshool, Bishweshwar P., Hem Raj P., Dipendra Raj P., Gopal P., Ki Taek N. ,, Cheol Sang K., & Hak Yong K., "Characterization and antibacterial properties of Ag NPs loaded nylon-6 nanocomposite prepared by one-step electrospinning process", Colloids and Surfaces A: Physicochem. Eng. Aspects 395.PP (94-99). (2011)

108 Sencadas V. , Correia D.M. , Areias A. , Botelho G. , Fonseca A.M. Neves I.C. , Gomez J., Ribelles & Lanceros S., "Determination of the Parameters Affecting Electrospun Chitosan Fiber Size Distribution and Morphology", Carbohydrate Polymers, Vol. 87, PP (1295-1301). 2012

109 Hyun J. , Hem R. , Young S. , Kyung Soo J. , Bishweshwar P. , Cheol S. , & Hak Y. , " Synthesis and Characterization of Spider - Web - Like Electrospun Mats of Meta - Aramid ". , Society of Chemical Industry , www.soci.org Poly . Intr . 2012

REFERENCES

110 Li Z. & Wang C., “Effects of Working Parameters on Electrospinning - One-Dimensional Nanostructures,” Springer Briefs in Materials. 2013

111 Ngadiman H. A., Noordin M. Y., Ani I., Denni K., “Effect of Electrospinning Parameters Setting towards Fiber Diameter”, Advanced Materials Research, Vol. 845.2014

112 Deng - Guang Y. , Xiao - Yan L. , Wei C. , Ying L. , & Xia W., "Influence of Sheath Solvents on the Quality of Ethyl Cellulose Nano Fibers in a Coaxial Electro Spinning Process", Jour . of Bio - Medical Mat . and Eng. Vol . 24. 2014

113 Zhou, Yuman; He, Jianxin; Wang, Hongbo; Nan, Nan; Qi, Kun; Cui, Shizhong (2017). Fabrication of superhydrophobic nanofiber fabric with hierarchical nanofiber structure. *e-Polymers*, 17(3), –. doi:10.1515/epoly-2016-0170

114 Yoon, Jae Won; Park, Yaewon; Kim, Jooyoun; Park, Chung Hee (2017). Multi-jet electrospinning of polystyrene/polyamide 6 blend: thermal and mechanical properties. *Fashion and Textiles*, 4(1), 9–. doi:10.1186/s40691-017-0090-4

115 Altan, A., Aytac, Z., & Uyar, T. (2018). Carvacrol loaded electrospun fibrous films from zein and poly (lactic acid) for active food packaging. *Food Hydrocolloids*, 81, 48-59

116 Yue, T. T., Li, X., Wang, X. X., Yan, X., Yu, M., Ma, J. W., ... & Long, Y.

Z. (2018). Electrospinning of carboxymethyl chitosan/polyoxyethylene oxide nanofibers for fruit fresh-keeping. *Nanoscale research letters*, 13(1), 1-8.

117 Jawad, K.H., Mohammed, D.B., Alsaffar, M.R. Performed of Filter Nano Textile for Purification of Aerosol Water by Electrospinning Technique. *Journal of Physics: Conference Series* 2019, 1298(1), 012023

118 Alehosseini, A., Gómez-Mascaraque, L. G., Martínez-Sanz, M., & LópezRubio, A. (2019). Electrospun curcumin-loaded protein nanofiber mats as active/bioactive coatings for food packaging applications. *Food Hydrocolloids*, 87, 758-771.

119 Somsap, J., Kanjanapongkul, K., Chancharonpong, C., Supapvanich, S., & Tepsorn, R. (2019). Antimicrobial activity of edible

REFERENCES

electrospun chitosan/cellulose acetate/gelatin hybrid nanofiber mats incorporating eugenol. *CURRENT APPLIED SCIENCE AND TECHNOLOGY*, 19(3), 235-247.

120 Wang, D., Liu, Y., Sun, J., Sun, Z., Liu, F., Du, L., & Wang, D. (2021). Fabrication and Characterization of Gelatin/Zein Nanofiber Films Loading Perillaldehyde for the Preservation of Chilled Chicken. *Foods*, 10(6), 1277.

121 Phuong N. Tuan Anh N. Pascal C. and Cuong N. (2018) Nanocomposite Coatings: Preparation, Characterization, Properties, and Applications . *International Journal of Corrosion* Volume 2018, Article ID 4749501, 19.

122 Talal J. H., Mohammed D. B . and Jawad K. H . (2018)

Fabrication of Hydrophobic Nanocomposites Coating Using Electrospinning Technique For Various Substrate. *IOP Conf. Series: Journal of Physics: Conf. Series* 1032 (2018) 012033.

123 Wang, Ling; Wang, Hao; Li, Bei; Guo, Zheng; Luo, Junchen; Huang, Xuwu; Gao, Jiefeng (2020). Highly electrically conductive polymer composite with a novel fiber-based segregated structure. *Journal of Materials Science*. doi:10.1007/s10853-020-04797-y

124 Daems, N.; Milis, S.; Verbeke, R.; Szymczyk, A.; Pescarmona, Paolo P.; Vankelecom, Ivo F. J. (2018). High-performance membranes with full pH-stability. *RSC Advances*, 8(16), 8813–8827. doi:10.1039/C7RA13663C

125 Al Dabbagh B M., Khadim H J., Dayah N. R. Studying the Effect of some Parameters on PS Microfibers by Electrospinning Technique. *Journal of University of Babylon* . 24, (3), PP 577-586 (2016)

126 Kadhim H J . Micro Fiber composite by Electrospinning Technique. PH.D thesis University of technology . Materials Branch, applied science department. 2015

127 Shin, Y. M., M. M. Hohman, M. P. Brenner, and G. C. Rutledge, “Electrospinning: a whipping fluid jet generates submicron polymer fibers.” *Applied Physics Letters* 78 (8): 1149-1151. (2001a)].” Shin

128 , Y. M., M. M. Hohman, M. P. Brenner, and G. C. Rutledge, “Experimental characterization of electrospinning: the electrically forced jet and instabilities.” *Polymer* 42 (25): pp (9955-9967) (2001b)

REFERENCES

129 Anthony L. Andrady, "Sciences and Technology of Polymer Nanofibers," Copyright by John Wiley & Sons, Inc. All rights reserved. 2008

130 He J. H., Wu Y., and Pang N., "A mathematical model for preparation by AC- Electro spinning process. International Journal of Nonlinear Sciences and Numerical Simulation 6 (3), pp (243-248). 2005

131 Huan, Siqi; Liu, Guoxiang; Han, Guangping; Cheng, Wanli; Fu, Zongying; Wu, Qinglin; Wang, Qingwen (2015). Effect of Experimental Parameters on Morphological, Mechanical and Hydrophobic Properties of Electrospun Polystyrene Fibers. *Materials*, 8(5), 2718–2734. doi:10.3390/ma8052718 .

132 Su, F., & Yao, K. (2014). Facile Fabrication of Superhydrophobic Surface with Excellent Mechanical Abrasion and Corrosion Resistance on Copper Substrate by a Novel Method. *ACS Applied Materials& Interfaces*, 6(11), 8762–8770.

133 Zhai, L., Ling, G., Li, J., & Wang, Y. (2006). The effect of nanoparticles on the adhesion of epoxy adhesive. *Materials Letters-25*60 , .3033–3031 ,(26

134 Mukesh K., Nisha K. , & Neha R. (2017). The Effect of Zinc Oxide Nanoparticles on Cohesive and Adhesive Bond of Epoxy/Amine Coating on Carbon Steel Substrate. *IOSR Journal of Applied Chemistry (IOSR-JAC)* . Vol. 10, Iss. 7 Ver. II ,(PP 47-58)

الخلاصة

يتناول البحث دراسة الخواص الفيزيائية لاليف النانوية المنتجة

1 استخدام AC-HV

2 استخدام DC-HV

تم انتاج اليف من مواد فلوريد البولي فينيلدين و البولي ستايرين و بتاثير عوامل مختلفة منها تتعلق بالمحلول مثل (اللزوجة ، التوصيلية ، الشد السطحي) و الاخر تتعلق بتتصيب مثل (قدرة ضخ السائل ، قيمه الفولتية ، نوع الفولتية) وكما تمه إضافة مادة طبيعیه مستخلصه من النباتات وهي زيت اركان على افضل العينات المحضره لمعرفة تاثيره على المحاليل المعدة و خصائص الاليف الناتجة . تم إجراء العديد من الاختبارات ، بما في ذلك اختبارات للمحلول ، والتي تشمل التوتر السطحي واللزوجة ، التوصيلية الكهربائية ، وكذلك الفحوصات الاليف والتي تشمل فحص الأشعة تحت الحمراء الاليف المنتجة بواسطة DC-HV لتحديد نوع التفاعل بين المكونات ومعرفة الروابط الناتجة والتركيب ، وزاوية الترطيب الفحص لتحديد ما إذا كانت الألياف المحضرة محبة للماء أو كارهة للماء وظهرت النتائج ان الزاوية الترطيب لاليف المنتجة بواسطة DC-HV اكبر من نتائج AC-HV ، اختبار مجهري للقوة الذرية لمعرفة خشونة السطح ومؤشر تحمل السطح وظهرت النتائج ان خشونة السطح لاليف المنتجة بواسطة AC-HV اكثر من الاليف المنتجة بواسطة DC-HV ، مسح المجهر الإلكتروني لدراسة مورفولوجيا الألياف وتوزيعها وظهرت النتائج ان الاليف المنتجة باستخدام DC-HV تحوي على خرز و اكثر انتظاما من الاليف المنتجة بواسطة AC-HV . تمت دراسة اختبار التآكل للطلاء وأظهرت النتائج أن مقاومة التآكل تزداد عندما تزداد نسبة ب (PVDF). كما تمت دراسة نتائج مقاومة الالتصاق عن طريق اختبار السحب حيث تزداد مع زيادة نسبة PVDF .



جمهورية العراق
وزارة التعليم العالي والبحث العلمي
جامعة بابل / كلية هندسة المواد
قسم البوليمر والصناعات البتروكيمياوية

تحضير الياف نانوية مركبة فائقة الكراهية للماء بتقنية الغزل الكهربائي ذات الفولتية العالية المستمرة و المتناوبة

اطروحة مقدمة لقسم البوليمرات والصناعات البتروكيمياوية بكلية هندسة
المواد / جامعة بابل في استيفاء جزئي لمتطلبات درجة الماجستير في
هندسة المواد / البوليمر

اعداد الطالب
عمار كريم كاظم

اشراف
أ.د. هناء جواد كاظم